RESILIENT MODULUS OF ASPHALT CONCRETE MIXTURES

BY

TARA LEIGH LAW

A Thesis
Submitted to the Faculty of Graduate Studies
In Partial Fulfillment of the Requirements
For the Degree of

MASTER OF SCIENCE

Department of Civil Engineering
University of Manitoba
Winnipeg, Manitoba

THE UNIVERSITY OF MANITOBA

FACULTY OF GRADUATE STUDIES

*****

COPYRIGHT PERMISSION

RESILIENT MODULUS OF ASPHALT CONCRETE MIXTURES

BY

TARA LEIGH LAW

A Thesis/Practicum submitted to the Faculty of Graduate Studies of The University of Manitoba in partial fulfillment of the requirement of the degree

Of

MASTER OF SCIENCE

Acknowledgements

I would like to acknowledge Thomas J. Pounder Family, EBA Engineering, Transportation Association of Canada, and Manitoba Department of Transportation and Government Services for providing me with the financial assistance to complete this project.

I would like to express gratitude to my supervisor, Dr. Ahmed Shalaby, for his support and dedication towards the completion of this project. His enthusiasm inspired me and gave me devotion.

Special thanks to my parents and family for their encouragement throughout the competition of my Master's Degree, and throughout all my accomplishments. If my parents had not believed in me first, I would have never made it this far in my studies. I would especially like to thank my husband, Lonnie, for his loving, caring and endless support through all my endeavors.

Abstract

This research investigates the properties of the two standard asphalt paving mixes used in Manitoba, Bituminous B (Bit B) and Bituminous C (Bit C). Bit B is a well-graded, dense mix while Bit C is a lower class product with smaller aggregates and lower asphalt content. The aim of the research is to characterize the relationship between material properties and strength parameters measured in the laboratory and in the field.

Eight test sites located throughout the Province of Manitoba were identified for this research. Each test site had a test section that consisted of at least 1 km of a Bit B surface course over a Bit B binder course (Bit B/B) and a side-by-side section with a Bit B surface course over a Bit C binder course (Bit B/C). Twenty cores were extracted from each test site, ten from the Bit B/B section and ten from the Bit B/C section. Four cores per section were tested for the physical properties and the remaining cores were tested for strength and deformation parameters using a modified form of the indirect tensile strength test.

The tensile strength and the elastic properties from static loading were determined using the indirect tensile strength test. A moisture sensitivity analysis was conducted on the paving mixtures to evaluate the long-term performance of the mixes. To assess the layer stiffness of the asphalt concrete mixes, some of the cored samples were dynamically loaded in the laboratory under controlled temperatures to determine the resilient modulus and the effects of temperature.

The overall pavement strength and deflection response of the pavement layers for Bit B/B and the Bit B/C sections were determined using data from a Falling Weight Deflectometer (FWD). An elastic layer analysis was completed using the ELMOD computer program, and the backcalcuated resilient modulus was determined. The Inertia Method was then used to estimate the modulus of each asphalt layer.

Test results show that the Bit C mixes tested in the static mode show greater tensile strengths than the corresponding Bit B mixes. Through dynamic loading it was found that, Bit B mix generally has a greater resilient modulus value than the corresponding Bit C mix. The backcalculated resilient modulus values demonstrated similar trends to the resilient modulus calculated from dynamic loading.

Table of Contents

List of Tables

List of Figures

Chapter 1
INTRODUCTION

1.1 The Research Need

Over the years, great strides have been made to better understand the behaviour of hot mix asphalt and the many factors that affect its performance. There is much work that still remains to fully understand the factors that influence the level of performance of asphalt paving mixtures, such as the aggregate characteristics, binder characteristics, environmental conditions and traffic loading.

Conventional flexible pavements consist of the more stiffer mixture on the top where the stresses are greater than the underlying layers where the stresses are lower. This makes it possible to use lower grade asphalt mixtures for underlying layers, to make use of local materials that are of lower grade resulting in a more economical design. There is a need to determine the relative performance of asphalt mixes in order to optimize pavement design.

It has been widely accepted that the strength of a pavement structure is a good indicator of mixture quality. The traditional mixture design methods have had associated strength tests that are empirical. The Marshall stability test has been, and is currently, being used by many agencies to determine the stability of asphalt paving mixtures as an indication of strength. A rational and reliable test method is needed to determine the strength of asphalt paving mixtures.

Through this research, the procedures, recommendations and limitations of strength test methods of asphalt mixtures in the laboratory were evaluated. The Federal Highway Administration (FHWA) has developed the Long Term Pavement Performance (LTPP) Protocol P07 (FHWA, 2001), a test method to determine the resilient modulus of asphalt mixtures with the use of indirect tensile testing and dynamic loading.

1.2 Objectives of the Research

The purpose of this research is to evaluate the properties of two asphalt concrete paving mixtures, in the laboratory and using nondestructive in-situ tests. The aim is to characterize the relationship

between material properties and strength parameters obtained through laboratory and field testing. Experience and understanding gained in this area will be used to compare the relative performance of asphalt paving mixtures and to aid in the selection of a suitable mix design.

To determine the material and strength properties of an asphalt mixture, a large sample size is required. For this research, the Manitoba Department of Transportation and Government Services (MTGS) provided two distinctly different asphalt concrete mixture samples to be tested. Bituminous B (Bit B) is an asphalt mixture that is a well-graded, dense mix and is identified to have good wearing resistance. Bituminous C (Bit C) is a lower grade product consisting of finer aggregate size (poorly graded) and lower asphalt content. This Bit C mixture has less stringent gradation specifications and could be considered an "open-graded" mixture.

Samples of these two paving mixtures taken from various paving projects in Manitoba were used in this research to evaluate the material properties that affect the strength, and in turn, the performance of asphalt paving mixtures. Falling Weight Deflectometer (FWD) data was obtained from field testing and the indirect tensile strength test, incorporating static loading and dynamic loading, were used in the laboratory to gain information on the material properties. The physical mix properties were also evaluated to compare each mix and to relate them to laboratory and field test results.

1.3 Scope

This research investigates the strength parameters of asphalt concrete by examining the physical mixture properties through field and laboratory testing. The physical mixture properties such as air voids, asphalt content, voids in mineral aggregate, density and gradation were examined to for affect on the structural performance of the asphalt pavement such as stiffness, and durability, as determined in the laboratory.

The stiffness of the asphalt mixtures was determined from the indirect tensile strength test using static and dynamic loading and from deflection data obtained from FWD testing. The subgrade strength was also determined using backcalculation of FWD deflections by using the computer software ELMOD and by a procedure presented by the American Association of State Highway and Transportation Officials in the 1993 Design Guide (AASHTO, 1993). The subgrade strength was determined when examining the entire pavement structure response to FWD loading. No

laboratory testing was conducted on the aggregate base or the subgrade material, as these are not the focus of this research.

A relative comparison of the durability of the two asphalt paving mixtures was conducted by an accelerated moisture conditioning test and static loading. The results from the durability testing of the Bit B mixture was only briefly addressed. The durability of the Bit C mixture was not determined, as further testing is required. The Bit C mix did not withstand the moisture conditioning process and therefore a different test method is required.

Dynamic testing is in the early stages of development at the University of Manitoba. LTPP Protocol P07 was followed as much as possible but modifications to the testing procedure were made as needed to accommodate equipment at the University of Manitoba.

All material properties were determined through tests conducted at Manitoba Department of Transportation and Government Services Central Laboratory. The test results were forwarded to the University of Manitoba to enable an evaluation of the material properties to be made for this research. The aggregate gradation and composition were examined but no additional testing was conducted on the aggregates.

1.4 Thesis Organization

This thesis is divided into six chapters. The chapters are organized as follows:

Chapter 1 - The need for this research, the aim and objectives of this research, the boundaries and terminology used throughout the thesis.

Chapter 2 - A literature review that covers the pavement analysis methods, material properties of asphalt cement, aggregates and asphalt mixtures, laboratory test methods and field test methods.

Chapter 3 - A description of the test site locations and characteristics, data collection, sampling, and an outline of laboratory tests conducted.

Chapter 4 - Presentation of the test results from the material property testing, FWD deflections, and the indirect tensile strength test using static and dynamic loading. The loading history and the interpretation of the data is summarized.

Chapter 5 - Analysis and discussion of the FWD deflections using backcalculation to determine the resilient modulus, the indirect tensile strength test (IDT) using static loading to compare Bit B and Bit C and for a moisture sensitivity analysis, and the IDT using dynamic loading to compare Bit B and Bit C response to moving loads. An overall comparison between the test procedures and the mixtures are presented and correlations are made between the asphalt parameters.

Chapter 6 - A summary of research and findings, conclusions and recommendations for future work.

1.5 Terminology

The following terms and definitions are used interchangeably in this thesis:

Hot mix asphalt

asphalt concrete
asphalt mixture
asphalt paving mixture
bituminous paving mixture
bituminous concrete

This material is a high quality pavement surface composed of asphalt cement and aggregates, hot-mixed in an asphalt plant and then hot-laid (Atkins, 1997).

Asphalt binder or asphalt cement is defined as a fluxed or unfluxed asphalt specially prepared as to quality and consistency for direct use in the manufacture of bituminous pavements, and having a penetration at 25°C (77°F) of between 5 and 300 units, under a load of 100 g applied for 5 seconds (ASTM D8-02). Asphalt cements fall within the broad category known as bitumens. Bitumens are defined as a class of black or dark-colored (solid, semisolid, or viscous) cementitious substances, natural or manufactured, composed principally of high-molecular-weight hydrocarbons, of which asphalts, tar, pitches, and asphaltites are typical.

Poisson's ratio, ν, is defined as the ratio of the lateral strain to the axial strain (Huang, 1993). Poisson's ratio is usually assumed in the design of asphalt pavements due to it's small effect on pavement response.

Modulus

- The *resilient modulus* refers to the elastic modulus of the asphalt concrete that is used with elastic theory (Huang, 1993) and is obtained through repeated loading. The loads applied and the displacements experienced are measured on uniaxial compression or indirect tensile specimens (Roberts et al., 1996). The loading is of a haversine waveform with a rest period. The modulus a measure of the ratio of repeated stress to corresponding recoverable or resilient strain under repeated loading. It is also referred to as the elastic stiffness of the asphalt mixture after many load repetitions.
- The *stiffness* is the relative deformability of a material under load and is measured by the rate of stress to the rate of strain (Davis et al., 1982).
- *Young's modulus*, E, can be used to characterize the linear elastic characteristics of the material. It is defined as the slope of the straight line portion of the stress-strain curve. This term can only be applied to the linear portion of the stress-strain curve during the loading-unloading of asphalt concrete. If there is no straight portion of the curve, the tangent of the curve at the origin can be used to represent the Young's modulus.
- The *tangent modulus* is the modulus calculated at a location along a stress strain curve at a given stress, as shown by Figure 1.1.

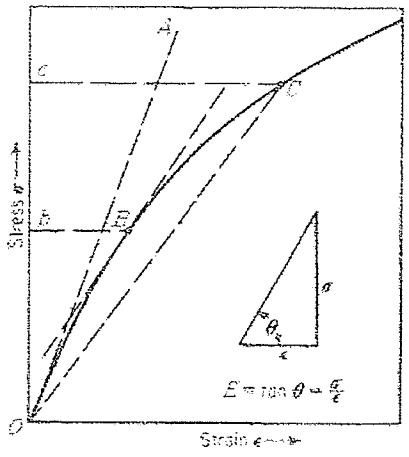

Figure 1.1 **Stress-Strain Curve** *(Davis et al., 1982)*

- The tangent modulus would be the slope of line OB. The *secant modulus* is the slope of the line from the origin to any point on the stress-strain curve, as illustrated by line OC in Figure 1.1. It is representative of the average modulus between the load in which the straight line intercepts and zero load. It is only determined when a static load is applied.
- The *complex modulus* test is similar to the resilient modulus test except that the former applies a continuous sinusoidal or haversine loading while the resilient modulus applies any waveform loading with a given rest period. The complex modulus is a complex quantity; the real part represents the elastic stiffness while the imaginary part characterizes the dampening. The inelastic as well as elastic deformations are measured and can provide information on the stiffness and dampening.
- The *dynamic modulus*, E^*, is the absolute value of the complex modulus and is determined from the test procedure outlined in ASTM D3497-79 (1995), *Standard Test Method for Dynamic Modulus of Asphalt Mixtures*. A repeated sinusoidal or haversine load is applied to a specimen with a height to diameter ratio of at least 2 to 1. The dynamic modulus is calculated by dividing the axial stress by the recoverable axial strain (Huang, 1993).

The *stability* is related to the strength of the asphalt concrete and refers to the ability of the pavement to resist deformation under application of loads (Derucher et al., 1998). It depends on the distribution of loads by point-to-point contact of the aggregate particle, aggregate interlocking developed and the cohesiveness supplied by the asphalt cement.

Chapter 2
LITERATURE REVIEW

2.1 Linear Elastic Theory

Over the years, there has been a change in the philosophy of flexible pavement design from the empirical methods to a more mechanistic approach. The mechanistic approach incorporates elastic layered theory.

The behaviour of a flexible pavement due to loading can most easily be characterized if assumed to be a homogenous half-space. The half-space has an infinitely large area and an infinite depth with a top plane on which the loads are applied. In 1885, the original Boussinesq's theory was implemented. Boussinesq's theory is based on a concentrated load applied to a homogeneous, elastic half-space (Huang, 1993). The assumption of the material to be elastic is not valid when dealing with stationary loads but is acceptable when assuming moving traffic loads. This is because for moving loads, the deformations were assumed to be recoverable and therefore, can be considered elastic.

The concept of layered pavement systems was introduced to better analyze flexible pavement structures that consisted of various layers. Donald M. Burmister presented the layered system in the 1940s. The two-layered system was first developed followed by the three-layer system in the 1950s. The elastic layered theory assumed that:

- Layers are homogeneous
- Layers are isotropic
- Each layer has a finite thickness (with the exception of the subgrade layer)
- All layers have finite lateral expanse
- There is full bond between the layers as indicated by the compatibility of interface strains and displacements.
- No surface shear forces are present
- Stress solutions are characterized by the resilient modulus and Poisson ratio.

The linear elastic theory requires the use of the elastic properties of the asphalt mixtures. The most commonly calculated value used to determine the elastic properties of an asphalt mixture is

the resilient modulus, through the use of the indirect tensile mode (Brown et al., 1989). The resilient modulus is one of the most widely used stress-strain measurements used to evaluate the elastic properties of an asphalt mixture for use in multilayer elastic theories (Mamlouk and Sarofim, 1988). The resilient modulus is considered the most appropriate parameter to be used because it represents the elastic stiffness of the asphalt mix after many load repetitions. Other elastic properties of asphalt mixtures that have been determined in the laboratory are Young's modulus, shear modulus, bulk modulus, complex modulus, dynamic modulus, and double punch modulus values, but are not discussed in this thesis.

2.1.1 Stress, Strain, and Deflection Criteria

Through the theory of layered pavement systems, different criteria have been used for pavement design. Figure 2.1 illustrates the general distribution of a load that is imposed at the surface of a pavement structure.

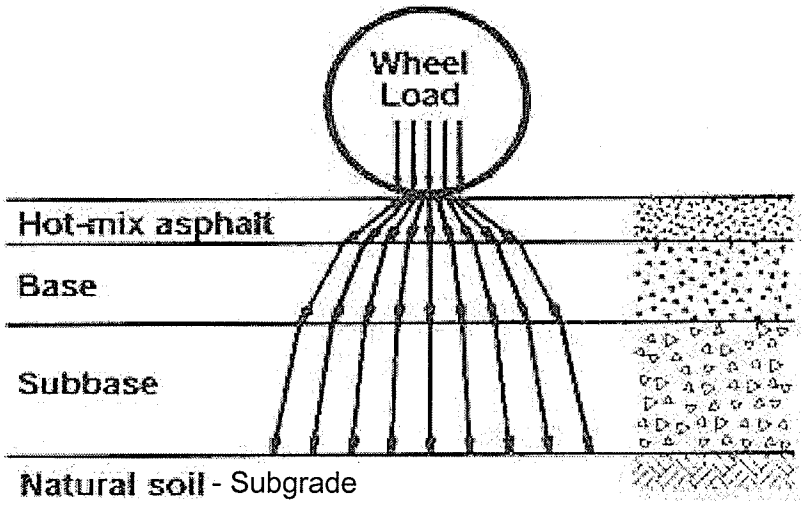

Figure 2.1 Load Distribution in a Layered System *(ERES, 2001)*

Over the years, the design philosophy shifted from the early purely empirical design methods to the modern more mechanistic-empirical methods. The advantages of the mechanistic approach are the improved reliability of a design, the ability to better predict the type of distress, and the feasibility to extrapolate parameters from limited field and laboratory data (Huang, 1993). The mechanistic-empirical design methods are based on limiting horizontal tensile strain at the bottom of the asphalt layer and vertical compressive strain at the surface of the subgrade. The primary goal in pavement design is to minimize the critical stresses, strains and deflections experienced

by the pavement structure. Stresses within flexible pavements vary greatly on the type of flexible pavement and the ratio of moduli (or stiffness) of the various layers of the pavement structure. Figure 2.2 identifies the location of tension and compression within the pavement structure when subjected to a load.

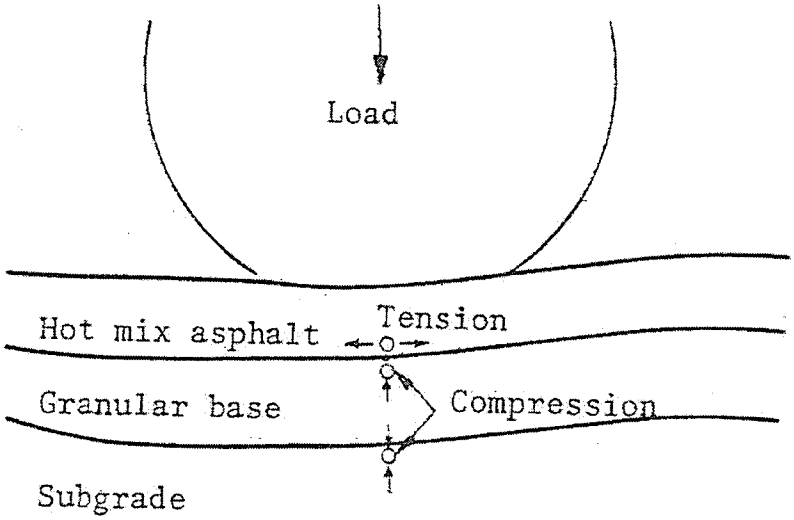

Figure 2.2 Location of Critical Tensile and Compressive Strains *(Huang, 1993)*

Most often, the vertical compressive strain at the subgrade is used as the design criterion. The aim is to reduce the vertical stresses at the top of the subgrade material. When the vertical stresses exceed the strength of the subgrade material, permanent deformations may take place. A method of minimizing the critical stresses, strains and deflections is to; reduce the modulus ratio in the upper layers; and or increase the thickness ratio of the upper layers (Mahoney and Newcomb, 1990). To reduce the vertical stresses on the top of the subgrade, increase the thickness of the base or surface layer or increase the stiffness of the base.

To prevent pavement fatigue cracking, the tensile strains at the bottom of the asphalt layer have been used as a design criterion. Surface deflections due to traffic loading have been limited to maximum allowable values to reduce the deflection experienced by the pavement structure.

2.1.2 Limitations of Elastic Theory

There are some limitations associated with the layered elastic model, such as:

- Tire-pavement contact to be represented as a uniformly loaded circular area is incorrect. Research has shown that the actual contact area shape varies with tire pressure and tire stiffness, resulting in a highly non-uniform distribution of load;
- The vertical and lateral variation in the resilient modulus are not accounted for;
- Unbound material is stress sensitive and therefore the stresses and strains calculated in the unbound materials may be unreasonable;
- Inertial forces are neglected; and
- An asymmetric approach is required when wheel loads are applied close to cracks or edges.

2.2 Pavement Performance

The performance of a pavement is directly related to the construction, materials, and maintenance of the existing structure. If a pavement structure fails, the causes must be identified to improve the design procedure. Pavement failure can be prevented during the design process by addressing each potential failure criterion.

Great strides have been made to understand the behaviour of bituminous mixtures and the many factors that affect their performance. The structural performance of a pavement is dependant upon its ability to distribute stresses, resist permanent deformations, resist cracking, and the ability to resist moisture damage (Epps et al., 2000). These factors are related to the materials, environment, load and construction process.

Pavement performance can be classified in two categories: structural failure and functional failure. Structural failures are associated with the pavement structure not being able to carry the design load. Functional failures are concerned with vehicle stability, comfort of the ride and safety. Often, functional failures trigger the rehabilitation of pavement structures although the pavement structure may still be structurally sound.

2.2.1 Pavement Distresses

Pavement distresses are visible failures of a pavement structure. There are non-load induced distresses and load-induced distresses. Non-load distresses are such distresses as thermal cracking, which are a type of structural failure. Fatigue cracking is an example of a load induced

structural failure. Rutting is classified as a load-induced functional failure, with no structural damage but may produce an uncomfortable and unsafe ride.

2.2.1.1 Fatigue Cracking

Fatigue cracking exists in asphalt pavement structures when the horizontal tensile stresses or strains at the bottom of the asphalt concrete layer are the highest due to traffic loading. Cracking initiates at the bottom of the asphalt layer as microcracks and propagates to the surface in longitudinal cracks from the increase or repetition of tensile stresses, shear stresses or a combination of both. This type of failure is identifiable by alligator cracking.

An asphalt mix is designed to resistant cracking when subjected to repeated loads over a period of time. With the development of a better understanding of the mechanisms of failure, improved mixture tests and improved materials and pavement models to predict field performance of bituminous mixtures are more reliable. The increase of knowledge will lead to improved design procedures and specifications (Epps et al., 2000).

2.2.1.2 Thermal Cracking

Thermal cracking can be classified into two different types based on two different environmental conditions: low-temperature cracking and thermal fatigue cracking (Epps et al., 2000). In Canada, low temperature thermal cracking exists in regions where winter temperatures fall below –23°C (10°F). Cracks form because the binder is unable to withstand the stresses induced by cold temperatures. The asphalt binder is primarily responsible for resisting thermal cracking through its ability to undergo tensile strain without failure. When the asphalt binder fails, thermal cracking starts and the pavement structure is prone to the intrusion of water and fines.

Thermal fatigue cracking occurs when the asphalt binder selected for the mix has a high stiffness or has hardened due to aging. The stiffness of the asphalt binder increases tensile strain in the asphalt layer due to the multiple cycles of temperature change with thermal stresses below the tensile strength of the mixture. The binder properties of the asphalt mixture have been used to control the threshold at which thermal cracking initiates. The indirect tensile strength test and the thermal stress restrained specimen test (TSRST) are the tests that are currently being used to determine the fatigue properties of an asphalt mixture.

2.2.1.3 Permanent Deformation

Due to the increase in traffic volume, axle load and truck tire pressure, there has also been an increase in rutting in asphalt pavement highways. Rutting has been defined as the accumulation of permanent deformation or strain in one or more layers of the pavement structure (Thiessen, 2001). Rutting can be identified as the longitudinal depressions in the wheel path that may affect vehicle handling which is a hazard for highway users. Rutting is a result of the failure of the asphalt pavement structure to carry the loads imposed by traffic.

Collop et al. (1995) have suggested that there are two major factors that contribute to rutting: densification (compaction) during construction; and plastic shear deformation. The potential for rutting can be decreased by ensuring the pavement structure is well compacted during the construction process.

The resistance to permanent deformation is crucial during hot summer months when the viscosity of the asphalt binder is low and the traffic loading is mainly carried by the aggregate structure. The initial step to control the permanent deformation is during the mix design process. Quality aggregates with proper gradation should be selected along with an asphalt content that will guarantee adequate voids. The permanent deformation of a mixture can be determined in the laboratory using static or dynamic creep tests. There are many time-dependent permanent deformation models that have been developed over the years to aid in the prediction of rutting, but will not be discussed in this thesis.

2.2.1.4 Stripping (moisture susceptibility)

Stripping of an asphalt pavement is the loss or weakening of bond between the aggregate surface and asphalt binder. The loss of bond is usually caused by the presence of moisture between the aggregate and binder, although other factors do amplify the problem. The presence of moisture reduces the cohesion, interlock and friction between the aggregate structure, resulting in rapid deterioration of the asphalt. Structural strength in the asphalt pavement decreases with stripping and in turn causes an increase in the tensile strains in the upper layers. Rutting and fatigue cracking have also been associated with stripping (Shatnawi and Van Kirk, 1993).

2.3 Material Properties

There are many tests that are used to characterize the physical properties and the mechanical properties of an asphalt mixture. Physical mix properties are determined from tests to measure the density, air voids, and voids in mineral aggregate. Mix characteristics such as Marshall stability, resilient modulus, indirect tension and moisture susceptibility are determined through mechanical tests.

2.3.1 Aggregate Properties

There are many aggregate properties that affect pavement performance. The physical properties of the aggregates that could be looked at are: voids in mineral aggregate (VMA), mineralogy; durability; particle shape; gradation; and specific gravity.

2.3.1.1 Voids in Mineral Aggregate (VMA)

The voids in mineral aggregate (VMA) is primarily a function of the aggregate gradation, shape and surface texture of the aggregate and affects the performance of an asphalt mixture. It is the total amount of voids in the compacted aggregate.

As the maximum particle size of an aggregate mix decreases, the minimum VMA increases. If the VMA is too low, asphalt binder cannot be added to the mix without overfilling the voids, which may lead to durability problems with the mixture. On the other hand, if the VMA is too large the voids will not be filled and the mixture may show stability problems and be uneconomical to produce (Kandhal and Chakraborty, 1996). There must be enough VMA to allow for adequate asphalt cement film thickness and for enough voids to remain after compaction to allow for future compaction from traffic and to compensate for thermal expansion.

2.3.1.2 Mineralogy

The mineral composition of the aggregates are usually examined for the properties of hardness or toughness, resistance to stripping and polishing due to traffic, soundness to resist breakdown due to freezing and thawing, surface texture and crushed shape, which all have an important effect on the performance of an asphalt mixture.

It is well known that asphalt cement adheres better to some aggregates than others. This property is extremely important when the aggregates are subjected to moisture. Some siliceous aggregates are hydrophilic, which means they attract water more readily than asphalt cement due to their surface charge. This may lead to stripping by the asphalt cement coming away from the aggregates in the presence of water.

2.3.1.3 Durability

The aggregate must be tough enough to withstand the manufacturing, placing and compaction during the construction process. After this, the aggregate must be able to transmit the traffic load to the underlying layers without failure and be resistant to abrasion and polishing due to traffic.

The durability of an aggregate is defined as its ability to resist the deterioration under the action of wetting and drying, and freezing and thawing. Accelerated moisture induced tests, such as AASHTO T283-89 *Standard Method of Test for Resistance of Compacted Mixture to Moisture-Induced Damage*, are performed on aggregates to determine their susceptibility to moisture. In a study performed by Shatnawi & Van Kirk (1993), it was found that high air voids increase the moisture susceptibility of a mixture because there is an increase in the surface area exposed to moisture. Also, a high ratio of fines to asphalt may contribute to stripping, which is a type of moisture-induced failure.

2.3.1.4 Shape

Angular shaped particles provide greater aggregate interlock and internal friction than flat, thin or elongated particles. Thin, elongated aggregate particles break easily. Greater angularity also provides greater mechanical stability than rounder particles but the rounder particles offer better workability and require less compactive force to achieve the desired density. Asphalt pavements may continue to compact and increase in density under traffic loading.

2.3.1.5 Gradation

Aggregates used in asphalt mixtures are usually classified as coarse, fine or mineral fillers. The size limits for each of the three categories varies in each department or agency.

The gradation of an aggregate mix is the distribution of aggregate particle size determined by a sieve analysis. It is thought to be the most important properties of an aggregate mix (Roberts et al., 1996). The gradation of an aggregate mixture is important to ensure that the maximum aggregate size is not too small or too large, that the VMA requirements are met and that a satisfactory aggregate skeleton is obtained.

The gradation of an aggregate used in pavement design will affect many properties of the asphalt mixture, such as, stiffness, resistance, durability, permeability, workability, fatigue resistance, frictional resistance and resistance to moisture damage. The gradation used in an asphalt mix should be dense enough to achieve the desired density but also have enough voids to ensure adequate asphalt cement film thickness and to leave enough air voids to allow for future compaction from traffic and thermal expansion.

It has been reported that the asphalt film thickness is dependent upon the aggregate gradation (Stroup-Gardiner et al., 1995). The film thickness increased with an increase in the coarseness of the gradation, which had a smaller surface area. Without adequate film thickness, the asphalt cement may oxidize faster, the film will penetrate water easier and therefore the strength of the asphalt mixture decreases.

During the design process, a maximum aggregate size should be specified. If the maximum aggregate size is too small the mix may be unstable and if the maximum aggregate size it too large, workability and segregation may be a problem.

2.3.1.6 Specific Gravity

The specific gravity of an aggregate is useful when calculating the void content in a compacted asphalt mixture. It is the ratio of weight to volume, as shown in Equation 2.1.

$$specific\,gravity = \frac{weight}{volume(unit\,weight\,of\,water)} \qquad (2.1)$$

where

specific gravity is unitless

weight is in grams

$volume = \text{cm}^3$

$unit\ weight\ of\ water = 1\ \frac{g}{cm^3}$ (to be corrected for temperature)

The specific gravity can be expressed as the apparent, bulk effective and bulk impregnated specific gravity. The apparent specific gravity is only the volume of the aggregate particles. The bulk specific gravity used the overall volume of the aggregate particles and the volume of the pores that may be filled with water after a 24-hour soak. The effective and bulk impregnated specific gravity uses the overall volume of the aggregate particles and the pores that may be filled with water after a 24 hour soak, minus the large pores that absorb asphalt cement.

The effective specific gravity is dependant upon the degree to which the aggregate particles absorb asphalt cement. The effective specific gravity can be equal to or greater than the bulk specific gravity and equal to or lower than the apparent specific gravity.

2.3.2 Asphalt Binder Properties

The two main properties that the asphalt binder can possess are viscosity and penetration. Asphalt cement undergoes tests to determine the viscosity grade and penetration grade.

2.3.2.1 Viscosity

Viscosity is known as the resistance of a fluid to flow and can be defined as the ratio between the applied shear stress and the rate of shear. This measurement is called the coefficient of dynamic viscosity, which is the resistance to flow (Derucher et al, 1998). ASTM D3381-92 (1999) *Standard Specification for Viscosity-Graded Asphalt Cement for Use in Pavement Construction*, ASTM D2170-01a *Standard Test Method for Kinematic Viscosity of Asphalts (Bitumens),* and ASTM D2171-01 *Standard Test Method for Viscosity of Asphalts by Vacuum Capillary Viscometer* are standards that can be used to determine the viscosity. A fundamental approach is used when determining the viscosity of a binder and therefore is independent of the test system and sample size.

The absolute viscosity is determined at 60°C (140°F) to determine the properties of the pavement structure during the hot summer months. The kinematic viscosity is determined at 135°C (275°F)

to determine the properties during mixing and construction of the pavement structure. The temperature susceptibility of the asphalt binder can be determined through viscosity testing at multiple temperatures, representing a wide range of environments. Unfortunately low temperature performance is not adequately addressed.

2.3.2.2 Penetration

The penetration of asphalt cement is a measure of the consistency in terms of viscosity. ASTM D5-97, *Standard Test Method for Penetration of Bituminous Materials*, is the standard test method used to determine the penetration of the asphalt cement, and unfortunately is an empirical test and does not measure the consistency of the asphalt binder in fundamental units. The penetration of semisolid and solid bituminous materials is simply the measure of hardness or softness. Penetration grading is based on the binder temperature at 25°C (77°F), which is close to the average pavement temperature (Roberts et al., 1996). The temperature susceptibility of the asphalt binder can be determined by testing the binder over a range of temperatures, 4°C, 25°C, and 16°C (39.2°F, 60°F, 77°F).

2.3.2.3 Ductility

The ductility test is run in accordance with ASTM D113-99, *Standard Test Method for Ductility of Bituminous Materials*. The ductility of an asphalt binder is defined as the distance to which it will elongate before breaking when the two ends are pulled apart (see ASTM D113-99 for complete test procedures). The speed at which the specimen is pulled apart and the temperature are specified.

2.3.2.4 Aging

The short-term aging and long term aging of the asphalt cement is tested to determine the durability of the binder. Short-term aging is the hardening of the binder at a fast rate during the mixing, processing and construction period. Long-term aging is the ongoing hardening of the asphalt binder throughout its lifetime due to environmental and other factors at a slower rate. The long-term age hardening will be accelerated during the life of the pavement structure if the percent air voids are greater than the original design. This allows air, moisture and light to enter the pavement structure and causes oxidation to take place.

2.3.2.5 Temperature Susceptibility

Asphalt binder properties play an important roll in the reaction of the asphalt mixture to temperature. Temperature susceptibility is the rate in which the consistency of the asphalt binder changes with temperature. Asphalt cements with high susceptibility to temperature are not desirable.

Stroup-Gardiner et al. (1995) reported that temperature susceptibility became more project-specific as the coarseness of the aggregate gradation increased. Temperature affects the elastic and viscoelastic properties of an asphalt concrete mixture. The modulus of the asphalt is dependent upon the pavement temperature; with an increase in temperature there is a decrease in asphalt modulus. The susceptibility to temperature is a property of the asphalt binder and can be evaluated by evaluating the change in stiffness with temperature.

2.3.3 Mixture Properties

Pavement performance is greatly influenced by the interaction between the asphalt cement and aggregate. The mix design should be developed to resist the distresses that have been addressed in Section 2.2.2, be durable, resist moisture induced damage, and provide a safe pavement during normal turning and braking.

2.3.3.1 Material Properties

Air Voids

The percent of air voids in an asphalt mixture will decrease as the asphalt content increases, in turn, affecting the performance of the pavement structure. If the percent air voids is too low, then plastic flow may take place that can result in rutting. On the other hand, if the percent air voids is high, the mix will be permeable to air and water. This will accelerate the rate of oxidation of the asphalt binder and may result in premature cracking or raveling.

A high percent air voids will also decrease the expected life of the asphalt concrete layer (Mahoney and Newcomb, 1990). The effective thickness of the asphalt concrete layer is the thickness of the asphalt that is used to calculate the life of a pavement structure. Finn and Epps

(1980) showed that the effective thickness decreases with an increase of air voids. Table 2.1 shows 4-inch and 6-inch thick asphalt concrete at a starting point of 7% air voids, as highlighted. As the air voids increase to 12%, the effectiveness of the 4 and 6-inch thick pavement decreases to 2 and 4 inches, respectively.

Table 2.1 Air Voids versus Effectiveness Thickness Asphalt Concrete
(Finn and Epps, 1980)

Asphalt Concrete Air Voids (%)	4" @ 7% Air Voids	6" @ 7% Air Voids
7	4.0	6.0
8	3.5	5.0
9	3.0	4.5
10	2.5	4.0
12	2.0	4.0

In summary, Table 2.1 indicates that if a 4-inch thick asphalt concrete layer were only compacted to 12% air voids, then it would only effectively last as long a 2-inch thick asphalt concrete layer.

Theoretical Maximum Specific Gravity

The theoretical maximum specific gravity is the ratio of the weight in air of a unit volume of an uncompacted bituminous paving mixture to the weight of an equal volume of gas free distilled water at the same temperature. The standard test method used is ASTM D2041-00, *Standard Test Method for Theoretical Maximum Specific Gravity and Density of Bituminous Paving Mixtures.* The desired density of a mixture is often stated in terms of a percent of the theoretical maximum specific gravity.

Density

The field density is usually expressed as a percent of the theoretical maximum density. The density can be increased by increased compaction, increased asphalt content (to an optimum percent), increase filler content, or other available methods to reduce the voids in the mixture. These methods to increase the density of a mixture may not have a positive affect on the performance. Initially, when the asphalt content is increased there is an increase in density. The density will reach a peak with an optimum asphalt content. As the asphalt content continues to

increase, there is an increase in film thickness around each individual aggregate particle pushing the particle farther away from one another. This decreases the density of the asphalt mixture because lighter asphalt replaces some of the aggregates (Atkins, 1997).

The theoretical maximum density must be such that when the asphalt mixture is properly compacted there are still voids left to compact by traffic loading and room for thermal expansion.

2.3.3.2 Strength

Great strides have been made to understand the behaviour of bituminous mixtures and the many factors that affect their performance. The structural performance of a pavement is dependant upon its ability to distribute stresses, resist permanent deformations, resist cracking, and the ability to resist moisture damage (Epps et al., 2000). These factors are related to the materials, environment, load and construction process.

The stiffness, or modulus, of an asphalt mixture is an indicator of quality for the mixture design process or pavement evaluation and analysis. There has been much work done to relate the stiffness of an asphalt mix to field performance. The stiffness of a mixture is dependent on many variables, which include temperature, load frequency and stress state which can be determined through various test methods. The stiffness of an asphalt mix can be defined as the ratio of the stress to strain as a function of loading and temperature, as shown by Equation 2.2.

$$S(t,T) = \frac{\sigma}{\varepsilon} \qquad (2.2)$$

where

S = stiffness

t = time

T = temperature

σ = stress

ε = strain

The stiffness of a mix can be increased or decreased by altering the mixture gradation, asphalt content, air voids, filler content and binder type. An asphalt mix with a high modulus value will be stiffer and is more resistant to deformation than an asphalt mix with a low modulus value, but will be more susceptible to thermal and fatigue cracking (AASHTO, 1993).

The compressive and tensile response of an asphalt mix are expected to be different. Aggregate interlock and the stiffness of the asphalt binder both contribute to the compressive strength of the asphalt pavement. The tensile strength of an asphalt mix is primarily dependent on the stiffness of the asphalt binder. Studies have shown that the difference between the compressive and tensile strength is different at different temperatures due to the fact that the asphalt binder stiffness is largely sensitive to temperature and the aggregate stiffness is not (Khanal and Mamlouk, 1995).

2.3.3.3 Viscoelastic behaviour

Asphalt mixtures possess both elastic properties of a solid and the viscous properties of a liquid. The behaviour of viscoelastic materials is time dependent. This means that the longer the time, the more flow. Looking at the properties of hot mix asphalt, when there is a longer loading time, the mixture acts more viscous. There is no general theoretical method of determining the viscosity of asphalt mixtures for a wide range of environmental conditions found in literature (Collop et al., 1995).

One method that has been used to characterize viscoelastic materials is by the use of creep compliance curves at various times. The creep compliance is defined as the time-dependent strain under constant stress, as shown in Equation 2.3:

$$D(t) = \frac{\varepsilon(t)}{\sigma} \qquad (2.3)$$

where

D = creep compliance

ε = strain

σ = stress

Poisson's ratio has a very small effect on the behaviour of the pavement and therefore is assumed to be elastic and independent of time. On the other hand, the modulus is considered to be viscoelastic and time dependent.

2.3.3.4 Durability

The durability of an asphalt mix refers to the ability to resist the environmental effects of air and moisture. Moisture damage to asphalt pavements is a serious durability problem throughout

Canada (Emery and Seddik, 1997). Factors that accelerate the deterioration of an asphalt pavement are traffic, weather, change in pavement stresses, temperature and moisture conditions. The rate of deterioration in serviceability should be minimized to ensure the most cost-effective life-cycle performance from design, construction and maintenance perspectives.

The extent of degradation or disintegration of an aggregate caused by the freeze-thaw cycle, moisture or traffic loading will indicate the durability of an asphalt mixture. Moisture affects the stiffness of a mix adversely by the stripping of the binder from the aggregate. Moisture conditioning accelerates the damage to the mix caused by water.

There are two moisture damage tests that are widely used: AASTHO T283-98 *Resistance of Compacted Bituminous Mixture to Moisture Induced Damage* and ASTM D4867/D4867M-96, *Standard Test Method for Effect of Moisture on Asphalt Concrete Paving Mixtures*, also known as Tunnicliff-Root method. These are laboratory tests indicating the stripping potential of an aggregate in an-asphalt cement mixture.

Over the years, liquid anti-strip additives or hydrated lime have been added to asphalt concrete to mitigate moisture damage. These methods of reducing moisture related problems have been successful but require plant modifications and additional worker and environmental safety considerations (Stroup-Gardiner et al., 1995). A more desirable approach is to recommend alternative mix design procedures and parameters that are related to the durability, such as asphalt film thickness.

Asphalt Film Thickness

Various studies have shown that the durability of an asphalt mix is directly related to the film thickness but usually not directly considered as part of mixture design (Roberts et al., 1996). Thicker binder film increases the durability by decreasing the permeability of the mixture to air and water.

It has been recognized that a dense graded asphalt mix that has a thick asphalt film is more flexible and durable (Kandhal et al., 1998). On the other hand, a dense graded asphalt mixture with a thin asphalt film will produce a mix that is brittle, susceptible to cracking and ravels excessively. The thin asphalt film thickness is the cause of high air voids and high permeability

leading to oxidation and premature distresses, which contribute to lack of durability of the asphalt mix (Kandhal & Chakraborty, 1996).

All particles in the same mix will not have the same asphalt film thickness, as the film around an aggregate particle is a function of the diameter of the aggregate and the percent asphalt cement in the mixture. In the early 1930s, Hveem initially assumed that each aggregate particle had the same film thickness. He later discovered that the film thickness decreased as the diameter of the particle decreased and presented Equation 2.4 to calculate it (Roberts et al., 1996).

$$T_F = \frac{V_{asp}}{SA * W} * 1000 = \frac{Pbe}{SA} * Gb * 1000 \qquad (2.4)$$

where

T_F = average film thickness (microns)

V_{asp} = effective volume of asphalt cement (liters)

SA = surface area of the aggregate (m^2 per kg of aggregate)

W = weight of aggregate (kg)

Pbe = effective binder content by weight of mixture (percent)

Gb = specific gravity of the asphalt

Asphalt particles may possess the same effective film thickness but require more or less asphalt binder, depending on the absorptive properties of the aggregate, as shown in Figure 2.3 (Nukunya et al., 2002). The effective volume of asphalt cement is defined as the binder that is available to coat the aggregate particles and does not include the asphalt binder that has been absorbed by the aggregate particles.

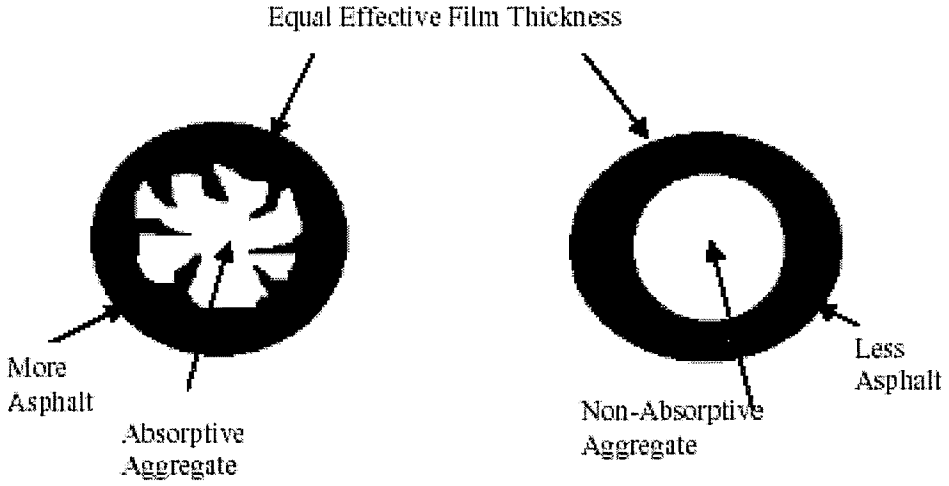

Figure 2.3 Schematic of Absorptive and Non-absorptive Aggregates

In contrast to Hveem, Kandhal et al. (1998) found that fine aggregate particles have a thicker asphalt film thickness compared to coarse grain aggregate particles. Other researches have presented different methods to determine the effective film thickness of mixtures. One method is based on the fine aggregate of the mixture as shown by Equation 2.5 (Nukunya et al., 2002). The fine aggregate portion of a mixture is defined as the percent aggregates passing the # 8 (2.36 mm) sieve.

$$T_f = \frac{V_{be}}{SA * W_T * PF_{Agg}} = \left[\frac{Pb - \left(\frac{Abs}{100} \right) * P_{Agg}}{SA * PF_{Agg} * G_b} \right] * 1000 \qquad (2.5)$$

where

P_{Agg} = Percent aggregate by mass of total mixture

PF_{Agg} = Percent fine aggregate by mass of total mixture

V_{be} = Effective volume of asphalt

SA = Surface area (m^2/kg of aggregate)

Pb = asphalt content percent by mass of total mixture

Abs = absorption

G_b = specific gravity of asphalt

The asphalt film thickness is of great interest when meeting the VMA requirements of an asphalt mix design criterion. Currently, the conventional method to determine the asphalt film thickness does not take into account the degree of compaction (Radovskiy, 2003). Figure 2.4 represents the film thickness calculated after compaction, termed the 'separating film'.

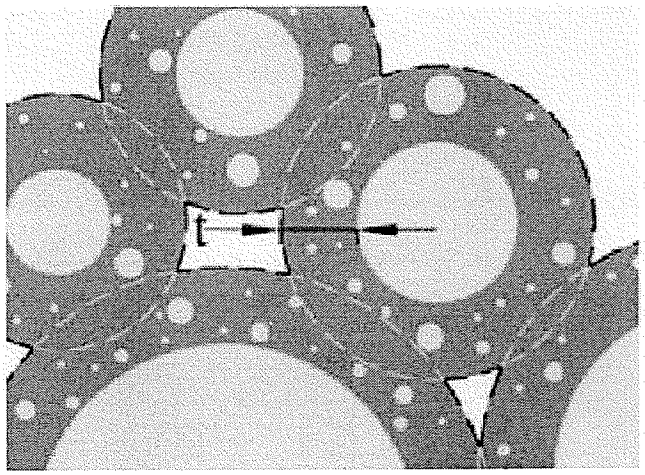

Figure 2.4 Film Thickness
Proposed by Nukunya et al. (2002)

The separating film thickness, t, represents the smallest distance from the outer edge of an aggregate particle to the air void. The film thickness is then assumed to be the same for all particles. When the diameter of the aggregate particle becomes smaller than the defined film thickness, it is assumed the particle to be embedded within the binder material.

2.4 Laboratory Test Methods

In the laboratory, many different modes of loading have been used to determine the material properties of asphalt. Direct tension, indirect tension, direct compression, and a combination of tension and compression have been used.

The indirect diametral tension and the triaxial compression have been considered to be the simplest, most practical, and most economical test methods to determine various properties of an asphalt mixture. Generally, the indirect diametral tension test is used for bound materials while the triaxial compression is used for unbound materials. The indirect diametral tension test will only be discussed in this thesis, as no testing was conducted on unbound materials.

Over the years, there have been a number of tests that have been used to determine the resilient modulus of asphalt concrete in the laboratory. The following four tests are repeated load tests that have been used (Vinson, 1990):

1) Direct tension
2) Beam flexure (bending or rotating cantilever)
3) Indirect diametral tension
4) Triaxial compression

2.4.1 Indirect Tensile Test

The indirect tensile test has been widely used to determine the structural properties of an asphalt mixture through laboratory testing (Mohammad and Paul, 1993). This test has the ability to determine the tensile strength, resilient modulus and creep compliance of an asphalt sample using three different loading modes. The tensile strength of the asphalt mixture can be determined by applying a load at a predetermined rate, the resilient modulus can be determined through the use of dynamic loading and the creep compliance can be determined by loading the specimen with a constant load.

The indirect tensile test is closely related to the field conditions under the wheel path, as shown by Figure 2.5. When the wheel path is loaded, the asphalt material just outside the wheel path experiences an outward lateral movement due to the vertical compressive force. The lateral movement is resisted by an equal and opposite confining pressure imposed on the material directly below the wheel path, as shown by Figure 2.5. If the asphalt concrete around the wheel path is weak, over time the asphalt concrete may experience plastic flow, resulting in rutting.

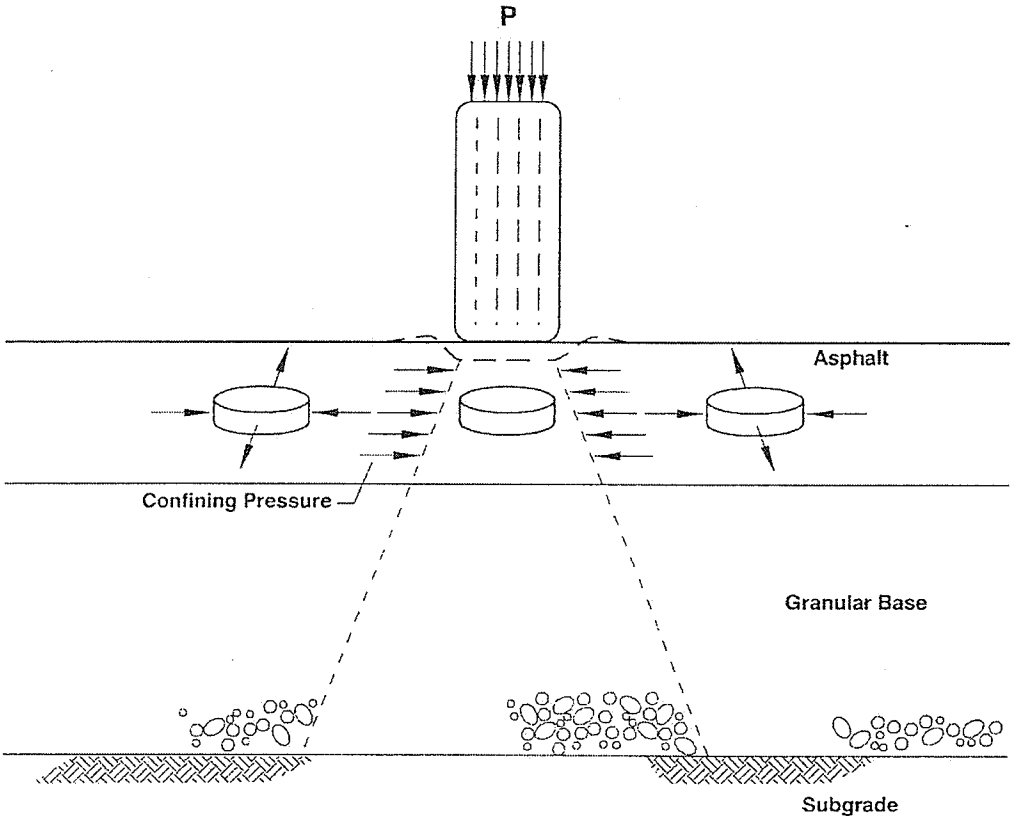

Figure 2.5 Relationship of IDT Test to Field Conditions *(Thiessen, 2001)*

Figure 2.6 illustrates the basic loading configuration of the indirect tensile test. A load is applied along the vertical axis, creating a compressive load parallel to the vertical axis. The curved loading strips are used to reduce the vertical compressive stresses experienced at the point of loading. A uniform stress is developed along the vertical axis of the specimen causing failure along the vertical plane, as shown by Figure 2.6. Following ASTM D4123-82 (1995), *Standard Test Method for Indirect Tensile Test for Resilient Modulus of Bituminous Mixtures*, diametral testing provides an estimate of the material properties at the inner portion of the asphalt core.

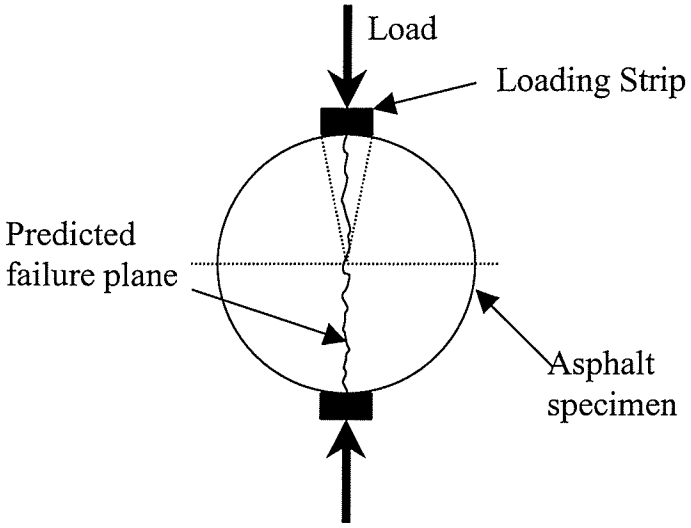

Figure 2.6 Basic Loading Configuration

Consensus as to where the vertical and horizontal measurements should be taken has changed over the years. In the early years of testing, it was suggested to place the LVDTs in contact with the edge of the sample surface. Some variations of this placement of the LVDTs also included having a thin membrane placed between the LVDT and the asphalt sample, such as paper or aluminum foil. This was done because it was thought that the LVDT may be placed in a small depression on the sample and would alter the resilient modulus, increasing the error (Brown and Foo, 1989). Wallace and Monismith (1980) have concluded that 80 percent of the diametral deformation occurs within the inner 63.5 mm (2.5 inch) of a 100 mm (4 inch) diameter specimen. In recent studies, the practice was to capture the deformations at the center of the specimen (FHWA, 2001).

2.4.1.1 Stresses

Compressive strength is developed in the asphalt mixture when subjected to compression due to the interlocking of the aggregate particles and the stiffness of the asphalt binder. When the asphalt mixture is subjected to tension, it is the binder that resists the tensile stresses. There is little, if any, aggregate interlock when the asphalt mix is in tension. The asphalt mixture will behave different under compressive and tensile stresses and at different temperatures due to the temperature sensitivity of the asphalt binder. Figure 2.7 represents an asphalt specimen under diametral loading.

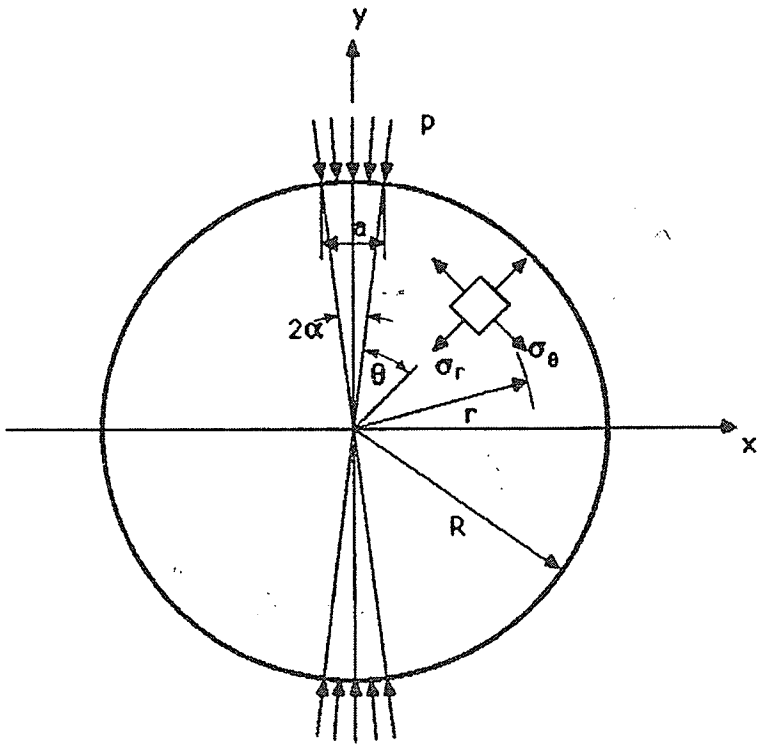

Figure 2.7 Definition Sketch of a Diametrally Loaded Circular Element *(FHWA, 1990)*

Four stresses (radial stress along the vertical axis, radial stress along the horizontal axis, tangential stress along the vertical axis, tangential stress along the horizontal axis) are created by the load and can be calculated from Equation 2.6.

$$\sigma = \pm \frac{2P}{\pi a t}[f(r, R, \alpha)] \qquad (2.6)$$

where

P = load

a = width of loading strip

t = thickness of asphalt sample

r = radius from origin to point of interest

R = radius of asphalt samples

2α = angle at origin subtended by the width of the loading section

It is assumed that the specimen is subjected to plane stress ($\sigma_z = 0$), the material is linear elastic, homogeneous, and isotropic, and the load applied to the specimen is a line load. Poisson's ratio must also be known, but when it is not known, then a value of 0.35 is assumed for asphaltic material. The following equations (Wallace & Monismith, 1980) can be used to calculate the

maximum horizontal stress, $\sigma_{x(max)}$, minimum vertical stress, $\sigma_{y(min)}$, and the corresponding average stresses when the above mentioned factors are satisfied:

maximum horizontal stress $$\sigma_{x_{max}} = \frac{2P}{\pi dt} \quad (2.7)$$

minimum vertical stress $$\sigma_{y_{min}} = \frac{-6P}{\pi dt} \quad (2.8)$$

average horizontal stress $$\overline{\sigma}_x = \frac{0.273P}{dt} \quad (2.9)$$

average vertical stress $$\overline{\sigma}_y = \frac{-P}{dt} \quad (2.10)$$

where

d = specimen diameter (mm)

t = specimen thickness (mm)

P = load (N)

During the indirect tensile test, the true stress-strain response of the material can be captured during loading. The strain experienced by the asphalt core can be measured at the center of the sample. The stress analysis assumes a perfectly elastic, homogeneous, isotropic and weightless circular element. The horizontal strain can be calculated from Equation 2.11.

$$\overline{\varepsilon}_x = \frac{\overline{\sigma}_x}{E} - \upsilon\frac{\overline{\sigma}_y}{E} = \frac{0.273P}{Et} + \frac{\upsilon P}{Edt} \quad (2.11)$$

where

ε_x = horizontal strain (mm/mm)

E = Young's modulus (kPa)

ν = Poisson's ratio (usually assumed to be 0.35)

The deformation experienced by the specimen is equal to the horizontal strain times the diameter, as shown in Equation 2.12.

$$\Delta = \overline{\varepsilon}_x d = \frac{0.273P}{Et} + \frac{\upsilon P}{Et} \quad (2.12)$$

By rearranging Equation 2.12, Young's modulus can be calculated from Equation 2.13.

$$E = \frac{P}{\Delta t}(0.273 + \upsilon) \quad (2.13)$$

When Young's modulus is calculated using Equations 2.7 through 2.13 then it is said to be the resilient modulus of the material (Wallace and Monismith, 1980).

Figure 2.8 represents the stress distribution that develops in the asphalt specimen during the indirect tensile test. The stresses shown in Figure 2.8 are only valid if the thickness of the specimen is small compared to the diameter. Due to the use of the loading strips, the stress changes from compression to tension in the lateral direction along the y-axis. The magnitude of the lateral tensile stresses are virtually unaffected by the loading strips at the center of the asphalt specimen. Therefore it has been suggested to record the deformations at the center of the specimen.

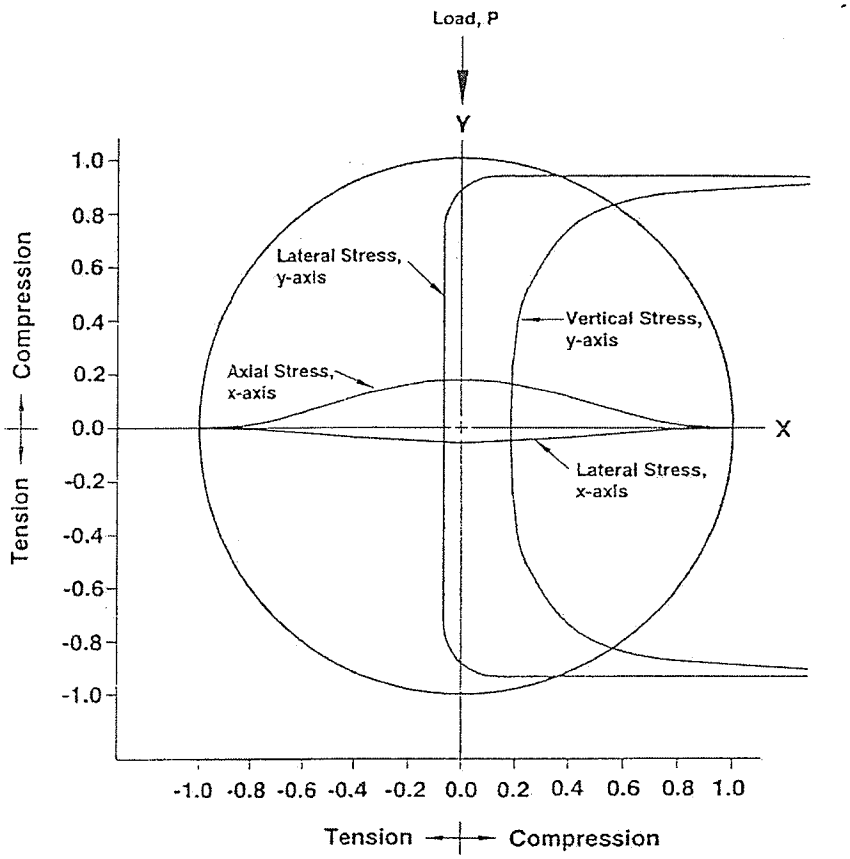

Figure 2.8 Relative Stress Distributions of the Indirect Tensile Test
(Mamlouk and Sarofim, 1998)

2.4.1.2 Static Indirect Tensile Test

In accordance to ASTM D4123-82 (1995) the tensile stress characteristics of an asphalt mixture can be determined by applying a diametral load to the specimen at a constant rate, or static

loading. The static indirect tensile test has many advantages, as determined by Kennedy and Hudson (1968).

- Relatively simple and quick test to perform
- Equipment is generally available
- Failure is not significantly affected by the surface conditions
- Failure is initiated in a region of relatively uniform tensile stress
- The test has a low coefficient of variance
- The test provides information to calculate the tensile strength, modulus of elasticity, and Poisson's ratio
- The test captures the stress-strain response of the material.

Rutgers Asphalt Pavement Laboratory at the State University of New Jersey has used the static indirect tensile test as a predictive model to determine fatigue and low temperature cracking characteristics, which are strain failures. Asphalt mixtures that can tolerate high strains prior to failure have a higher resistance to cracking than an asphalt that cannot tolerate high strains. A load of 12.5 mm/min at temperatures of –20, -10 and 0°C were used to determined the low temperature cracking and a load rate of 50 mm/min at temperatures of –10, 4 and 20°C were used to test for fatigue cracking.

The tensile strength, S_T, can be calculated according to ASTM D4123-82 (1995) from Equation 2.14.

$$S_T = \frac{2 P_{ult}}{\pi t D} \qquad (2.14)$$

where

P_{ult} = ultimate applied load (N)

t = thickness of specimen (mm)

D = diameter of specimen (mm)

Moisture Susceptibility

The tensile strength is often used to evaluate the water susceptibility of an asphalt mixture. The two commonly used moisture susceptibility tests being used by highway departments are AASHTO T283-89 Standard Method of Test for *Resistance of Compacted Bituminous Mixture to*

Moisture Induced Damage and ASTM D4867/D4867M-96. The test evaluates the moisture susceptibly of the asphalt mixture with the use of the tensile strength test. The tensile strength of the conditioned samples is compared to that of the samples that are not conditioned. A loss of strength in the conditioned samples exhibits the damage, the loss of cohesion and adhesion due to moisture.

Both standard test methods have test value ranges for the degree of saturation and the air voids. Equation 2.15 shows that the tensile strength ratio varies with a change in air voids and degree of saturation (Khosla et al., 2000). Some test samples that were at the higher limit of saturation and air voids failed the criterion while samples from the same test sample passed at lower saturation and air void levels. The variability of these two factors will affect the reliability of the test results.

$$TSR = \frac{S_m}{S_d} \times 100 \qquad (2.15)$$

where

TSR = tensile strength ratio

S_m = average tensile strength of moisture conditioned sample

S_d = average tensile strength of unconditioned (dry) sample

2.4.1.3 Dynamic Indirect Tensile Test

Dynamic loading, in the form of a haversine wave, is used to simulate moving traffic load over a pavement structure in the laboratory. Figure 2.9 shows the stresses and strains that are developed during the loading and unloading of an asphalt pavement caused by moving traffic (Khanal and Mamlouk, 1995). The figure indicates that pavement layers are mainly subjected to vertical compressive stress while tensile stresses are developed at the bottom of the stiff layers.

At a point in a pavement structure, the magnitude of the load increases from zero when the load is far away from the point, to a peak value when the load is directly over the point. The magnitude of the load will then decrease as the moving load departs from the point. The point will experience a period of relaxation before the onset of the sequential moving load from the following wheel. This will cause the point to experience the dynamic load and unload cycle to be repeatedly.

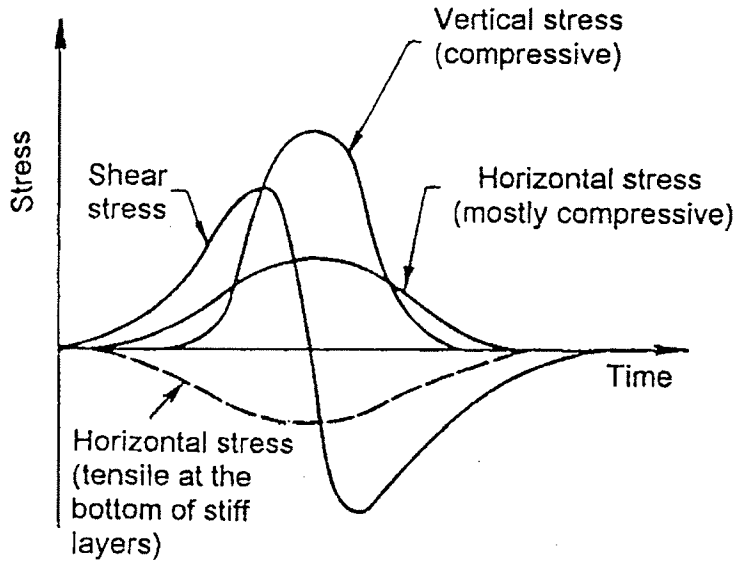

Figure 2.9 Pattern of Stresses and Strains Developed in the Pavement System Under a Wheel Load Moving on a Smooth Pavement Surface *(Khanal and Momlouk, 1995)*

The tensile strain at the center of the specimen is calculated using Equation 2.16.

$$\varepsilon_t = \left[\frac{0.16 + 0.49\upsilon}{0.27 + \upsilon}\right] H \qquad (2.16)$$

where

ε_t = tensile strain at the center of the specimen (microstrain)

υ = Poisson's ratio

Poisson's ratio can also be calculated if vertical strains were recorded during testing, as shown in Equation 2.17.

$$\upsilon = \frac{-3.50 - 0.27\left(\frac{V}{H}\right)}{0.063 + \left(\frac{V}{H}\right)} \qquad (2.17)$$

where

V = total recoverable vertical deformation

H = total recoverable horizontal deformation

The pulse-rest loading sequence used to simulate moving traffic over a pavement structure consists of haversine loading of a duration of $2d$ followed by a rest period, as illustrated by Equations 2.18 and 2.19 (Drescher et al., 1997).

$$P(t) = P_1 - P_0 \cos\frac{\pi}{d}t \qquad (pulse) \qquad (2.18)$$

$$P(t) = 0 \qquad (rest) \qquad (2.19)$$

The unloading portion of the loading-unloading cycle, the sample rebounds in accordance with the viscoelastic properties of the mix (Qi and Witczak, 1998). It has been suggested that when using a pulse-rest loading sequence, determining the viscoelastic properties of the asphalt concrete is impractical, near almost impossible (Drescher et al., 1997).

Resilient Modulus

H. C. Seed first introduced the resilient modulus in the 1960s. The resilient modulus is defined as the ratio between an applied stress and the recoverable strain that takes place after the applied stress has been removed and a specified time has passed (Fairhurst et al., 1990). The resilient modulus can be used to estimate the response of a pavement structure due to traffic loads or in pavement design procedures.

The lateral constraint experienced by the asphalt pavement for in-situ conditions varies when the structure is vertically loaded. When tested in the laboratory, asphalt specimens are not laterally constrained and therefore the resilient modulus values determined in the laboratory may be lower than the in-situ resilient modulus values (Fairhurst et al., 1995).

In 1972 Schmidt was the first to propose the use of repeated load and the indirect diametral tension test to determine the resilient modulus of asphalt concrete in the laboratory. Figure 2.10 illustrates the stress-strain relationship experienced by the asphalt specimen (a plastic material) from one load cycle.

The stress-strain relationship in the linear portion of the loading cycle is used to calculate the elastic modulus. Beyond the elastic range of the material and removal of the load, the material will experience plastic deformations. The resilient modulus is calculated from the unloading portion of the load-unload cycle.

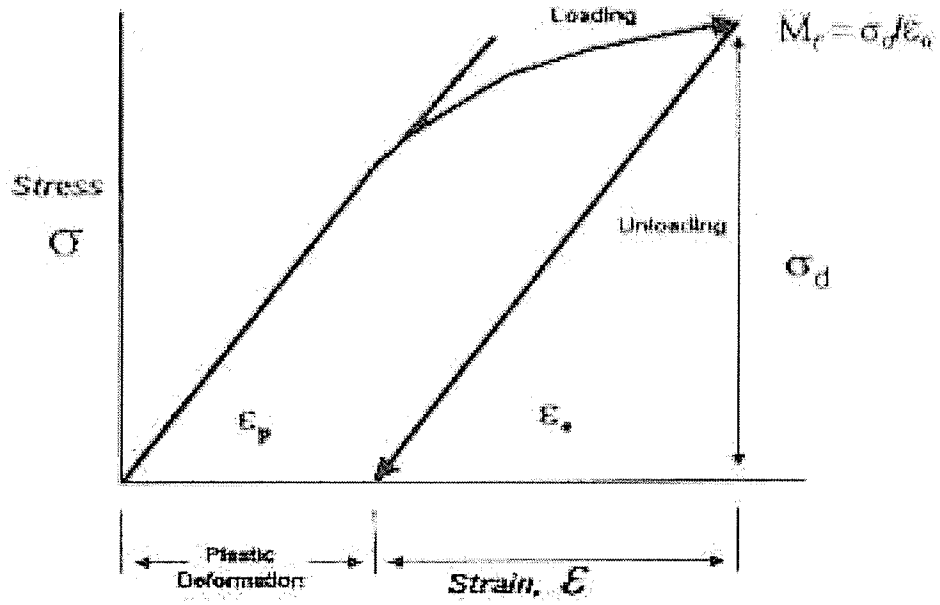

Figure 2.10 Stress and Strain During Loading and Unloading of a Plastic Material *(ERES, 2001)*

Equation 2.20 was used to calculate the resilient modulus of the specimen (Vinson, 1990).

$$M_R = \frac{P}{Ht}(\upsilon + 0.27) \qquad (2.20)$$

where

M_R = resilient modulus

P = repeated load

H = total recoverable horizontal deflection

t = specimen thickness

υ = Poisson's ratio

Poisson's ratio is usually assumed to be 0.35. When not assumed, Poisson's ratio can be calculated from Equation 2.21 (ASTM D4123-82 1995).

$$\upsilon = 3.59\frac{\Delta H_t}{\Delta V_t} - 0.27 \qquad (2.21)$$

where

ΔH_t = horizontal deformation

ΔV_t = vertical deformation

From substitution of Equation 2.21 into Equation 2.20, the resilient modulus can then be calculated from Equation 2.22 (Farihurst et al., 1990).

$$M_r = \frac{3.59P}{t\Delta V_t} \qquad (2.22)$$

It is apparent from Equation 2.22 that the horizontal deformation can be an unknown if the Poisson's ratio is known.

In the laboratory, ASTM D4123-82 (1995) and LTPP Protocol P07 were used to determine the resilient modulus, M_R, of the asphalt mixtures through the use of the indirect tensile test and dynamic loading. The resilient modulus value calculated from the laboratory test outlines in LTPP Protocol P07 is a measure of the elastic modulus of the asphalt mixture recognizing certain nonlinear characteristics. The dynamic loading is in the form of a haversine wave shaped load pulse and can be applied over a range of load durations, load magnitudes and rest periods. Equation 2.23 is proposed in LTPP Protocol P07.

$$M_r\{I,T\}_j = \frac{lP_{avg_j}}{\Delta H\{I,T\}n_{avg_j} d_{avg} t_{avg} Cmr\{I,T\}} \qquad (2.23)$$

where

$M_r\{I,T\}$ = instantaneous or total resilient modulus (MPa)

l = gauge length (mm)

P_{avg} = average cyclic load (N)

$\Delta H\{I,T\}n_{avgj}$ = average instantaneous or total horizontal deformation (mm)

d_{avg} = average specimen diameter (mm)

t_{avg} = average specimen thickness (mm)

$Cmr\{I,T\}$ = resilient modulus correction factor

j = cycle number

The resilient modulus correction factor, *Cmr*, is calculated from Equation 2.24.

$$Cmr\{I,T\} = 0.6345 * \left(\frac{\Delta V\{I,T\}ncycleavg}{\Delta H\{I,T\}ncycleavg}\right) - 0.332 \qquad (2.24)$$

where

$\Delta V\{I,T\}ncycleavg$ = average vertical cycle deformations

$\Delta H\{I,T\}ncycleavg$ = average horizontal cycle deformations

Previous research has found the repeatability of the resilient modulus test, following ASTM D4123-82 (1995) to be low (Brown and Foo, 1989). It was found that the resilient modulus is stress sensitive and therefore it was recommended that the stress should be specified in the test procedure. There was also a greater variance in the resilient modulus values of field samples than with laboratory samples. Some studies have concluded that determining the resilient modulus in accordance with ASTM D4123-82 (1995) does not have a high degree of precision (Brown and Foo, 1989). Factors such as local segregation and the presence of larger aggregates may affect the results from diametral testing (Wallace and Monismith, 1980). Other factors such as the indirect tensile device, deformation measurement system and the operator could significantly affect the results and therefore the asphalt mixture should be tested under the same conditions.

Khanal and Mamlouk (1995) compared the compressive and tensile resilient modulus. From the literature review, it was found that the compressive strength of asphalt concrete was ten times the tensile strength and the dynamic modulus of asphalt concrete in tension was half of the dynamic modulus in compression. The difference between the compressive and tensile modulus values varies as the temperature changes (Khanal and Mamlouk, 1995). For lower temperatures (for example, 5°C), asphalt concrete has similar compressive and tensile modulus values. At higher temperatures (for example, 40°C), the difference between the compressive and tensile modulus values is more significant and it was found that the tensile modulus was always lower than the compressive modulus.

Instantaneous and Total Deformations

The instantaneous and total horizontal deformations are recorded and used to calculate the instantaneous and total resilient modulus values. The instantaneous resilient modulus more accurately represents elastic theory than the total resilient modulus (Mamlouk and Sarofim, 1988). The instantaneous values measure the recoverable or elastic deformations while the total values take into account the permanent deformations. It has been stated that the deviation from perfect elasticity of the asphalt concrete mixture is simplified by determining two resilient modulus values, the instantaneous resilient modulus and the total resilient modulus (Drescher et al., 1997).

Poisson's ratio can be calculated using measured recoverable vertical and horizontal deformations. This test is performed over a range of temperatures and stresses to simulate

moving vehicles over the pavement structure and the service life of the pavement. Calculating a range of resilient modulus values at different temperatures and frequencies of loading can be designed into a master curve for characterizing asphalt concrete for pavement thickness design and performance analysis (Barksdale et al, 1997).

2.4.1.4 Factors Influencing the Dynamic Resilient Modulus

Throughout the literature review it was found that many test procedures can influence the resilient modulus values obtained from laboratory compacted samples, including test temperature, load frequency, load duration, time allowed for recovery between loading cycles and the load-induced diametral strain level. Due to these influencing factors, clear, precise guidelines must be established to ensure that the laboratory test results can be comparable (Fairhurst et al., 1995). Currently, there are two standards that are available to follow to determine the resilient modulus of a mix in the laboratory, ASTM D4123-82 (1995) and LTPP Protocol P07. A comparison between the two standards is shown in Table 2.2.

Table 2.2 Resilient Modulus Test Conditions

Test Procedure / Test Condition	**ASTM D4123-82**	**LTPP Protocol P07**
Temperature	5, 25, and 40°C	5, 25, and 40°C
Load Duration	0.1 to 0.4 seconds	0.1 seconds
Load Frequency	0.33, 0.5 and 1.0 Hz	1.0 Hz
Load/Strain Level	induce 10 to 50 % of the indirect tensile strength	range between 0.038 and 0.089 mm
Contact Load	3 to 5 % of the maximum load	10 % of the maximum load

ASTM D4123-82 (1995) requires that the sample be pre-conditioned. To pre-condition the sample, a pre-load (contact load) of approximately 3-5% of the maximum load is applied to the specimen. This load is maintained on the sample until the rate of deformation is constant. When five consecutive cycle deformations are measured and are less than 2% change, conditioning is complete and recording of data commences. ASTM D4123-82 (1995) also recommends the specimens to be tested at 0° and then rotated 90°.

Temperature

The resilient modulus of the asphalt specimen is highly dependent on the temperature due to the material properties of the mix. The asphalt mix will show a decrease in modulus as the temperature increases. The resilient modulus of different mixes will decrease at different rates (Boudreau et al., 1992). As the temperature increases, so does the ductility of the asphalt binder, decreasing the strength of the asphalt mix.

Stress State

The stiffness of an asphalt cement mixture may be more influenced by the stress state at higher temperatures (example, above 25°C) because of the decrease in stiffness of the binder (Monismith, 1990). At lower temperature, below 25°C, the asphalt mixture can be considered independent of stress state.

Material Properties

The material properties of the asphalt mix will affect the resilient modulus values obtained through dynamic loading and unloading. As the air voids of an asphalt mix increase, the resilient modulus values decrease. Other studies have shown that with an increase of asphalt content, the resilient modulus value decreased (Almudaiheem and Al-Sugair, 1991). The differences between asphalt concrete mixtures, (i.e. air voids, aggregate type and additive type), is more apparent at the 5°C temperature than at the higher temperatures. This is a greater variance of the resilient modulus values from the different asphalt mixtures at 5°C. Studies have shown a high degree of material sensitivity at 5°C and a low degree at 25°C (Boudreau et al., 1992). The stiffness of a mix is dependant on binder and mix rheology, the relative amount of elastic, delayed elastic and viscous response (Roque et al., 1998).

Specimen Diameter

It should be noted that the diameter of the asphalt core tested might affect the resilient modulus values obtained from dynamic testing (Barksdale et al., 1997). It is shown in Figure 2.11 that the 4-inch (100 mm) diameter specimens have greater resilient moduli values than the 6-inch (150 mm) diameter cores.

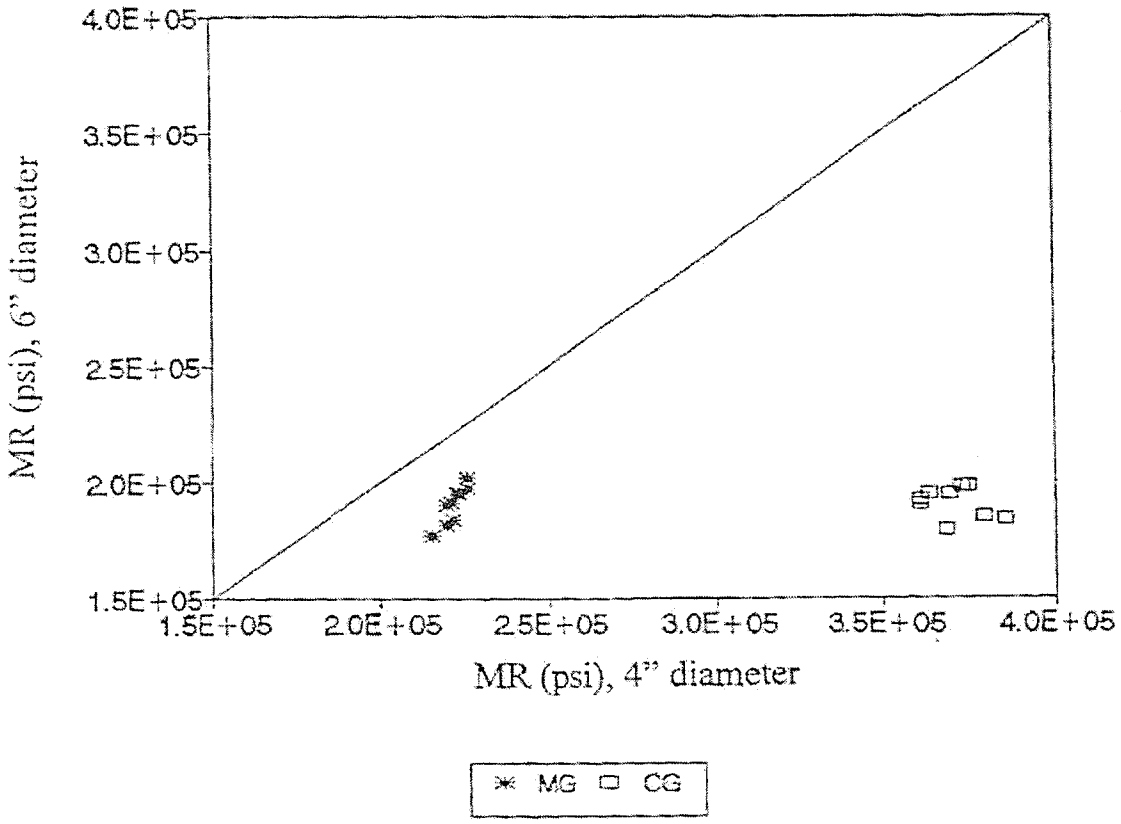

Figure 2.11 Effect of Specimen Diameter on M_R, for Stage 2 tests at 104°F
(Barksdale et al., 1997)

At lower temperatures the diameter does not affect the resilient modulus as much as at the higher testing temperatures (Barksdale et al., 1997). At higher temperatures, the asphalt mix shows more non-homogeneity, which causes the increase in diameter to decrease the resilient modulus due to the aggregate size to diameter ratio.

Specimen Thickness

In early studies, it has been recommended that the thickness of a 100 mm (4 inch) diameter sample be at least 50 mm (2 inches) for aggregates up to 25 mm (1 inch) maximum size (Vinson, 1990). For aggregates up to 38 mm (1.5 inches), it is recommended that a 150 mm (6 inch) diameter core be used with a minimum thickness of 75 mm (3 inches). LTPP Protocol P07 now recommends a thickness range of 25 to 50 mm (1 to 2 inches) for the 100 mm (4 inch) diameter core, but does not state a range for the 150 mm (6 inch) diameter core.

Load or Cycle Frequency

Fairhurst et al. (1990) indicated that the resilient modulus slightly increases with increasing load cycle frequency. A higher load cycle frequency results in a shorter rest period and a shorter time for recovery of strains to take place, resulting in higher resilient modulus values.

Load Duration

Studies have shown that at the 5°C test temperature that asphalt specimens act like an elastic material and therefore there is little affect by the load duration on the resilient modulus. It has been found that a greater loading duration considerably reduces the resilient modulus and produces more damage compared to a shorter loading time at the 25°C and 40°C test temperature (Barksdale et al., 1997). The longer loading duration will cause larger deformations and with a shorter rest period, the core will have less time to recover from the deformation experienced.

In early testing, it was recommended to use load durations ranging from 0.1 to 0.4 seconds (Vinson, 1990). The 0.1-second loading duration was considered to be more representative of moving vehicles.

A 0.05 second loading rate is representative of high vehicle speeds but too small to achieve reasonable results in the laboratory. The 0.1-second loading rate recommended by LTPP Protocol P07 represents slower traffic conditions. A loading period of 0.2 seconds is considered to be too long, even for slow moving traffic (Barksdale et al., 1997).

Rest Period

The ratio of rest period to load period should be considered because it would directly affect the amount of recoverable strain (Kim et al., 1992). A smaller recoverable strain will result in a greater resilient modulus value. Initially, it can be seen from Figure 2.12 that an increase ratio of rest period/loading period (time off/time on) will result in a decrease in the resilient modulus. As the temperature decreases, the dependency of the rest period/loading period ratio decreases. This plot is at 25°C.

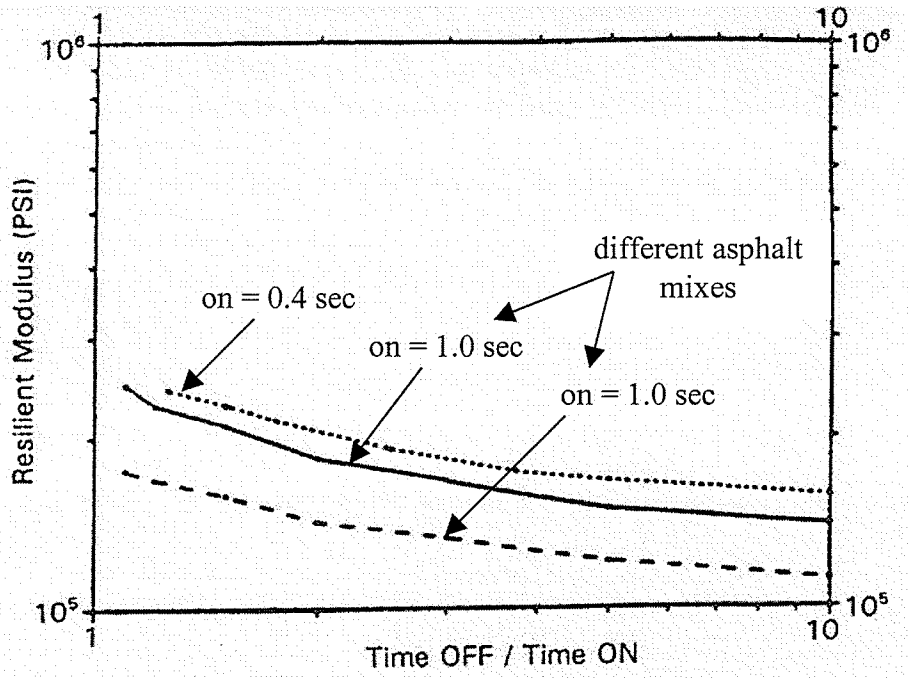

Figure 2.12 Influence of Time Interval Between Load Applications on Resilient Modulus
(Monismith, 1990)

The loading time of each line has been identified. The dotted line has a loading time of 0.4 seconds while the solid and dashed lines have a loading time of 1.0 second. The dotted line and the dashed line are the same asphalt mixtures. From this, it can be seen that with a decrease of loading time there is an increase in resilient modulus. Therefore, if the 0.3 and 0.1 second loading times were to be extrapolated from this figure, the 0.1-second loading time would have higher resilient modulus values than the 0.3 second loading time. Figure 2.13 also shows that there will be a difference in the resilient modulus values for different asphalt mixtures.

Figure 2.13 points out a resting/loading ratio of 2.33 and 9.00, the ratios that were used for this research and the ratio that is recommended by LTPP Protocol P07, respectively. For the same loading period, a smaller resting/loading ratio will have greater resilient modulus values. Fairhurst et al. (1990) reported that with a decrease in rest period, there is an increase in resilient modulus. The shorter rest period results in less time for rebound strain. No conclusion can be made about impact of a 0.1 and 0.3-second loading period, as there is no data from these loading periods.

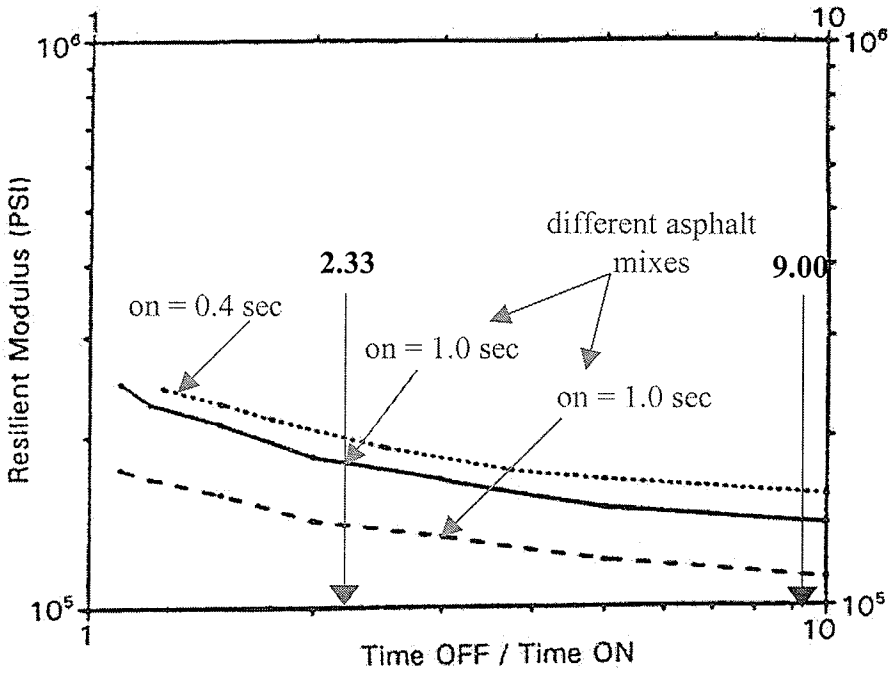

Figure 2.13 Different Ratios *(Monismith, 1990)*

Other studies have found that the ratio of the rest period to load period does not make a significant difference in the resilient modulus (Barksdale et al., 1997). Very little effect can be found in the resting period as the ratio approaches 8 and greater, the effect of the rest period is not very significant (Kim et al., 1992).

Total and Instantaneous Deformations

The total resilient modulus takes into account the instantaneous recoverable deformation and the time dependent recoverable deformation during the rest period of one cycle of loading (the total recoverable deformation). The determination of instantaneous deformation requires more judgmental than the total deformation measurement because it is calculated during the unloading portion of one cycle. This will cause greater imprecision when calculating the instantaneous resilient modulus. For this reason, it has been recommended that only the total resilient modulus will be reported (Boudreau et al., 1992).

Loading Magnitude

Early research of the loading magnitude following ASTM D4123-82 (1995) recommend to induce a load of 10-50% of the tensile strength of the asphalt (Vinson, 1990). Other testing has been conducted in accordance to ASTM D4123-82 (1995) using fixed loading magnitudes at the test temperatures. The applied loads used were as follows (Fairhurst et al., 1990):

5°C - 1.6 kN

25°C - 1.1 kN

40°C - 0.2 kN

The loading magnitude has been observed to affect the value of the resilient modulus following ASTM D4123-82 (1995) (Almudaiheem and Al-Sugair, 1991). Laboratory compacted samples were prepared at different asphalt contents. It was observed that when the specimens with the same asphalt content were tested using different magnitudes of loading, the resilient modulus decreased with an increase in load as shown by Figure 2.14. 'Dry' resilient modulus refers normal environmental conditions without moisture conditioning.

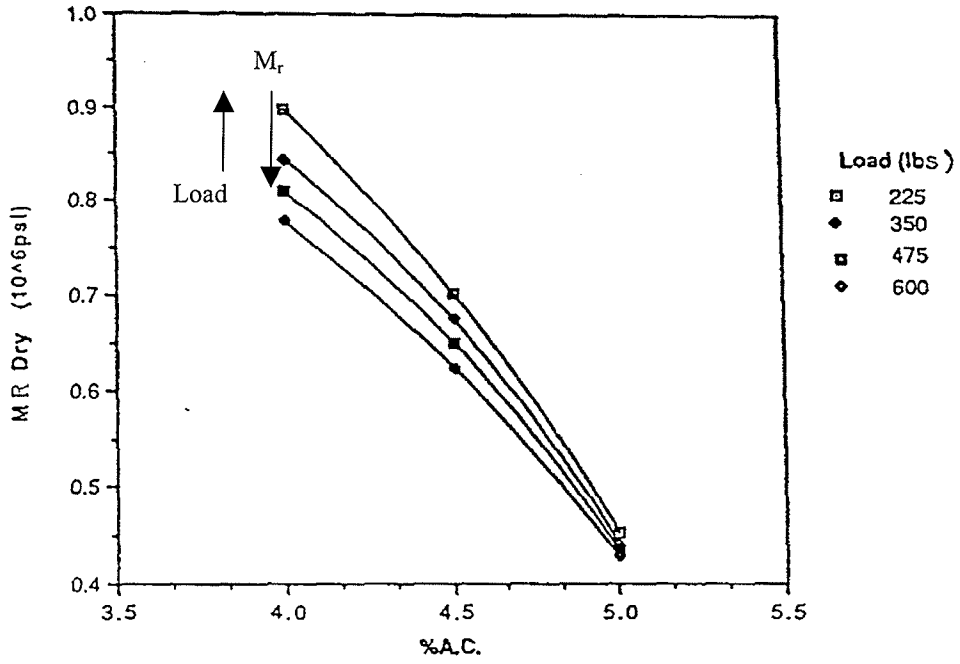

Figure 2.14 Resilient Modulus versus Asphalt Content under Different Loading Magnitudes *(Almudaiheem and Al-Sugair, 1991)*

The magnitude of load should be chosen in such a way that no permanent deformation be produced. During loading the specimen should experience only recoverable deformation. It is the recoverable deformation values that are used to calculate the resilient modulus.

2.4.2 Subgrade Resilient Modulus

The resilient modulus is the primary material property that is used to characterize roadbed soil and other structural layers for flexible pavement design in the 1986 and 1993 *AASHTO Guide for Design of Pavement Structures* (Von Quintus and Killingsworth, 1998). Many highways agencies suggest determining different subgrade strength parameters to calculate the resilient modulus. The subgrade parameters that are used for flexible pavement design are the California Bearing Ratio, R-value, Triaxial and the Soil Support Value. Von Quintus and Killingsworth (1997) report that the physical properties of the subgrade soil should not be used to estimate the design resilient modulus for structural pavement design for high-volume highways. The resilient modulus used for design purposes should be backcalcuated from deflection basin data or from resilient modulus testing of unbound materials in the laboratory.

2.5 Field Testing

In-situ testing is used to determine the material properties of asphalt pavements in the field.

2.5.1 Nondestructive Testing

Environmental conditions, materials and traffic loads are major factors that influence the effective structural capacity of a pavement section. The material properties of asphalt concrete layers are essential to evaluating the effective structural capacity of a pavement structure. To carefully evaluate the pavement structure, the in-situ material properties should be determined. Nondestructive testing (NDT) has been used to determine the in-situ material properties of asphalt concrete pavement layers.

The Benkelman beam, which was one of the first static nondestructive devices used, was introduced in the early 1950s (Ullidtz and Coetzee, 1995). The Benkelman beam is used for pavement deflection testing to measure road surface rebound deflection under standard wheel load and tire pressure. The results from this testing were representative of static or slow moving wheel loads. The maximum rebound deflection measured with a Benkelman Beam was compared to the design deflection for the expected traffic.

Manitoba Department of Transportation and Government Services (MTGS) uses Benkelman Beam Rebound (BBR) as a measure of pavement strength by simulating the rebound of a pavement under an applied load. For rehabilitation design purposes, Benkelman Beam Rebounds are the maximum spring rebound readings measured in the outer wheel path of a pavement lane.

Benkelman Beam results are representative of static or slow moving wheel loads. To better predict the behaviour of a pavement structure under moving wheel loads, it was apparent that different testing apparatus was needed to simulate moving loads.

2.5.2 Falling Weight Deflectometer (FWD)

The falling weight deflectometer (FWD) was developed in 1964 in Denmark at the Danish Road Institute, formerly the National Road Laboratory. It is commonly used to determine the deflection response of the pavement structure due to moving loads. The deflection basin produced by the pavement structure due to load can be used to determine the elastic properties of the asphalt concrete pavement. In conjunction with pavement deflections, the thickness of each layer must be known or estimated. Ground penetrating radar (GPR) measurements or field cores can be used to determine the asphalt concrete layer thickness, while the FWD device is used to determine the deflection response of the pavement structure from load. Other nondestructive testing methods include wave propogation, penetrometers, infrared and seismic technologies, which are not discussed in this thesis.

The FWD delivers an impulse force to the pavement surface. Loads can range from 5 kN to 250 kN with a duration of about 20 to 30 μsec, simulating various traffic loads. The pavement surface response to loads is the sum of the deflections of each layer of the pavement structure (Baladi, 1990). An example of the pavement response to load recorded by the sensors is shown in Figure 2.15. The typical deflection basin is shown.

Velocity transducers that are mounted on a bar at predetermined distances measure deflections. One transducer is located at the center of the loading plate and the six other transducers are placed at distances up to 2.25 m (7.4 ft) from the center of the loading plate, as shown in Figure 2.16.

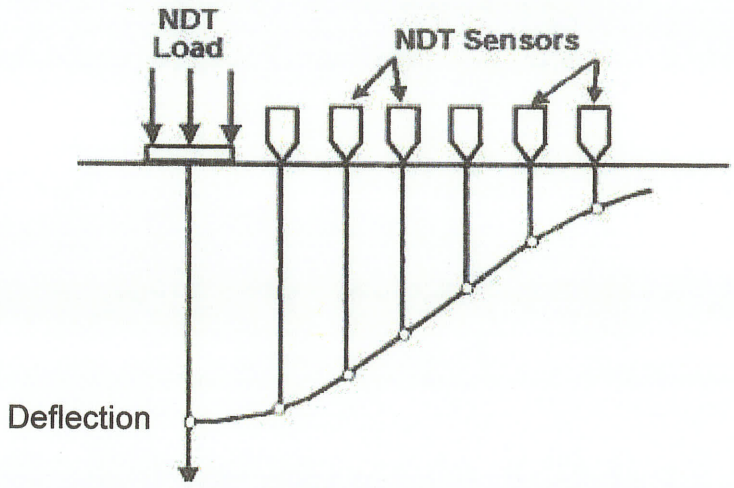

Figure 2.15 Measurement of Surface Deflections *(ERES, 2001)*

For the reason that the FWD is a non-destructive method to evaluate the pavement condition, it is sometimes preferred over destructive test methods. The FWD produces fast results, compared to laboratory testing, without the removal or destruction of pavement materials. The testing equipment is transportable and usually computer controlled.

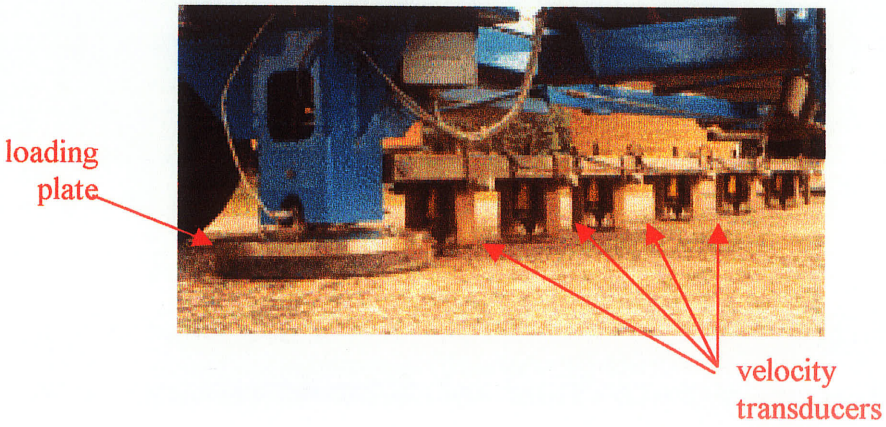

Figure 2.16 Load Plate and Sensors

The pavement properties of the asphalt structure can be determined through the use of backcalculation and the dynamic response of the pavement. The backcalculated material properties are dependant on the type of FWD device used, testing procedure and the method of backcalculation. All structural layers below the layer being loaded influence the FWD deflections. This issue sometimes requires complex or non-unique backcalculation techniques (Stubstad, 2002).

Currently there are five major FWD manufacturers: Dynatest; KUAB; Carl Bro (Phonix); JILS (Foundation Mechanics); and KEROS Mini FWD. The most commonly used FWD device in North America is the Dynatest Model 8000 FWD system, and is shown in Figure 2.17. It has the longest history of use throughout North America and currently is used in many provinces, states and local agencies (Haas, 1997).

Figure 2.17 FWD Equipment

2.5.2.1 Factors Influencing Deflections from FWD

There are three major factors that will affect the deflection values obtained by the FWD device;

1. stress state (loading);
2. temperature, moisture, seasonal variations; and
3. pavement condition.

Stress State (Loading)

It is desirable to normalize deflection values to an applied load of 40 kN, which is the design load. The load duration and frequency should simulate the magnitude and duration of moving vehicles.

Unbound materials are highly dependent on the stress condition. The modulus of a cohesionless, granular material does not have a unique modulus value, but only as a function of the stress state. Coarse-grained materials will show an increase in moduli with an increase in the applied stress level, it is a function of the stress invariant. This behaviour is the opposite of fine grained unbound materials as it is a function of the deviator stress. A load that causes a stress of 120 kPa at the top of a subgrade material may show the modulus to be approximately 20 MPa while the subgrade material that is deeper or at a larger radial distance away from the load, may have a modulus of 60 MPa or three times as much (Ullidtz, 2002).

Temperature, Moisture, and Seasonal Variations

The most important factor influencing asphalt concrete deflections is temperature (Chen et al., 2000). At high temperature, asphalt pavements are softer and are much more viscoelastic and therefore have greater deflection values than at lower temperatures. At colder temperatures, the material begins to approach the assumptions used for an elastic material (Von Quintus and Killingsworth, 1996).

Temperature has little effect on unbound and subgrade materials but moisture plays an important role in the strength. Dry granular materials will have a higher stiffness than wet granular materials. This can be explained by the decrease of internal friction due to the presence of excess water. This problem is manifested for fine-grained materials and the modulus of the material is lowest when completely saturated.

Figure 2.18 illustrates the variation in the pavement strength as a function of the season. Generally, during the winter months the pavement structure is the strongest due to deep frost in the subgrade material and will show little deflection values. In spring the deflection values will significantly increase because the pavement structure is at its weakest point when the frost starts to thaw. Spring is the most critical time for a pavement structure because the asphalt concrete has a relatively high modulus while the underlying unbound material is unable to provide adequate support of the upper layers. During summer and into the fall, the pavement structure begins to gain strength with the removal of excess water left from the spring thaw, deflection measurements begin to decrease. Regions that do not experience the deep frost followed by the thaw period tend to experience highest deflections during the wet season.

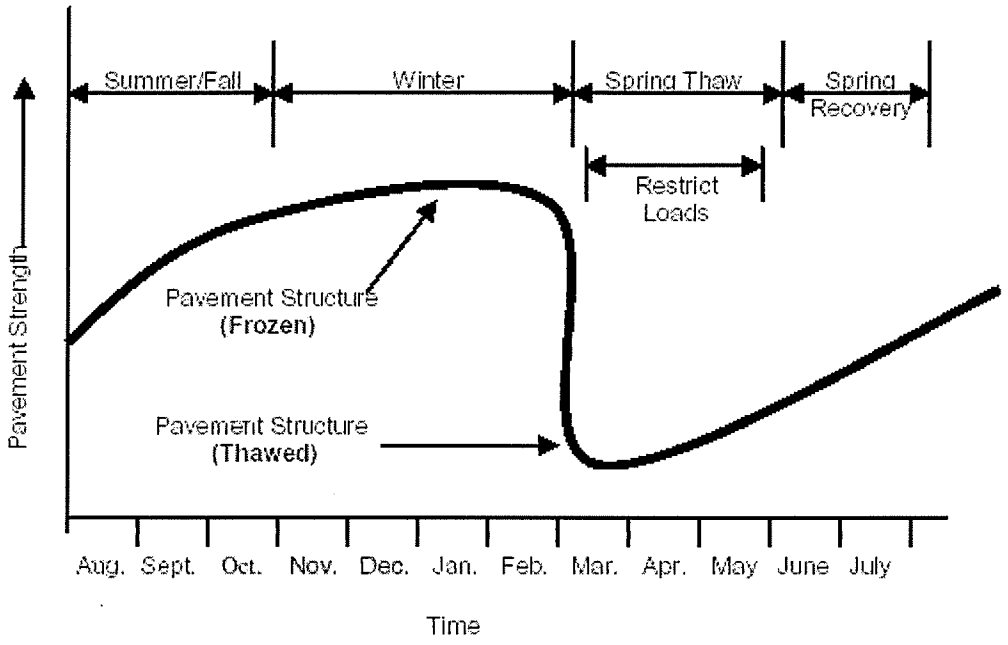

Figure 2.18 Pavement Strength versus Seasonal Variation *(Saskatchewan, 2000)*

Pavement Condition

Deflection measurements can be a good indication of the pavement conditions and vise versa, the pavement conditions can directly affect the deflection measurements. A pavement that has cracking and rutting will experience greater deflection values than a pavement that is free of such distresses. The subsurface variations and underlying voids can also affect the deflection values obtained by FWD testing (ERES, 2001)

2.5.3 Application of Deflection Data

2.5.3.1 Empirical Use

The early uses of NDT data was to relate the pavement structure to a threshold value that was determined by empirical methods.

Pavement Condition

There have been many uses for deflection data over the years. The maximum deflection directly under the applied load has been used as a pavement condition indicator in early studies of

deflection data (Ullidtz and Coetzee, 1995). A 'limiting maximum' deflection was usually used and compared to the maximum deflection experienced by the pavement structure. If the experienced maximum deflection exceeded the limiting deflection, corrective measures were taken to reduce the measured deflections.

The deflection measurements can be used to characterize the condition of the pavement structure, as shown in Figure 2.19. Generally, if the pavement experiences small deflections, the pavement is classified as 'strong'. If the deflections are high, then the pavement is classified as 'weak'.

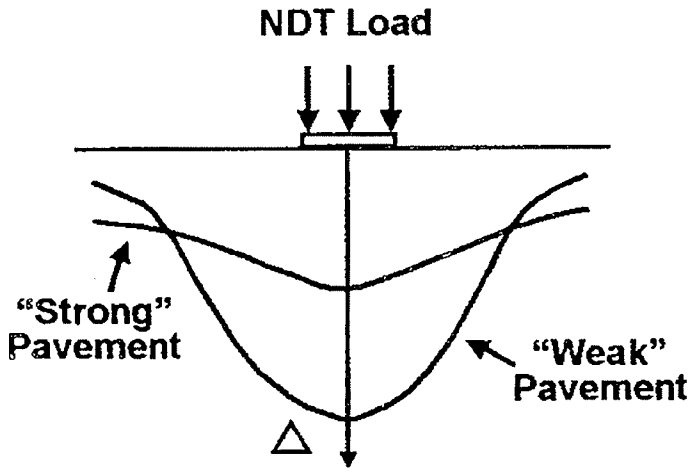

Figure 2.19 Strong versus Weak Pavement *(ERES, 2001)*

Pavement Thickness

The relative pavement thickness of different pavement structures can be determined from the deflection data. Pavements that have a thick asphalt layer have lower deflection values than pavements with thin asphalt layers, as shown by Figure 2.20.

Load Restrictions

Maximum deflections have also been used as an indicator to initiate spring load restrictions. The maximum deflections experienced by the pavement structure are monitored during the spring thaw and once a limiting maximum value is reached, spring load restrictions are placed in effect (Ullidtz and Coetzee, 1995).

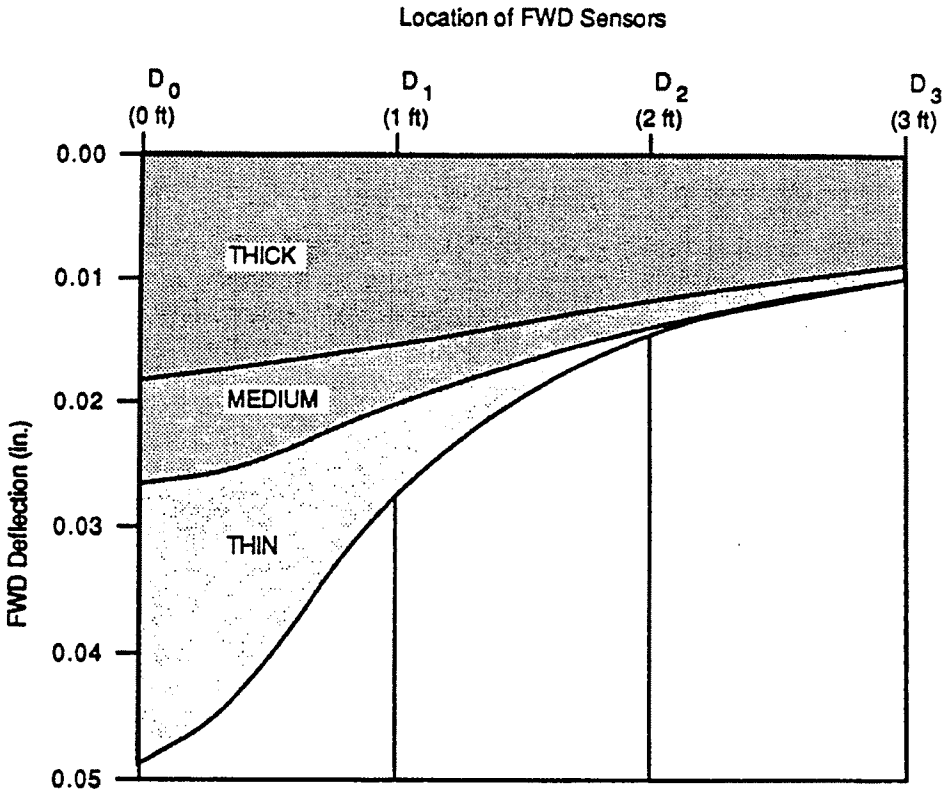

Figure 2.20 Comparison of Deflection Basins for the "Standard" Typical Pavement
(Mahoney and Newcomb, 1990)

Quality Control and Quality Assurance

Research has been conducted to evaluate the effectiveness of the FWD to assist in quality control and quality assurance (QC/QA) process during construction (Stubstad, 2002). Pavement quality, and in turn pavement performance, can be estimated from FWD data. The FWD is used on newly constructed sections, rehabilitated sections and during maintenance procedures to characterize the construction quality. Material variations could be detected for each layer during construction, which could lead to early detection of pavement failure. Hanna (2002) concluded that FWD data can be used to estimate material properties, the variations at each layer interface and an overall quality of the pavement structure, but should not be used to assess the "total" quality of the pavement structure. Good asphalt concrete mix designs and high quality aggregate base and subgrade materials are still vital in achieving well performing pavements. FWD testing is recommended as additional procedure for existing QC/QA procedures (Stubstad, 2002).

2.5.3.2 Mechanistic Design

Over the years, the use of NDT data has switched towards a more mechanistic approach based on fundamental engineering principles. The use of the deflection data has become much more refined than the early uses, incorporating backcalculation techniques to determine pavement structure properties. There are many computer programs that use backcalculation techniques to calculate the effective modulus of the pavement structure from deflection data.

Backcalculation of Modulus

A mechanistic-based approach has been the recent focus of pavement analysis and design, which is based on fundamental engineering principles. This requires the knowledge of material properties for the characterization of pavement layers.

Backcalculation procedures, along with pavement deflection basins and layer thicknesses, have been used to estimate the modulus of the pavement layers. The backcalculation procedure involves calculating the theoretical deflection and adjusting the resilient modulus until the measured deflection matches the theoretical deflection through an iterative procedure (Ullidtz and Coetzee, 1995). The modulus is representative of the pavement response to load. The thickness of the entire pavement structure can be found from as-built construction data or from extracting field cores.

The theoretical deflection usually involves the use of layered elastic theory or a variation thereof. Not all pavements follow the fundamental assumptions of the linear elastic theory and therefore the moduli values obtained through the various methods to calculate the theoretical deflections will vary to different degrees. Ullidtz and Coetzee (1995) also state that the backcalculated resilient modulus value is a layer parameter and not necessarily the layer material modulus.
Three computer programs that use backcalculation techniques to calculate the modulus are: WESDEF, MODULUS and ELMOD. WESDEF uses the approach to match the measured deflection basin to the theoretical deflection basin by altering the modulus values of the layers through a series of iterations. MODULUS calculates a number of deflection basins for a range of modulus values that best matches the calculated deflection basin with the measured deflection basin. ELMOD uses the Odemark equivalent thickness approach (Lukanen et al., 2000). These

computer programs do not necessarily result in a unique solution. Much engineering judgment is needed when using the computer programs.

Figure 2.21 is a general illustration of the stress zone in a three-layer pavement structure. The dotted line illustrates the load distribution throughout the various layers. As shown by Figure 2.21, sensors four and five are out of the stress zone for the hot mix asphalt and the granular base and therefore represent the deflections of the subgrade material only. Sensor two is representative of the hot mix asphalt, granular base and subgrade material, while sensor three measures the granular base and subgrade response to load. Knowing the modulus of the subgrade material from sensor five, the modulus of the granular base can be determined by matching deflection at sensor three with the calculated deflection at sensor three by varying the modulus of the granular base. Once the granular base modulus is calculated, the same procedure can be applied to sensors one and two to determine the modulus of the hot mix asphalt.

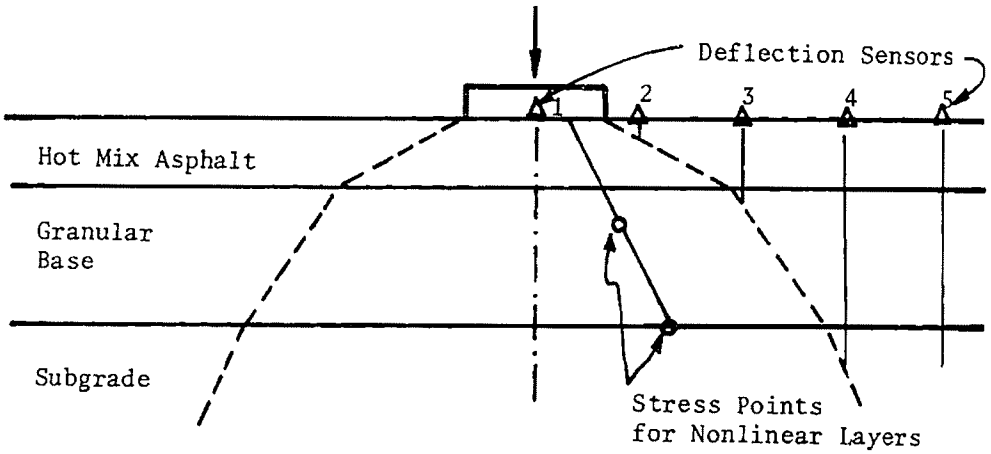

Figure 2.21 Stress Zone Within Pavement Structure *(Huang, 1993)*

The backcalculated modulus value describes layer stiffness, in turn, providing an indication of the layer condition. The in-situ material properties of the pavement layers will aid in the design and selection of the most suitable rehabilitation or reconstruction technique.

Other research has shown the backcalculation of the resilient modulus of the asphalt concrete layer to be very sensitive to the thickness of each layer (Cochran, 1990). The modulus of the subgrade material can be calculated with confidence, but the modulus of the asphalt concrete is questionable.

Some problems may be encountered when using backcalculation techniques to determine the resilient modulus. A single pavement structure may have different measured resilient modulus

values at different locations. These irregularities may result from variability in pavement thickness, pavement distresses, nonlinear material response, presence of bedrock or stiff layers and moisture effects (Ullidtz and Coetzee, 1995). Temperature corrections have been incorporated into many of the software programs available today.

AASHTO Subgrade Modulus Equation

The modulus of the subgrade was calculated using the AASHTO simplified Equation 2.25:

$$M_r\,(MPa) = \frac{P(1 - \mu^2)}{\pi d r} \qquad (2.25)$$

where

$P =$ *load (kN)*

$\mu =$ *Poisson's ratio, assumed to be 0.35*

$d =$ *FWD deflection (mm)*

$r =$ *sensor distance from centre of load plate (mm)*

Relative Layer Moduli

A direct method for analyzing FWD deflection data was presented by Wimsatt (1999). Assuming a two layer system, the deflection experienced by the pavement structure at a distance of 1828.8 mm (72 inches) away from the center of the loading plate divided by the deflection directly under the loading plate, relates directly to the ratio between the asphalt concrete modulus and the subgrade modulus.

This procedure assumes that the deflection experienced directly under the loading plate is a function of the asphalt layers and the subgrade, while the deflection experienced at the sensor farthest away from the loading plate is a function of the subgrade alone. Therefore, dividing the deflection value directly under the loading plate by the deflection at the sensor farthest away from the loading plate corresponds to the ratio between the asphalt modulus and subgrade modulus. The asphalt/subgrade modulus ratio is an effective value.

Detection of Weak Layers

Wimsatt (1999) suggested comparing all deflection ratios by the use of Equation 2.26:

$$\frac{d_{200}}{d_0}, \frac{d_{300}}{d_{200}}, \frac{d_{450}}{d_{300}}, \frac{d_{600}}{d_{450}}, \frac{d_{900}}{d_{600}}, \frac{d_{1200}}{d_{900}} \qquad (2.26)$$

where

d_x = deflection at sensor placed at distance x (mm) from the center of the load plate

Wimsatt (1999) found that it was a good indication that the base layer was much weaker than the surface layer if the ratio between the deflection of the second sensor, d_{200}, and the deflection directly under the loading plate, d_0, was not the minimum value.

Structural Number

AASHTO 1993 suggested a procedure to determine the effective structural number (SN_{eff}) from NDT by relating the pavement stiffness and layer coefficients. With NDT data and backcalculation techniques, the effective modulus of the entire pavement structure above the subgrade can be calculated. The determination of the SN_{eff} assumes a model based on stiffness theory and a two-layer pavement structure in addition to the subgrade. Equation 2.27 is used to calculate SN_{eff}

$$SN_{eff} = 0.045 D \sqrt[3]{E_P} \qquad (2.27)$$

where

SN_{eff} = total effective structural number for the pavement structure

D = total thickness of surface, base and subbase (inches)

E_P = effective modulus of the pavement (psi)

With the SN_{eff} known, the layer coefficients could be found for each layer by dividing the SN_{eff} by each layer thickness (Pologruto, 2000). AASTHO 1993 Design Guide recommends this approach to eliminate the backcalculation of the modulus for each layer.

2.5.4 ELMOD

The ELMOD computer program uses the Odemark-Boussinesq transformed method to backcalculate the resilient modulus of the layers. Odemark's layer transformation along with Boussinesq's equation is used as an iterative procedure assuming a homogeneous isotropic, linear elastic semi-infinite space (Appea and Al-Qadi, 2000). The ELMOD computer program backcalculates the modulus values that match measured deflections from the FWD testing.

ELMOD does not require the input of a seed modulus or a range of expected modulus values but has the ability to fix a modulus value input. A maximum of four layers can be analyzed, exclusive of the rigid layer. A non-linear analysis is completed for the subgrade material. Therefore the data collected is unique for that particular temperature and state of stress conditions.

The resilient modulus values calculated by ELMOD may be different than the resilient modulus values calculated by a different computer program that uses backcalculation techniques.

2.5.4.1 Inertia Method

When the pavement structure is composed of two layers, the modulus of each layer can be determined from the Inertia Method. This method was presented by CSHRP for the Study on the Normalization of Asphalt Concrete Overlay Design (EBA, 1996). The backcalculated asphalt modulus obtained from ELMOD can be used with in conjunction with the layer thickness and Equation 2.28.

$$E_{effective} = \left[\frac{d_1 \times \sqrt[3]{E_1} + d_2 \times \sqrt[3]{E_2}}{(d_1 + d_2)} \right]^3 \qquad (2.28)$$

where

$E_{effective}$ = overall asphalt modulus back-calculated from ELMOD (MPa)

d_1 = thickness of layer 1 (mm)

d_2 = thickness of layer 2 (mm)

E_1 = modulus of layer 1 (MPa)

E_2 = modulus of layer 2 (MPa)

Chapter 3
RESEARCH PROGRAM

Manitoba Department of Transportation and Government Services (MTGS) uses two different mixes for the asphalt pavements throughout the Province of Manitoba, Bituminous B (Bit B) and Bituminous C (Bit C). There are clear differences between the two mixes. Bit B is defined as a well graded dense asphalt mix with good wearing resistance. Historically, it has been used on the top and intermediate lifts of a pavement structure. Bit C is a lower class product with a less stringent gradation, with finer aggregate size, lower asphalt content and is usually used in the intermediate and lower lifts. Due to the less stringent requirements for gradation specifications, Bit C mix can utilize the more readily available local aggregates, which can lower the cost by approximately 30% of the Bit B mix. In the MTGS specifications, a minimum crush count of 50% is required for the Bit B mix, while the Bit C mix design has no specification for this property (MTGS, 2003).

3.1 Project Identification

During the 2000 construction season, MTGS randomly selected eight projects that were to be included in this research. As shown by the red markers in Figure 3.1, one project is located in Northern Manitoba, and the other seven projects are located in the southern region of the Province. Out of the eight projects, three were new construction and five were asphalt overlays. Each project included side-by-side comparison test sites that were used to collect pavement structure data, to extract cores, and for FWD testing.

3.1.1 Pavement Structure

All eight projects identified have a test section with two side-by-side pavement structures that had the same top two asphalt layers. Figure 3.2 shows the Bit B surface course over a Bit B binder course (Bit B/B) and a section with a Bit B surface course over a Bit C binder course (Bit B/C). See Appendix A for a detailed location of the test sections. Underlying these two top layers was either an existing pavement structure or additional asphalt layers that were constructed at the same time as the top two lifts. All laboratory testing was conducted on the binder course to

ensure that environmental factors did not affect the test results. The thickness of the two top asphalt lifts ranged from 37 mm to 68 mm in the as-built condition.

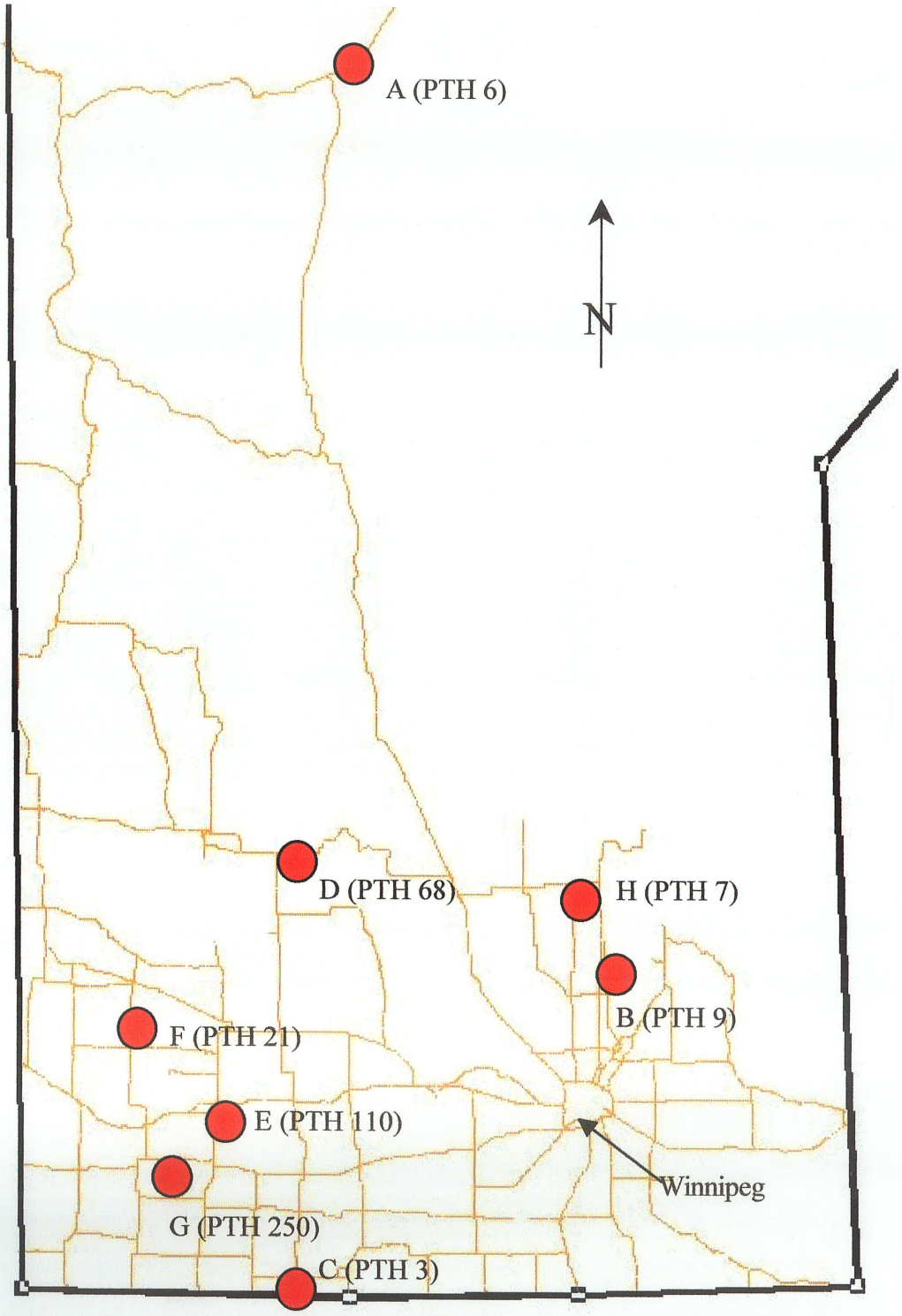

Figure 3.1 Map of the Province of Manitoba Indicating all Eight Test Site Locations using Their Designated Project Identification Letter

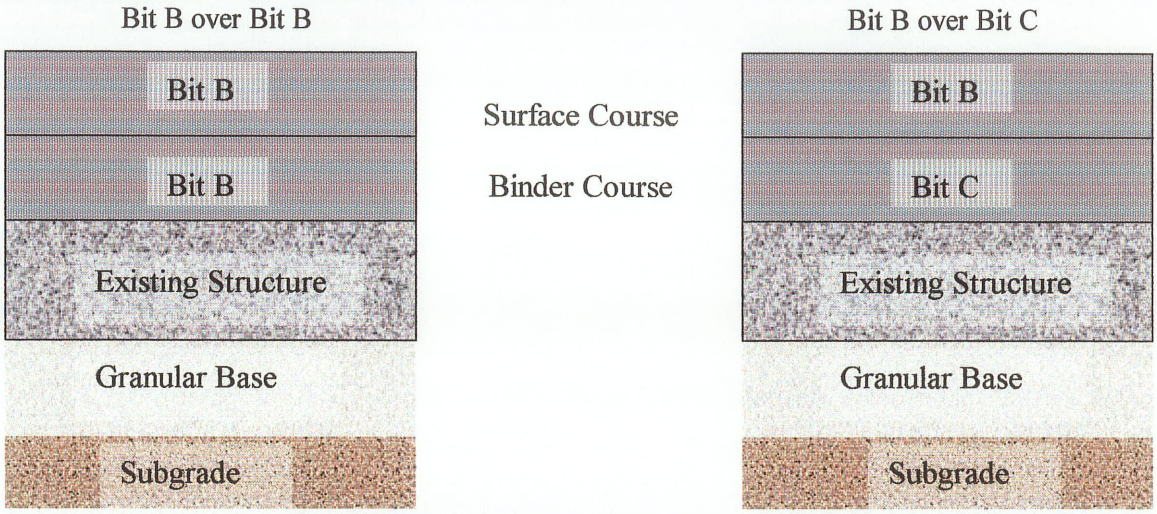

Figure 3.2 Bit B/B and Bit B/C Pavement Structure Identifying Surface and Binder Courses

3.1.2 Field Sampling

Twenty 150-mm (6 inch) diameter cores were extracted from each of the eight project sites throughout Manitoba. Ten of the cores were taken from the Bit B/B section, while the other ten cores were taken from the Bit B/C test section. All underlying asphalt pavement layers were extracted with the top two asphalt layers, and the thickness of the granular base material was recorded. The cores were taken between the wheel paths to reduce the effects of traffic compaction.

Table 3.1 includes the test site locations and a break down of the entire pavement structure. Each asphalt layer was measured from the cores that were extracted. The granular base was measured at two of the ten core locations and averaged.

Table 3.1 Test Site Locations and Pavement Structure

Project Identification	Location	Pavement Structure	
		Bit B over Bit B	Bit B over Bit C
A	PTH 6, North of PTH 39 to PR 373 (Ponton)	46 mm Bit B 43 mm Bit B 42 mm rotomilled 187 mm granular base fine subgrade	51 mm Bit B 48 mm Bit C 37 mm rotomilled 227 mm granular base fine subgrade
B	PTH 9, PR 519 to Willow Creek (Winnipeg Beach)	38 mm Bit B 61 mm Bit B 188 mm granular base fine subgrade	44 mm Bit B 37 mm Bit C 55 mm Bit C 193 mm granular base fine subgrade
C	PTH 3, PTH 5 to PR 442 (Cartwright)	65 mm Bit B 52 mm Bit B 109 mm Bit C 164 mm granular base coarse subgrade	58 mm Bit B 50 mm Bit C 57 mm Bit C 60 mm Bit C 175 mm granular base coarse subgrade
D	PTH 68, (Eddystone)	47 mm Bit B 49 mm Bit B 47 mm Bit C 164 mm granular base coarse subgrade	42 mm Bit B 54 mm Bit C 53 mm Bit C 162 mm granular base coarse subgrade
E	PR 110, PTH 10 to Richmond Ave. (Brandon)	51 mm Bit B 52 mm Bit B 111 mm Bit C 172 mm granular base coarse subgrade	52 mm Bit B 51 mm Bit C 105 mm Bit C 204 mm granular base coarse subgrade
F	PTH 21 (Hamiota)	68 mm Bit B 50 mm Bit B 52 mm Bit B 50 mm Bit C 112 mm Bit C 154 mm granular base coarse subgrade	51 mm Bit B 63 mm Bit C 85 mm Bit C 73 mm Bit C 76 mm Bit C 139 mm granular base coarse subgrade
G	PR 250, PTH 2 to Trans Canada Highway (Alexander)	45 mm Bit B 40 mm Bit B 39 mm Bit C 68 mm Bit C 194 mm granular base coarse subgrade	46 mm Bit B 41 mm Bit C 44 mm Bit C 60 mm Bit C 210 mm granular base coarse subgrade
H	PTH 7, PR 231 North (Arborg)	54 mm Bit B 55 mm Bit B 72 mm old asphalt layer 197 mm granular base coarse subgrade	51 mm Bit B 47 mm Bit C 47 mm Bit C 96 mm old asphalt layer 180 mm granular base coarse subgrade

3.2 Material Properties Data

From each test section within each of the eight projects, six of the ten cores were delivered to the University of Manitoba and the other four cores were delivered to the MTGS Laboratory to determine the material properties of the mixtures.

The following material properties were determined:

- percent air voids
- percent asphalt content
- percent asphalt absorbed
- percent effective asphalt content
- kinematic viscosity
- absolute viscosity
- stability
- flow
- recovered penetration
- percent VMA (voids in mineral aggregate)
- percent VFA (voids filled with asphalt)
- bulk density
- gradation

3.3 Laboratory Testing Program

A flow chart showing the details of laboratory testing is shown in Figure 3.3. From the field samples that were obtained from MTGS, the indirect tensile strength test was used with static and dynamic loading. In total, 64 asphalt cores were tested, with some cores having multiple tests performed on them.

3.3.1 Static Indirect Tensile Test

Indirect tensile testing was conducted on the asphalt cores in accordance with a modified version of the test outlined in LTPP Protocol P07. A 100 kN stepless drive load frame equipped with loading platens according to ASTM D4123-82 (1995) was used to load the sample. The load was transferred to the specimen via curved loading strips with curvature matching the 150 mm (6

inch) cylindrical specimens. The load frame was placed inside a temperature-controlled chamber capable of maintaining a desired temperature within one degree Celsius.

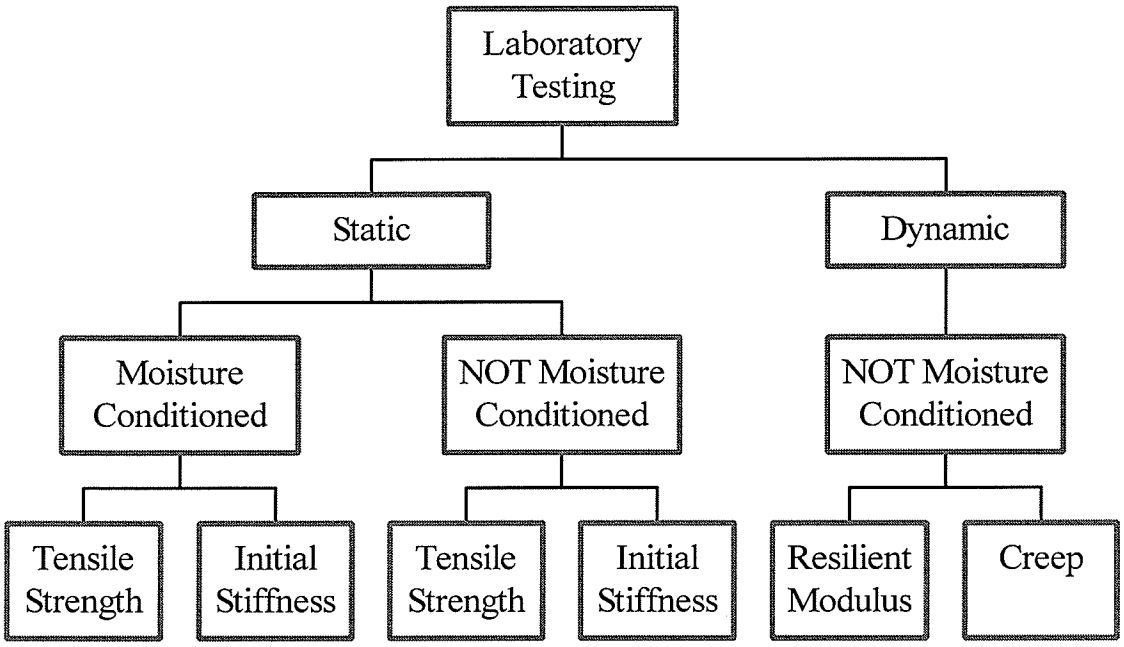

Figure 3.3 Overview of Laboratory Testing

3.3.1.1 Bit B – Bit C Comparison

The modified indirect tensile strength test was conducted on the binder course of the Bit B mix and the Bit C mix to compare the tensile strength and the initial stiffness of the two mixes used by MTGS. This will aid in characterizing the relationship between the material properties and strength parameters for each mix.

3.3.1.2 Moisture Sensitivity Analysis

Two sets of eight Bit B specimens were tested as follows. The first set of eight specimens were moisture conditioned in accordance to AASHTO T283-98 *Resistance of Compacted Bituminous Mixture to Moisture Induced Damage* and the corresponding ASTM D4867/D4867M-96 *Standard Test Method for Effect of Moisture on Asphalt Concrete Paving Mixtures.* The second set of eight specimens were not moisture conditioned.

The eight Bit B specimens that were moisture conditioned were partially saturated with distilled water using a vacuum chamber. The volume of water had to range between 55% and 80% of the total volume of air voids in the asphalt core sample. If the lower limit was not reached, the core was subjected to further vacuuming to increase the volume of water in the air voids. If the upper limit was exceeded, the core was deemed damaged and could not be further tested.

After the desired volume of water was achieved, the sample was sealed in plastic wrap and placed in a freezer at a temperature of –18°C ± 3°C for a minimum of 15 hours. The wrapped sample was then removed from the freezer and placed in a water bath at +60°C ± 1°C. After approximately 3 minutes of being submerged, the plastic wrap was removed and the sample was kept in the water bath for 24 ± 1 hours. The core was then brought back down to a temperature of 25°C by placing the core in the temperature chamber for a minimum period of 3 hours before testing. The conditioned cores were tested using the modified indirect tensile strength test and compared with the corresponding Bit B samples that were not conditioned.

Indirect tensile tests were performed on both sets of specimens in accordance with the procedures outlined in LTPP Protocol P07. The tensile strength and the initial stiffness were calculated and compared with the corresponding eight Bit B samples that were not moisture conditioned. The tensile strength was calculated at the ultimate load at failure, and the initial stiffness was calculated at 25% of the maximum load achieved.

3.3.1.3 Modifications to Indirect Tensile Strength Test Procedures

A modified version of the indirect tensile strength test outlined in LTPP Protocol P07 was used. A loading rate of 0.1 mm/min was applied to the sample until specimen failure. LTPP Protocol P07 suggests using a loading rate of 50 mm/min. The much slower loading rate was selected in order to capture the load deformation response of the mixture over time and to allow plastic deformation to take place. The slow loading rate creates conditions in which the strength and deformation properties of the mixture can be evaluated (Thiessen, 2001). This slower loading rate will affect the tensile strength results. Thiessen (2001) has reported that a decrease in loading rate will also decrease the tensile strength. It is not known to what degree the 0.1 mm/min loading rate will differ from the recommended 50 mm/min loading rate, although decreased strengths are expected.

The horizontal and vertical deformations were recorded by the data acquisition system until failure was reached. Since the tests were performed at a relatively slow rate of loading and at an intermediate to high temperature, all observed failures were at the binder/aggregate interface.

3.3.1.4 Sample Preparation

The 150 mm diameter asphalt cores were sawed into lift thickness ranging from 29 mm to 50 mm using a water-cooled masonry saw. The measured layer thicknesses are summarized in Appendix B. Aluminum gauge points were glued directly to the dry asphalt core using epoxy as shown in Figure 3.4, with a center-to-center spacing of 38.1 mm (1.5 inch). These gauge points were used to mount miniature linear variable differential transducers (LVDTs) to the front and back of the sample. One LVDT was placed horizontally to capture horizontal or lateral deformations and the other mounted vertically to capture the vertical deformations experienced by the core. All prepared asphalt core samples were placed in the temperature controlled chamber for a minimum of 12 hours to allow the epoxy to set and to ensure the temperature of the samples reached a uniform 25°C.

The LVDTs used were Trans-Tek Series 350, model number 350-0100. ASTM D4123-82 (1995) states that this type of LVDT is satisfactory.

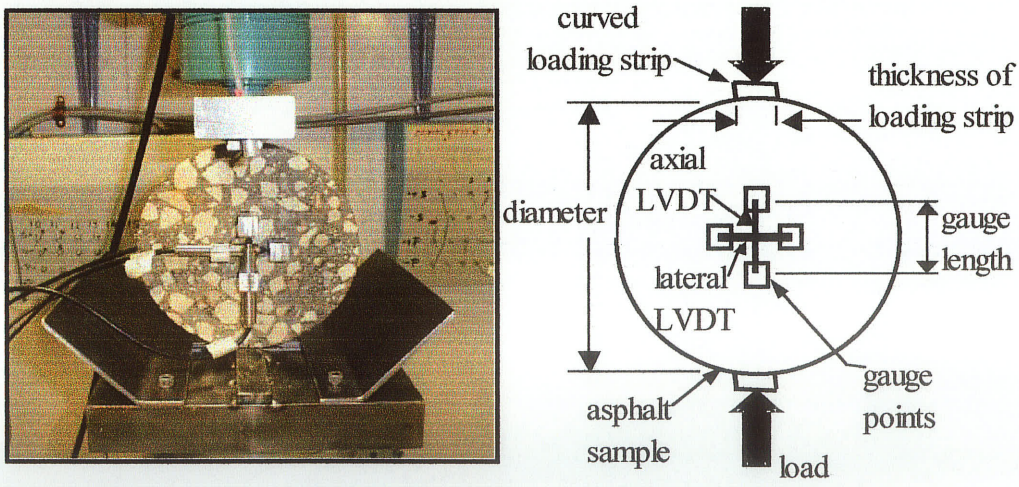

Figure 3.4 Indirect Tensile Test Setup and LVDT Configuration

3.3.2 Dynamic Indirect Tensile Test

Dynamic loading was utilized to determine the horizontal and vertical deformation response of the asphalt samples to cyclic loading. The amount of recoverable deformation between each cycle of loading is used to determine the resilient modulus of the asphalt mixture.

3.3.2.1 Resilient Modulus Test

Ideally, this resilient modulus test is a nondestructive test that will allow for different testing conditions to be used on each sample. The load applied to the asphalt specimen is dependant on the stiffness and the desired strain range; a higher load is needed at colder temperatures. Testing should begin at the lowest temperature, shortest duration and smallest load to reduce the permanent deformation experienced by the specimen. In accordance with LTPP Protocol P07, each asphalt core was tested in the following sequence using the MTS machine as shown in Figure 3.5:

Testing Sequence	
Creep	-10°C
Resilient Modulus	5°C
Creep	5°C
Resilient Modulus	25°C
Creep	25°C
Resilient Modulus	40°C
Tensile Strength	25°C

The creep test is performed at the same temperature minutes after the resilient modulus test is complete. The horizontal and vertical deformation data can be used to determine the creep compliance of the asphalt mixture at the given temperature, but was not calculated for this thesis. The tensile strength test was not carried out at 40°C due to the fact that most of the asphalt samples failed at the 40°C resilient modulus test temperature, as outlined in Section 5.1.2.1.

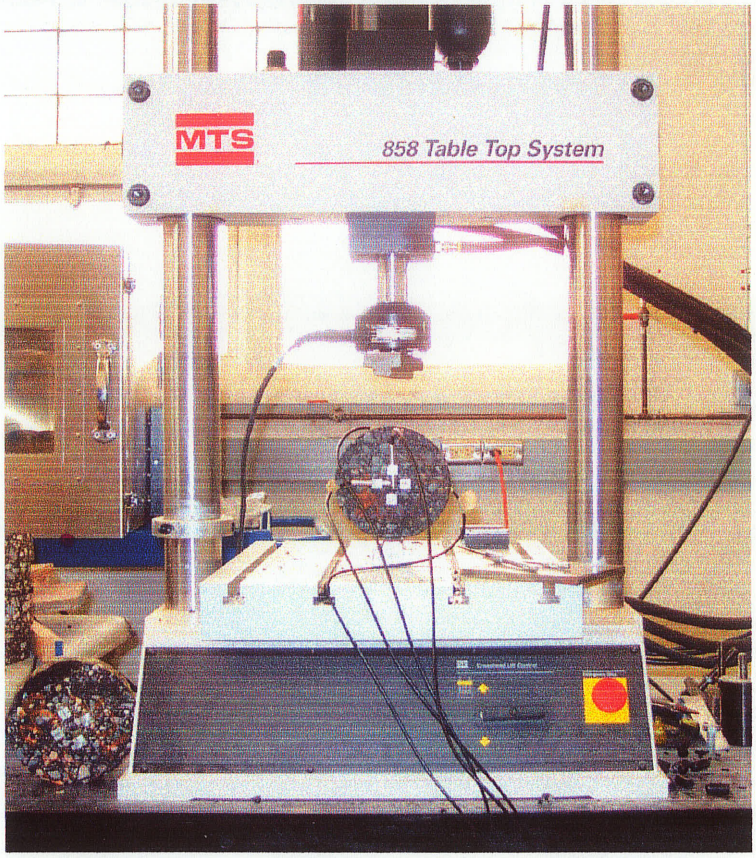

Figure 3.5 MTS Dynamic Loading Machine

3.3.2.2 Sample Preparation

The asphalt cores were prepared for testing as outline in Section 3.3.1.4. Temperature conditioning was completed in accordance to the testing sequence outlined in Section 3.3.2.1. The asphalt cores were conditioned for a minimum of 24 hours prior to testing at the -10, 5 and 25°C test temperatures. At the 40°C test temperature, the asphalt cores were conditioned in an environmental chamber for a minimum of 3 hours, not exceeding 6 hours.

3.3.2.3 Limitations of the Test Procedure

A few limitations were encountered with respect to the testing procedures that were outlined in LTPP Protocol P07 and with equipment limitations: static loading rate; dynamic load period; core diameter; test temperatures and analysis of data.

Core Diameter

LTPP Protocol P07 outlined the test procedures for 100 mm (4 inch) diameter cores. The testing done at the University of Manitoba was carried out on the field-extracted cores supplied by MTGS that were 150 mm (6 inch diameter). LTPP Protocol P07 states that the testing procedures can be adapted for the use of 150 mm (6 inch) diameter cores.

Test Temperature

When the specimens were conditioned in the 40°C temperature chamber, some of the cores collapsed under their own weight and were not tested. The cores that were tested failed under very small dynamic loads. Due to the limitations of the data acquisition equipment, the minimum contact load that could be applied to the asphalt core sample was 40 N, and in some instances this contact load was greater than 10% of the maximum load. Also, due to the fact that most of the specimens failed during the 40°C test temperature, the indirect tensile strength test at 25°C was not conducted.

LTPP Protocol P07 indicates that the resilient modulus and creep tests are to be conducted at 5°C, 25°C and 40°C. Due to equipment limitations, the stated 5°C test temperature was actually at 10°C and will be referred to as 10°C throughout the report.

3.4 FWD Deflection Data

John Emery Geotechnical Engineering Ltd. (JEGEL) conducted tests on each of the sections using a Dynatest Falling Weight Deflectometer in 2001 in accordance to *Standard Test Method for: Dynatest Falling Weight Deflectometer* (MTGS, 1998). The deflection data files were sent to the University of Manitoba and were analyzed using the ELMOD software.

The loading plate was 300 mm in diameter and the geophones spacing was 0, 200, 300, 450, 600, 900, and 1200 mm from the center of the loading plate. A seating drop of 40 kN was applied to the asphalt pavement before testing was initiated. A minimum of two load drops were applied at 25, 40, 60, and 70 kN load levels. The tests were conducted every 100 m for a one km section and were performed on the outer wheel path of the outermost lane.

The deflection data obtained from JEGEL was initially evaluated for any obvious structural problems in the pavement structure. This was carried out by plotting the deflection basins. The modulus of the asphalt pavement structure and the subgrade material was determined from the FWD data. The modulus of the entire asphalt concrete layer was estimated using backcalculation techniques through the use of ELMOD software and the deflection data. The Inertia Method was then used to estimate the modulus of each individual asphalt layer.

ELMOD uses layer thicknesses and structural characteristics and condition of pavement systems to predict the deflection basin of the pavement structure. ELMOD utilizes the Boussinesq-Odemark pavement analysis approach to approximate the complex relationships between pavement performance, material quality, traffic loading and environmental factors. ELMOD software uses the load-deflection data file generated by FWD to perform backcalculation, calculate stresses and strains and to determine overlay requirements.

ELMOD software analyzes pavements through the use of calculated and allowable stresses and strains at critical points within the pavement structure under load. The calculation of existing stresses and strains within the pavement structure is accomplished through analytical or mechanistic methods. The relationship between the allowable stresses and strains and the pavement distress is empirical.

The effects of temperature on the modulus of the asphalt concrete were briefly evaluated. ELMOD uses three different factors or equations to adjust the backcalculated modulus values for temperature. Each method was examined and applied to the backcalculated modulus values to illustrate the affects of temperature.

The Inertia Method, as presented in the Saskatchewan Surfacing Manual (1984), was used to estimate the asphalt modulus of each individual layer of the pavement structure. The individual asphalt layer thickness and the effective modulus of the entire pavement structure are variables used in the Inertia Method.

The modulus of the subgrade material was calculated by ELMOD during the backcalculation process to determine the modulus of the asphalt layer. The subgrade resilient modulus was also estimated using an equation presented by AASTHO (1993).

Chapter 4
PRESENTATION OF RESULTS

4.1 Physical Mix Properties

Four of the ten cores obtained for each test section were tested by MTGS to determine the physical mix properties of the two asphalt mixes. The results of the tests were forwarded to the University and presented in this study. The physical mix properties being investigated are: gradation; material properties and stability.

4.1.1 Gradation

A sieve analysis was performed by MTGS laboratory and the percent passing each sieve was recorded. The percent passing was plotted to determine the gradation of the aggregate of each mix. The main difference between the Bit B and the Bit C mixes is the aggregate grading specifications (MTGS, 2003). The Bit B mixes have a narrow sieve range specification and the mixes are well graded, as shown in Figure 4.1. Generally, the percent passing falls in the middle of the upper and lower limits. Six out of the eight projects have a nominal maximum aggregate size (NMS) of 12.5 mm, while the other two projects have a NMS of 16 mm.

The Bit C mixes have a wider specification range and show a greater variance within the range, falling towards the upper and lower limits, as shown in Figure 4.2. The NMS is also 12.5 mm for six of the Bit C projects, while the other two projects have a NMS of 9 mm. The Bit B specifies a minimum crush count of 50% and a minimum VMA range of 14% to 16% while there is no crush count or VMA range specification for the Bit C mix.

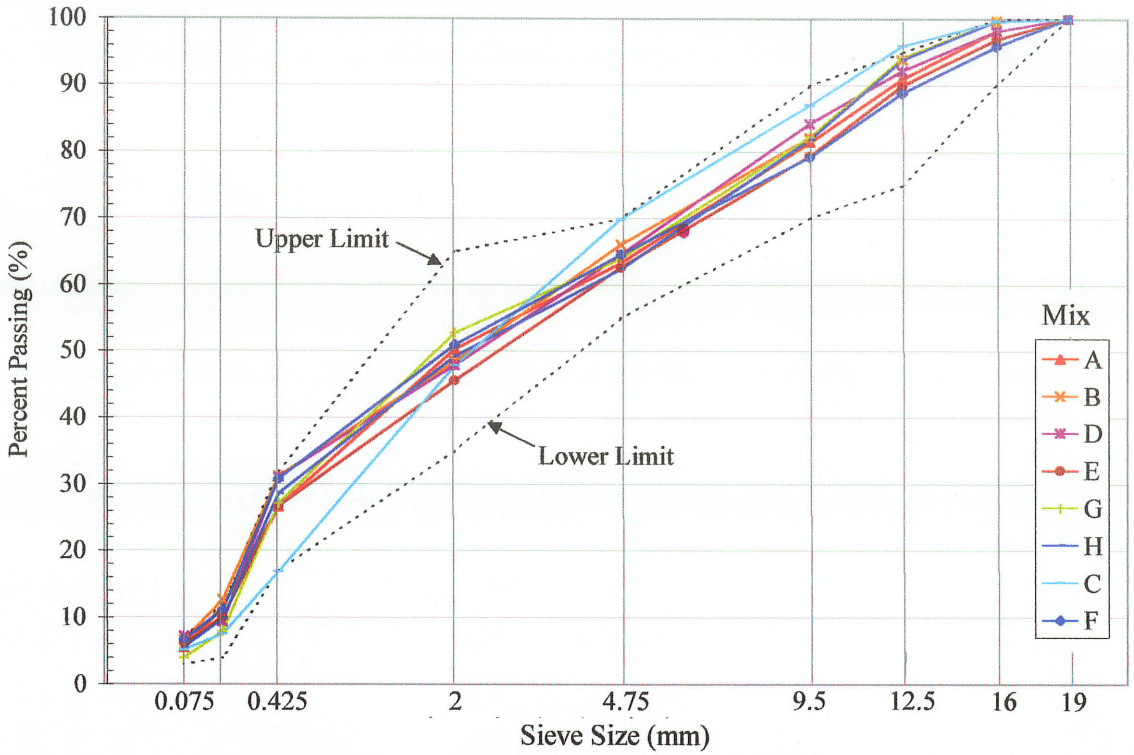

Figure 4.1 Bit B Gradation of Tested Mixes

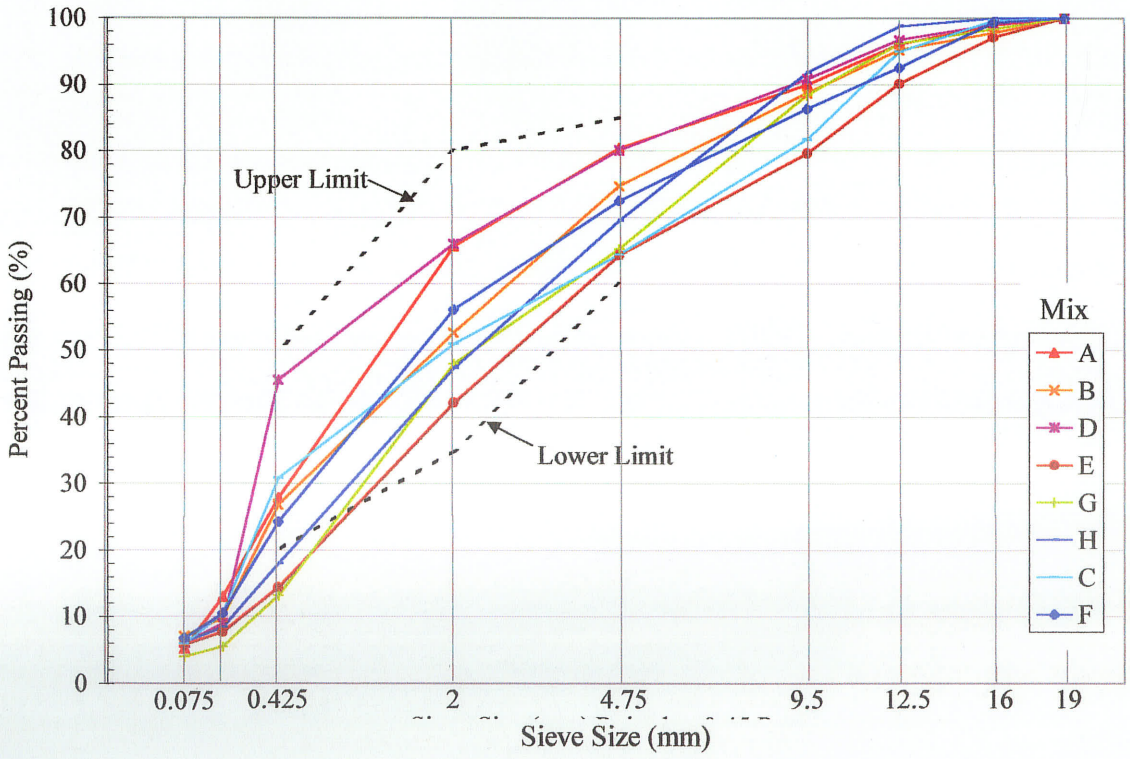

Figure 4.2 Bit C Gradation of Tested Mixes

4.1.2 Material Properties

The binder test results from the four cores that were tested for each of the two mixes were averaged. The average values of the Bit B and Bit C mixes that were used in this study are presented in Appendix C. The testing program consisted of the following tests on the lifts to evaluate the binder properties:

- Bulk density
- In-place air voids
- Marshall stability and flow
- Voids analysis to measure air voids, VMA, and VFA
- Abson method to recover the aged asphalt cement to determine asphalt content
- Recovered binder penetration at 25°C and absolute and kinematic viscosity

Table 4.1 is a summary of 32 cores (8 projects, 4 cores per project) of Bit B and 32 cores of Bit C mix. The averages for the air voids and asphalt content of the 32 cores fell within the ranges specified by MTGS. It can be seen that the Bit B mix has higher asphalt content and lower air voids. There is no specification range for the bulk density but it must be at least 95% of the standard density.

Table 4.1 Summary of Mix Air Voids, Asphalt Content and Bulk Density

	Bit B			Bit C		
	Air Voids (%)	Asphalt Content (%)	Bulk Density (kg/m^3)	Air Voids (%)	Asphalt Content (%)	Bulk Density (kg/m^3)
Minimum	2.5	5.4	2253	5.5	4.6	2164
Maximum	8.9	6.9	2417	13.2	5.0	2391
Average	4.3	6.1	2355	8.4	4.8	2164
MTGS range	3 - 5%	5 - 7%	N/A	8 - 12%	4 - 5%	N/A

4.1.3 Stability

The Marshall stability of the cores was also examined. Figure 4.3 represents the comparison between the Bit B and Bit C Marshall stability values.

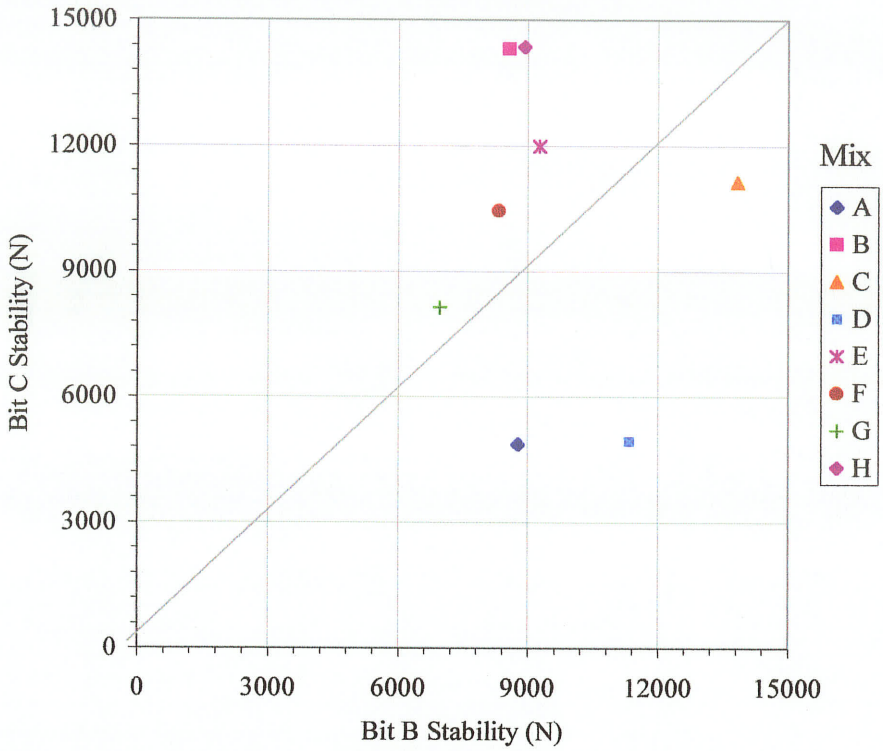

Figure 4.3 Bit B Marshall Stability versus Bit C Marshall Stability

It can been seen in Figure 4.3 that the stability ranged from 5000 to 15000 N and that there is no general trend in relating the Marshall stability of the Bit B mix to that of the Bit C mix. In some cases the stability is greater in the Bit C mix, while for other project locations the Bit B stability is greater. This could be due to the small sample size.

4.2 Laboratory Testing

In the laboratory, the indirect tensile strength test was used to test the asphalt samples, incorporating both static and dynamic loading.

4.2.1 Static Testing

A static load with a constant increasing rate of 0.1mm /min was applied to the asphalt cores till failure. The load-deformation response of each sample was measured and the ultimate load and corresponding failure strains were determined from the test data. An example of the load data collected is shown in Figure 4.4. The decrease in load can be seen, indicating failure of the

specimen. An example of the deformation data collected during static loading can be found in Figure 4.5.

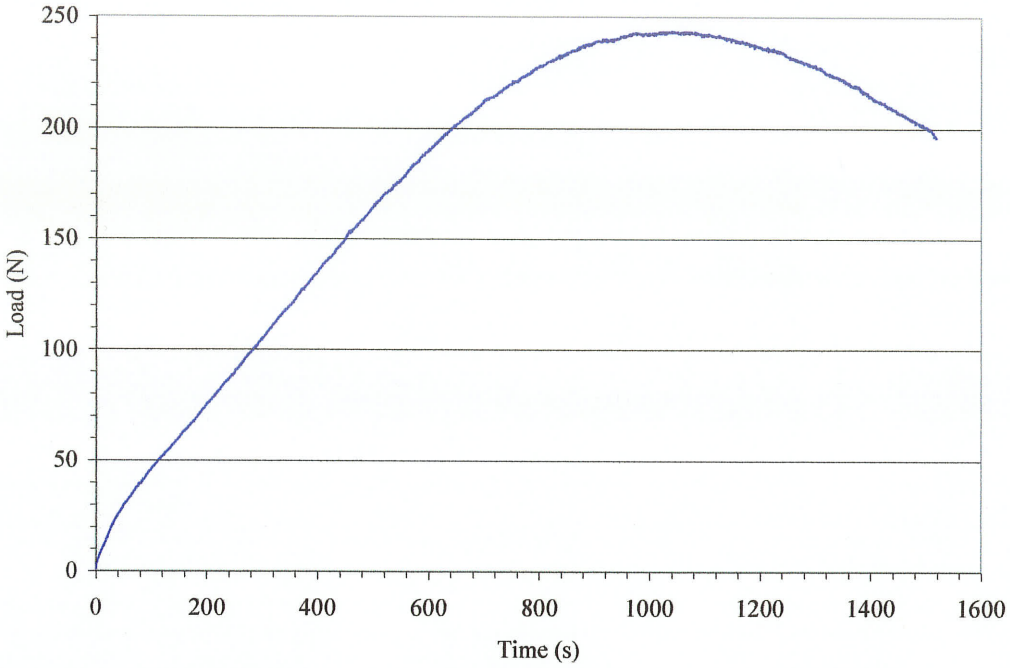

Figure 4.4 Example of Load Data Collected from Static Test

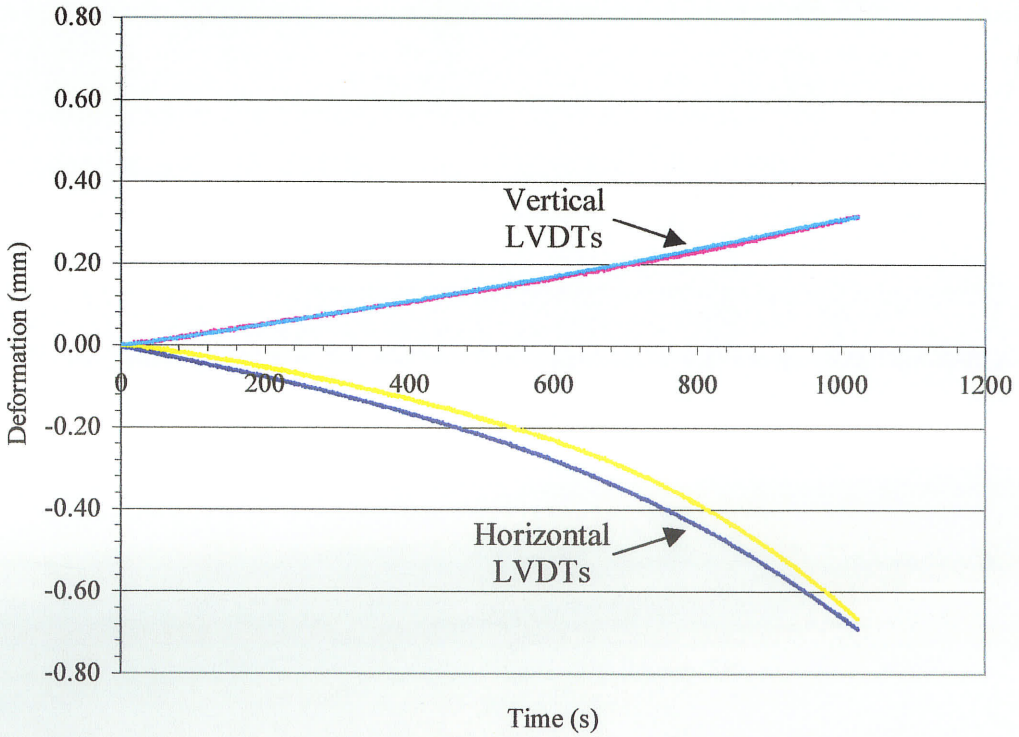

Figure 4.5 Example of Deformation Data Collected During Loading

4.2.1.1 *Bit B - Bit C Comparison*

Table 4.2 is a summary of the peak loads that were reached, as failure, for each core that was statically loaded while Figure 4.6 is a graphical comparison of the peak loads.

Table 4.2 Summary of Peak Load Achieved

Project ID	P_{ult} (N)	
	Bit B	Bit C
A	158	88
B	273	329
C	244	271
D	143	166
E	286	284
F	154	169
G	34	26
H	71	195
Average	170	191
Maximum	286	329
Miniumum	34	26

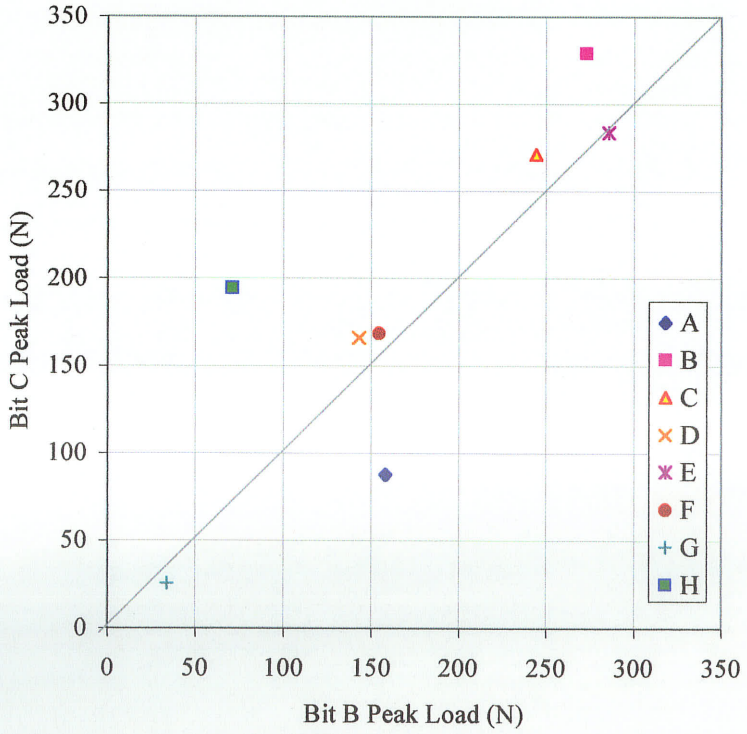

Figure 4.6 Peak Static Load of Bit B and Bit C

4.2.1.2 *Moisture Sensitivity Analysis*

AASHTO T283-89 *Resistance of Compacted Bituminous Mixture to Moisture Induced Damage* and the corresponding ASTM D4867/D4867M-96 *Standard Test Method for Effect of Moisture on Asphalt Concrete Paving Mixtures* standard test methods were followed to conduct a moisture sensitivity analysis of the mixtures. The test was performed on the Bit B mix only. During conditioning, the Bit C samples disintegrated and could not be tested.

Table 4.3 is a summary of the peak loads that were reached before failure for each Bit B core that was statically loaded according to the indirect tensile strength test. The conditioned samples were the cores that experienced moisture conditioning as outlined in Section 3.3.1.2. The control samples are the cores that were tested without moisture conditioning.

The conditioned sample from Project G failed during the conditioning process and the control sample failed during the temperature conditioning process; therefore no data is reported for Project G.

Table 4.3 Summary of Peak Load

Project ID	P_{ult} (N)	
	Conditioned	Control
A	180	158
B	34	60
C	81	79
D	52	40
E	30	78
F	68	136
G	n/a	n/a
H	48	20
Average	70	82
Maximum	180	158
Miniumum	30	20

Figure 4.7 shows a comparison of peak loads that the control samples reached versus the peak loads that the conditioned samples reached.

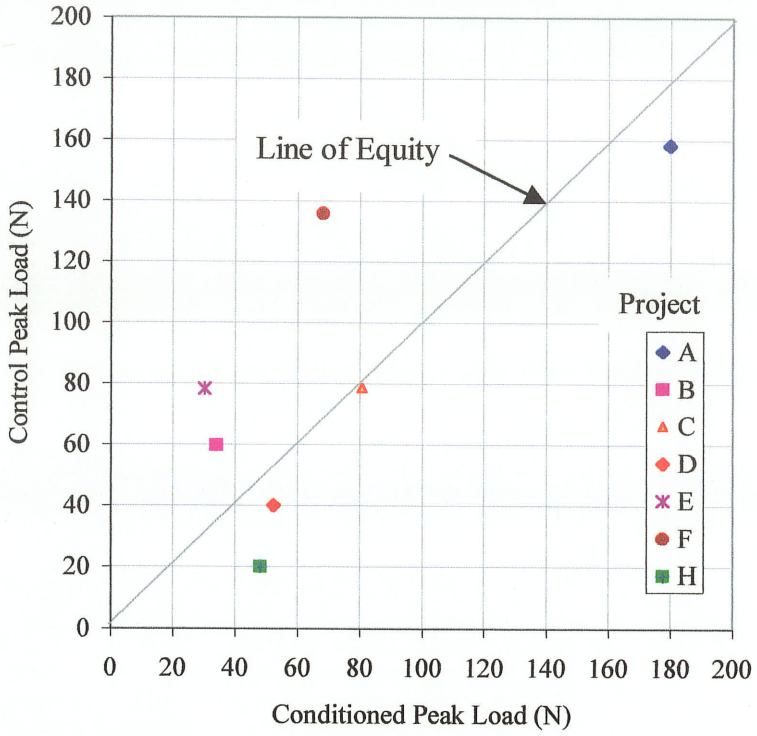

Figure 4.7 Peak Load of Conditioned Samples and Control Samples

4.2.2 Dynamic Testing

Dynamic loading of the specimens was conducted in accordance with LTPP Protocol P07. The data acquisition system recommended by P07 should be able to record 500 points per load cycle, time, temperature, load and four deformation measurements. The data acquisition system used was only capable of recording 200 points per load cycle and could not record temperature. LTPP Protocol P07 recommends the use of an automated data reduction and analysis system to process that data as manual data reduction and analysis is possible but impractical due to the subjective nature of manual work. Manual data reduction was utilized for the analysis in this research due to the limitation of time.

4.2.2.1 Interpretation of Data

The data acquisition system recorded the load and the horizontal and vertical deformation response of the asphalt cores during loading. The data analysis procedure varied from the procedure outlined in LTPP Protocol P07, as did the data acquisition system.

Figure 4.8 shows the repeated haversine waveform load response that was generated and recorded by the data acquisition system. The x-axis plots the data points collected and the y-axis plots the load. The data was collected at a rate of 200 samples per second. The duration of the pulse load was 0.3 seconds followed by a rest period of 0.7 seconds. In contrast, LTPP Protocol P07 recommends a load period of 0.1 seconds with a resting period of 0.9 seconds. This loading period was found to be too short because it exceeds the capability of the loading frame in a load-controlled test. The desired load could not be reached in the specified 0.1 seconds. After numerous trial tests in the laboratory, it was concluded that a load period of 0.3 seconds was long enough to allow the load to be within 5 to 10% of the desired load. For implications of the larger load duration and shorter resting period, refer to Section 2.4.1.4.

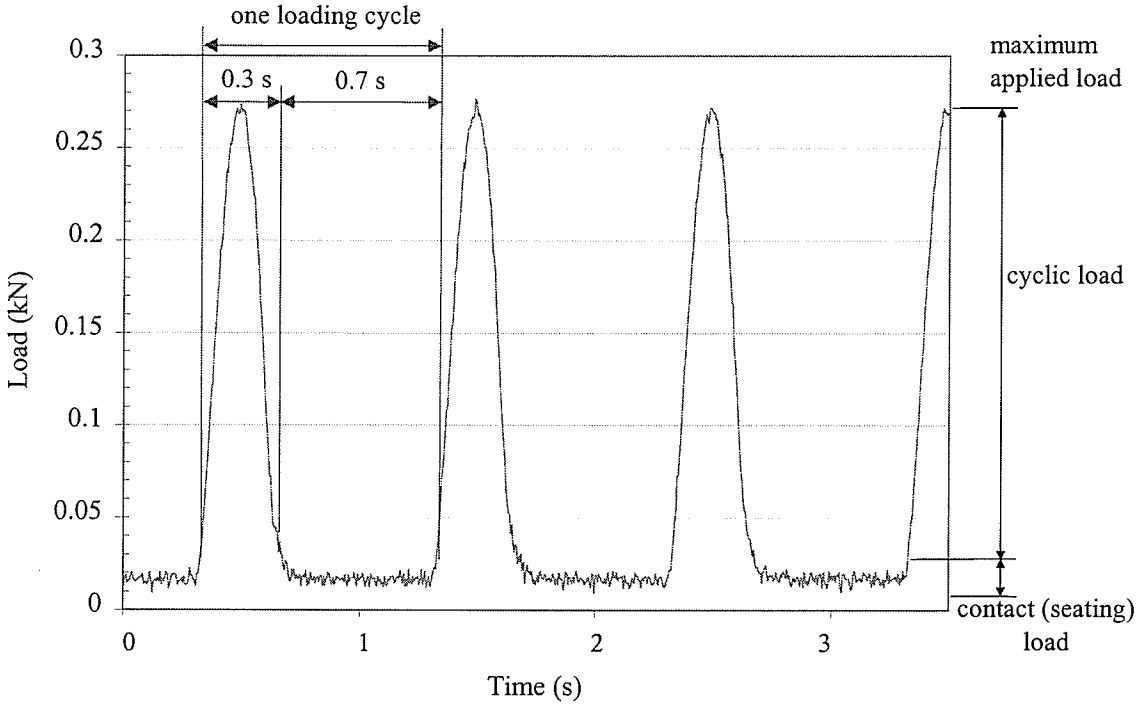

Figure 4.8 Typical Form of a Cyclic Load Pulse

The contact load was approximately 10% of the maximum load applied to the asphalt core. This load was placed on the specimen in order to maintain contact between the loading strip and the specimen and the numeric value was entered into the data acquisition system. While the cyclic load was being applied to the asphalt specimen, the horizontal deformations were closely monitored to ensure that they stayed within the recommended 0.038 to 0.089 mm range.

In accordance to LTPP Protocol P07, the load applied to the asphalt core had to produce horizontal deformations of 0.038 to 0.089 mm. This deformation range was recommended for the use of 100 mm (4 inch) cores, but was also used for the 150 mm (6 inch) cores that were tested at the University of Manitoba, as a conservative estimate.

The lower limit of the deformation range was used to prevent excess noise and drift associated with the sensors, while the upper limit was provided to ensure that the non-linear range of response of the sample was not reached. If the lower limit was not reached or the upper limit was exceeded, the test was stopped and a minimum recovery time of 5 minutes was allowed before reapplying a larger or smaller load.

LTPP Protocol P07 recommends recording five cycles of loading and corresponding deformation and usage of three cycles for analysis. At the University of Manitoba, the load was cycled for 60 seconds (60 cycles) and cycles 56, 57 and 58 were used for analysis. This was done to ensure that the horizontal deformations stayed within the ranges of 0.038 mm to 0.089 mm and to maintain some consistency with the testing procedure.

4.3 FWD Data

FWD testing was conducted and the raw deflection data was obtained from MTGS. The pavement deflection response was examined using the raw data obtained by John Emery. This enabled a comparison between the Bit B/Bit B structure and the Bit B/Bit C structure.

A Dynatest Falling Weight Deflectometer (FWD) was used to determine pavement deflections under applied loads. Load levels of 25, 40, 60 and 70 kN were imposed on the asphalt layers. Two drops are made at each load level at approximately 100 m apart along each test section, until ten test stops were completed.

The deflection response from the two-drops at each load level were averaged for each of the ten test locations. The 60 kN load level deflections were plotted and Equation 4.1 was used to verify the shape of the deflection basin. This was to identify any abnormal deflection values and to ensure that the deflection response decreased as the distance from the load plate increased.

$$d_{1200} < d_{900} < d_{600} < d_{450} < d_{300} < d_{200} < d_0 \qquad (4.1)$$

where

1200, 900, 600, 450, 300, 200, 0 = sensor distance from the center of load plate (mm)

d = deflection

The deflection response of a 60 kN load are plotted in Figures 4.9 and 4.10 for the Bit B/B and Bit B/C sections, respectively. The deflection bowls for the Bit B/Bit B test section are similar to the deflection bowls for the Bit B/Bit C section. Note, that the deflection measurements plotted are the average values for the entire test section (average of the ten test locations).

Although the deflection response of both pavement structures were of the same shape and trend, the Bit B/Bit C pavement structure exhibited generally greater deflections. This could indicate that the sections consisting of Bit B/Bit C layers are less flexible.

A comparison of Bit B/B and Bit B/C deflection bowls for each project can be found in Appendix D.

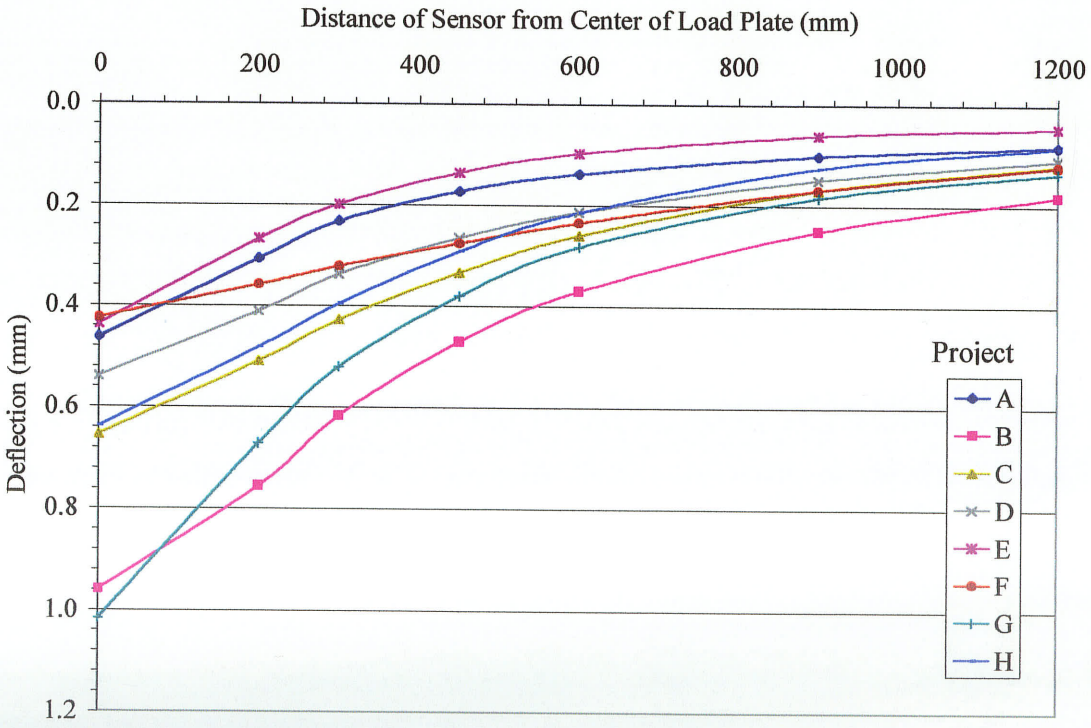

Figure 4.9 Deflection Plot of Bit B/B Sections

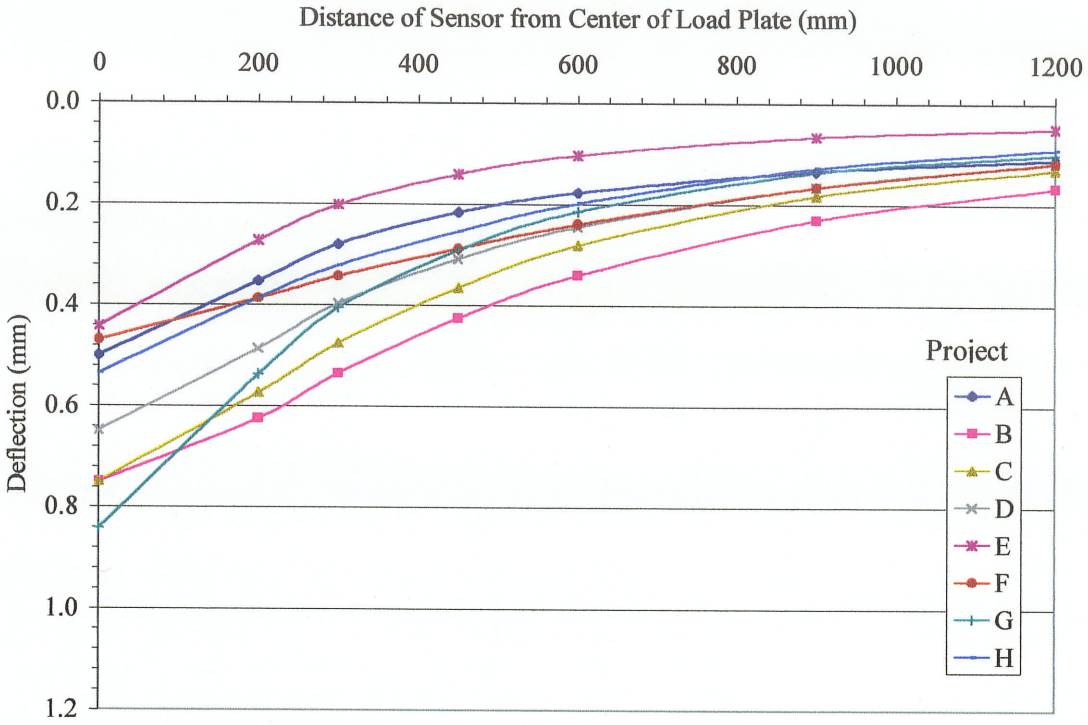

Figure 4.10 Deflection Plot of Bit B/C Sections

Chapter 5
ANALYSIS AND DISCUSSION

This chapter includes the analysis of static and dynamic test results and FWD rebounds. The results from a moisture sensitivity test are included and various comparisons of Bit B and Bit C moduli are presented.

5.1 Laboratory Testing

In the laboratory, the indirect tensile strength test along with different modes of loading was utilized to determine the tensile strength, initial stiffness, durability and resilient modulus of the samples. The tensile strength of the Bit B and Bit C mixtures were compared to each other. The initial stiffness was also found for each of the indirect tensile strength tests performed. Dynamic loading was utilized to determine the resilient modulus of the samples.

5.1.1 Static Loading

From static loading, the tensile strength, horizontal stresses and strains, and initial stiffness was calculated and examined. A comparison between the Bit B and Bit C mixes was made and the durability of the mixes was analyzed.

5.1.1.1 Tensile Strength

The tensile strength, S_T, of each sample was calculated according to ASTM D4123-82 (1995) using Equation 5.1.

$$S_T = \frac{2 P_{ult}}{\pi t D} \qquad (5.1)$$

where

S_T = tensile strength (kPa)
P_{ult} = ultimate applied load (kN)
t = thickness of specimen (m)
D = diameter of specimen (m)

The tensile strength that was experienced by the Bit B and Bit C specimens are shown in Figure 5.1. The peak load achieved and the tensile strength for each project can be found in Appendix E.

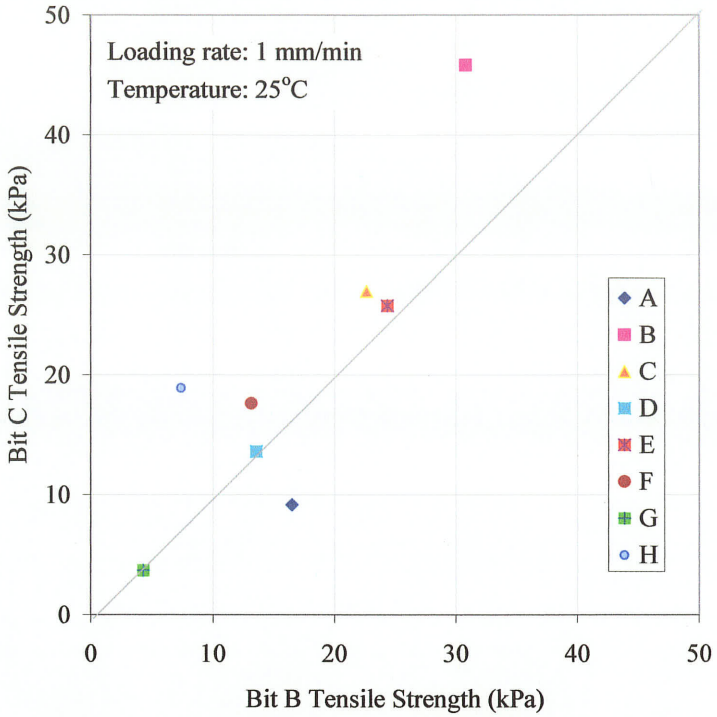

Figure 5.1 Tensile Strength from Static Test

Generally, the Bit C mixes demonstrated similar or higher tensile strengths than the corresponding Bit B mixes at each test location. The line of equality is shown to clearly identify when the Bit B and Bit C samples had equal strength. The greater tensile strength of the Bit C mix can be explained by reviewing the material properties of the mixes. The Bit C mixes consistently have lower asphalt contents and smaller aggregate size. The presence of smaller aggregates in Bit C mixes contribute to a higher tensile strength observed as there are larger specific surfaces providing better aggregate to binder bond. This finding may be limited to the test boundary conditions and not representative of field loading. In the latter case, the surrounding material will provide confinement not simulated in this test.

However, the tensile strength for both the Bit B and Bit C mix appears to be very low due to the use of softer binders. Most Projects used penetration grade 150-200 or PG 58-34 asphalt binder. The slow rate of loading could also contribute to the low tensile strengths.

Table 5.1 summarizes the tensile strength values for the Bit B and Bit C mix obtained from the indirect tensile strength test at 25°C. The B:C ratio is included. The tensile strength B:C ratio

ranges from 0.39 to 1.80, with two projects showing greater Bit B strength than Bit C, one project having the same tensile strength values and the remaining five demonstrating greater Bit C tensile strength.

Table 5.1 Summary of Tensile Strength

Project ID	Tensile Strength (kPa)		
	Bit B	Bit C	B:C ratio
A	16.5	9.2	1.80
B	30.8	45.8	0.67
C	22.6	27.0	0.84
D	13.6	13.6	1.00
E	24.3	25.8	0.94
F	13.2	17.6	0.75
G	4.3	3.7	1.17
H	7.4	18.9	0.39
Maximum	30.8	45.8	1.80
Minimum	4.3	3.7	0.39
Average	16.6	20.2	0.95

From the indirect tensile strength test, the Bit C mix has approximately 25% greater tensile strength than the Bit B mix. The greater tensile strength of the Bit C mix can be explained by reviewing the material properties of the mixes. Bit C mixes have lower asphalt contents and consistently show higher tensile strengths than the Bit B mix. The presence of the smaller aggregates in the Bit C mix also contributes to the higher tensile strength observed as there are greater surfaces providing better aggregate to binder bond.

The standard indirect tensile strength test has not shown high repeatability and a minimum of 3 tests should be completed to reduce random test variability. Because of the difficulty and cost involved with obtaining field samples and due to the premature failure of some of samples at the 25°C temperature, test results of only one sample per site were reported.

5.1.1.2 Horizontal Strain

The horizontal strain during loading was calculated using Equation 5.2. A summary of the tensile stress versus tensile strain for the Bit B and the Bit C samples can be found in Figure 5.2 and Figure 5.3, respectively.

$$\varepsilon = \frac{(HB + HF)}{2l} \qquad (5.2)$$

where

ε = microstrain (mm/mm)

HB = back horizontal displacement (mm)

HF = front horizontal displacement (mm)

l = gauge length (mm)

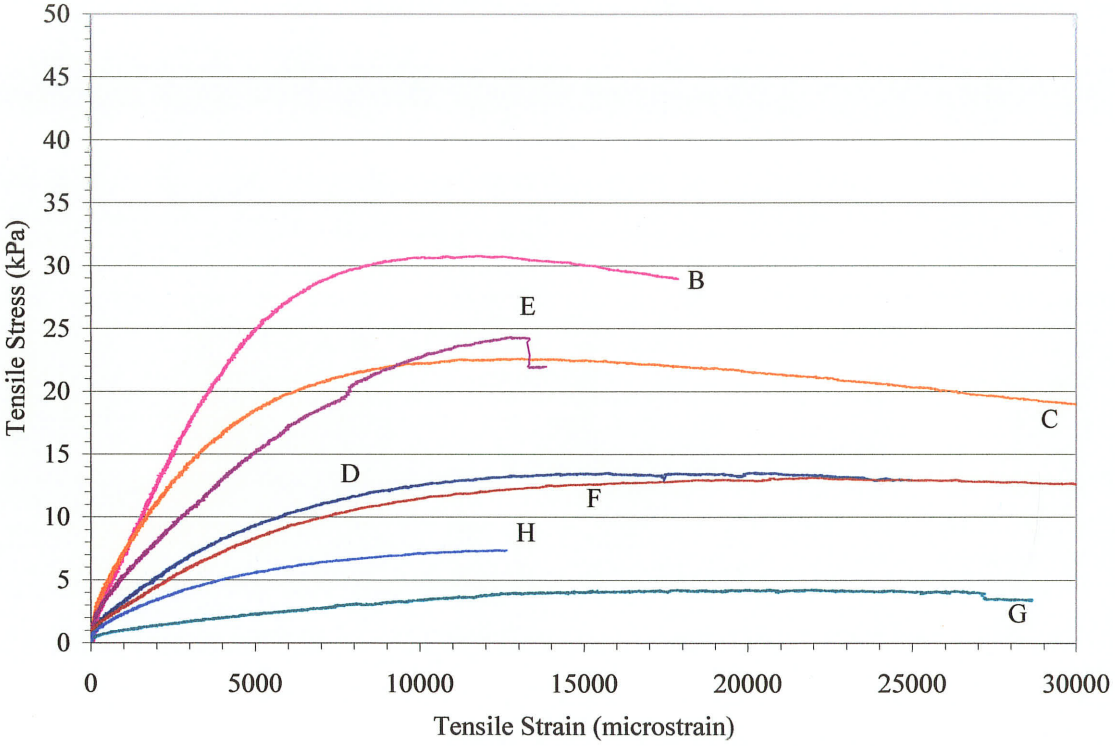

Figure 5.2 Stress versus Strain for Bit B Mixes

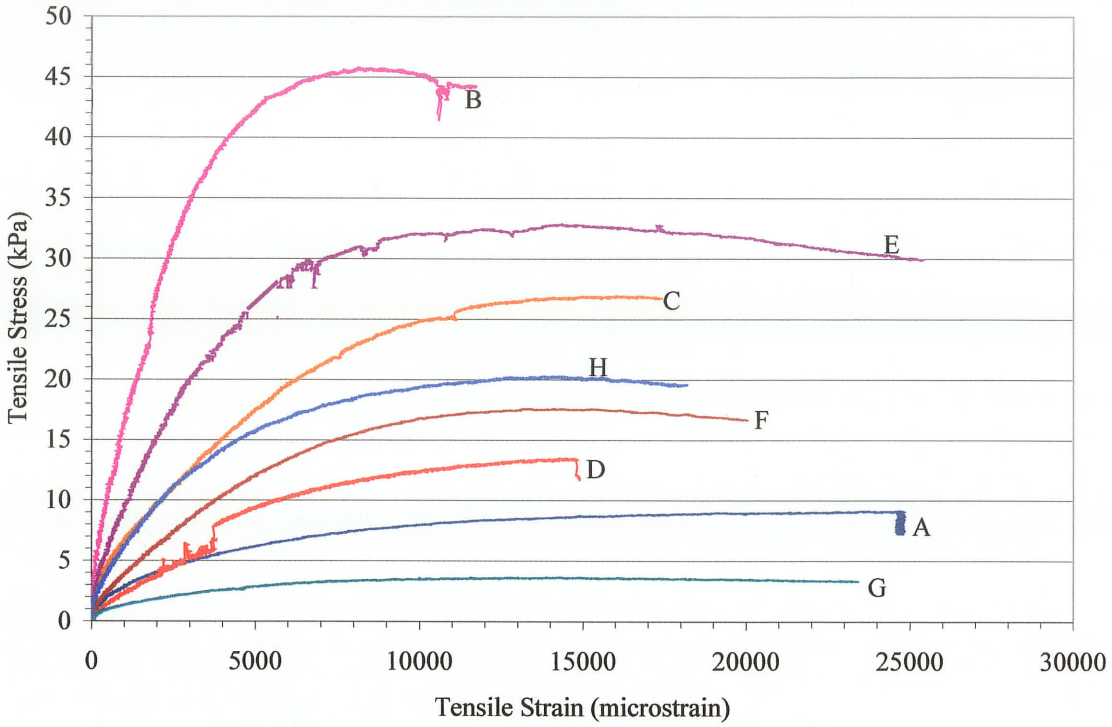

Figure 5.3 Stress versus Strain for Bit C Mixes

5.1.1.3 Initial Stiffness

In this research, the initial stiffness is defined as the stress divided by strain in elastic range of the asphalt specimen subjected to static loading during the indirect tensile strength test, as shown by Figure 5.4.

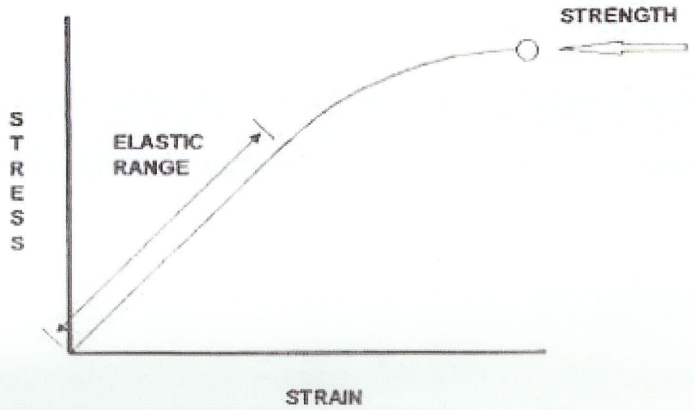

Figure 5.4 Elastic Range of the Static Indirect Tensile Strength Test *(ERES, 2001)*

The initial stiffness was calculated at 25% of the peak load achieved at failure during static loading using the indirect tensile strength test, as shown in Figure 5.5.

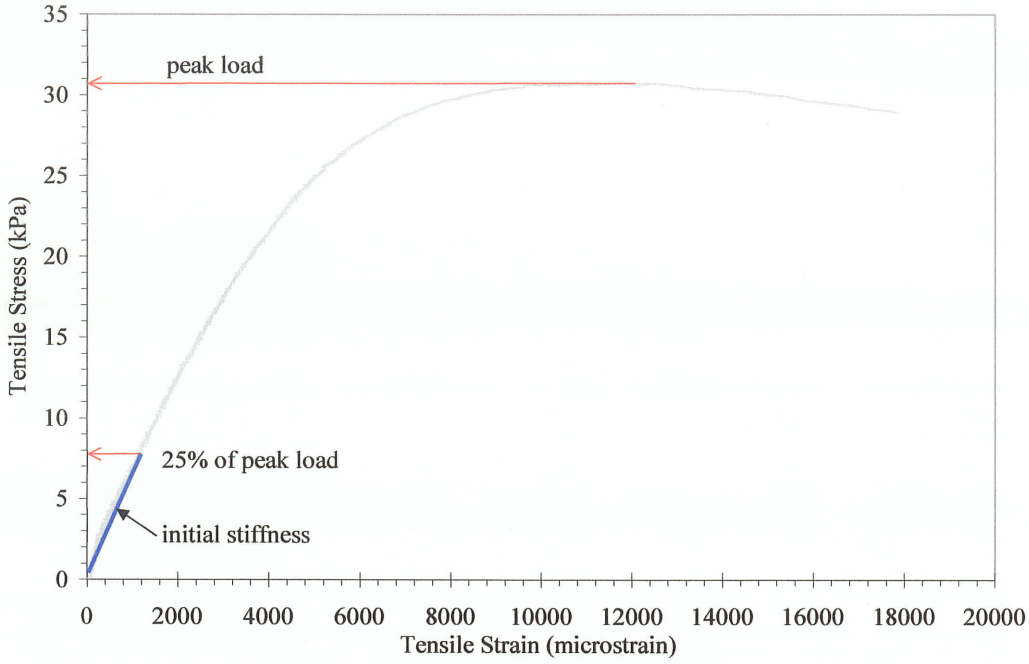

Figure 5.5 Initial Stiffness at 25% of the Peak Load

Figure 5.6 is a magnified example of the raw data at 25% of the peak load. During the analysis, a linear trendline was added to the raw data to calculate the initial stiffness of the specimen by calculating the slope of the line. This procedure was done for each specimen that was tested.

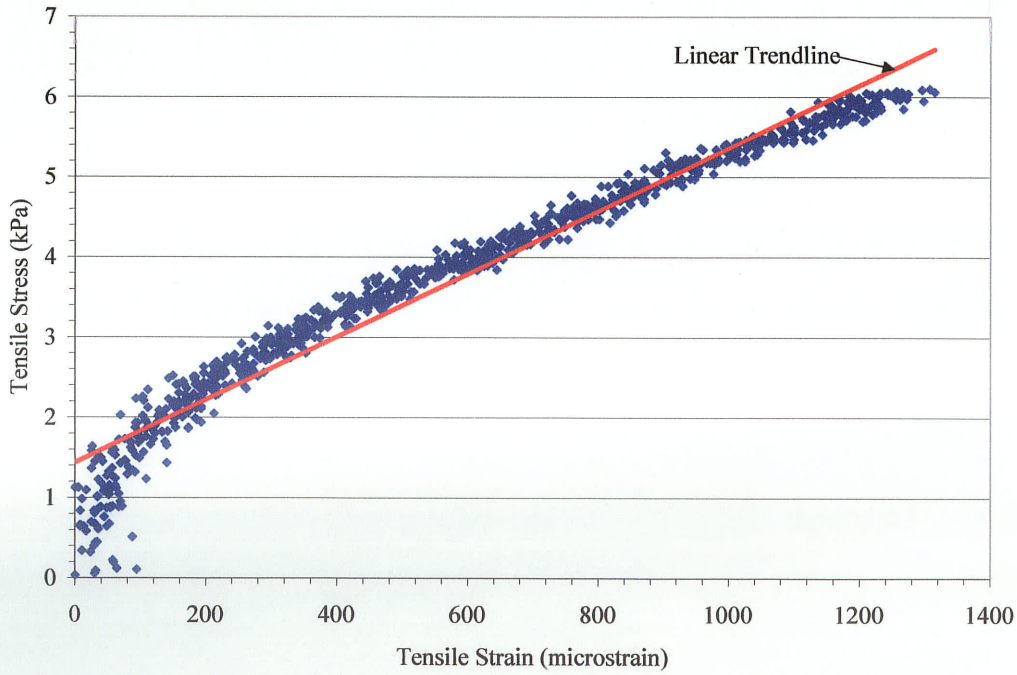

Figure 5.6 Stress versus Strain Data used to Calculate the Initial Stiffness

Figure 5.7 shows the relationship between the initial stiffness of the Bit B and Bit C mixes. project B has been highlighted because the Bit C sample had an extremely high initial stiffness. Although the Bit C sample from Project B was 'out of the range' of the other projects, the B:C ratio of the initial stiffness values were comparable to the other Projects, as shown in Table 5.2.

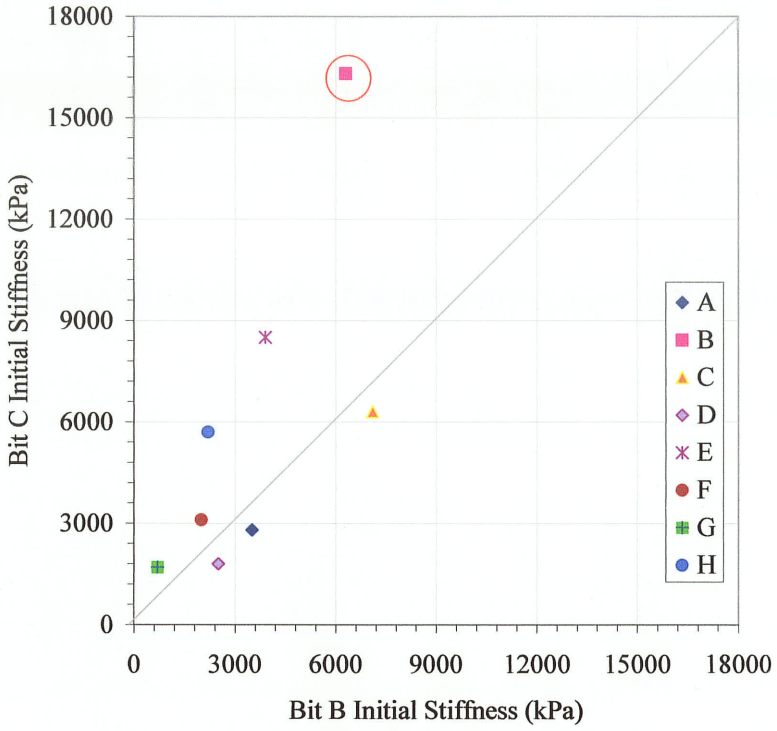

Figure 5.7 Initial Stiffness From Static Testing

Table 5.2 Summary of the Initial Stiffness Values

Project ID	Initial Stiffness (kPa)		
	Bit B	Bit C	B:C ratio
A	3500	2800	1.25
B	6300	16300	0.39
C	7100	6300	1.13
D	2500	1800	1.39
E	3900	8500	0.46
F	2000	3100	0.65
G	700	1700	0.41
H	2200	5700	0.39
Maximum	7100	16300	1.39
Minimum	700	1700	0.39
Average	3525	5775	0.76

From the B:C stiffness ratios shown in Table 5.2, three projects had greater Bit B initial stiffness values than the corresponding Bit C samples. The greatest variance between mixes was demonstrated in Project B and Project H, were the Bit C mixture was 2.6 times greater than the Bit B mixture. The smallest variance between the two mixtures was demonstrated in Project C, where the Bit B mixture was 1.1 times greater than the corresponding Bit C mixture.

5.1.1.4 Moisture Sensitivity

Figure 5.8 is a plot of the Bit B cores that were not conditioned to the Bit B cores that were conditioned with the corresponding strength ratios shown. A tensile strength ratio of 0.80 for the conditioned samples to the control (unconditioned) samples is the limiting value to determine if the mixture is sensitive to moisture (shown by the -20% strength line). Data points falling above the line indicate the mixture to be sensitive to moisture.

As shown by Figure 5.8, there is no definitive trend in the moisture sensitivity of the Bit B mixture. Three Projects, B, E and F showed to be sensitive to moisture. Project C Bit B mixture does not appear to be sensitive to moisture. Projects A, D and H show that the conditioned samples had greater tensile strength than the control samples. The conditioned sample from Project G failed during the conditioning process and the control sample failed during the temperature conditioning process, and therefore there is no data reported for Project G. It can be concluded that the Bit B mixture from Project G is very sensitive to moisture.

It appears that the sample size is too small to indicate any general trend. Therefore, a conclusive statement about the durability of the Bit B mix cannot be made. Bit C samples were prepared and the moisture conditioning process was started. The samples that were used as the conditioned samples disintegrated once placed in the water bath at the 60C temperature, and therefore could not be tested.

It is known that high air voids can have a detrimental effect on the moisture sensitivity of the mix. The Bit C mix has higher air voids than the Bit B mix, which could be the main factor for the high sensitivity of moisture in the Bit C mix. It has also been stated, that excessive fines or low asphalt content in a mix can lead to a decrease in durability (Shatnawi and Van Kirk, 1993). The excess fines contribute to the breakdown of aggregates.

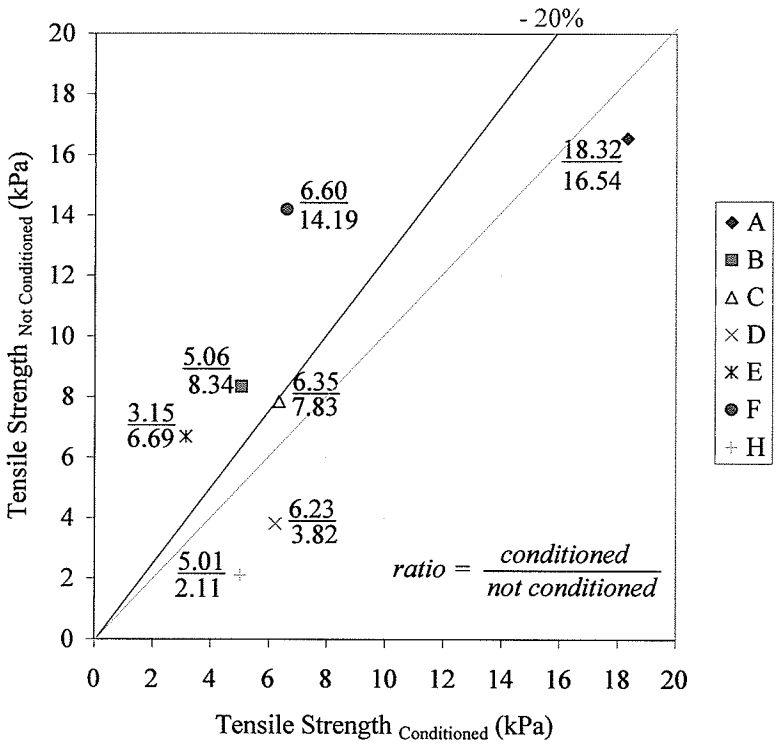

Figure 5.8 Tensile Strength of the Moisture Conditioned versus Control Bit B Mixes

5.1.2 Dynamic Testing

The load pulse that was recorded by the data acquisition system was analyzed to determine the maximum load, contact load and cyclic load. The maximum and contact load were determined by examining the raw data. The cyclic load was calculated by subtracting the contact load from the maximum load. The cyclic load is the load used to calculate the resilient modulus of the asphalt specimen in accordance with LTPP Protocol P07.

Figure 5.9(a) shows data from cycles 56, 57, and 58 of the horizontal deformation response to loading. As shown by Figure 5.9(a), the overall horizontal deformation to the sample increased with each additional cycle applied. Shown by Figure 5.9(b), the raw data was filtered and reduced through a 10-point moving average to decrease the noise experienced by the LVDTs during testing.

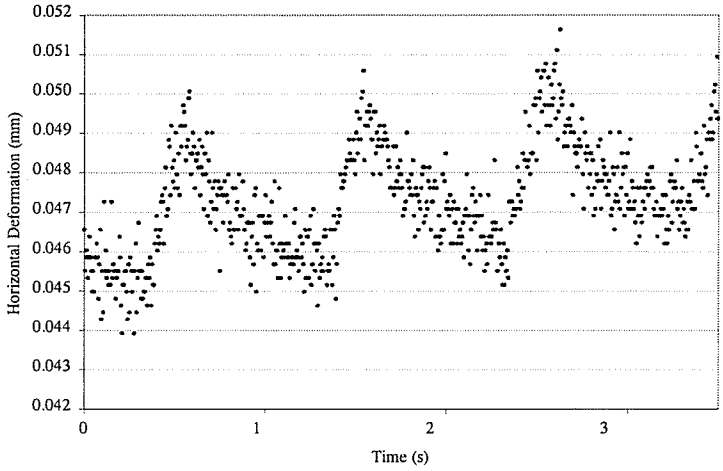

(a) Time-deformation test results

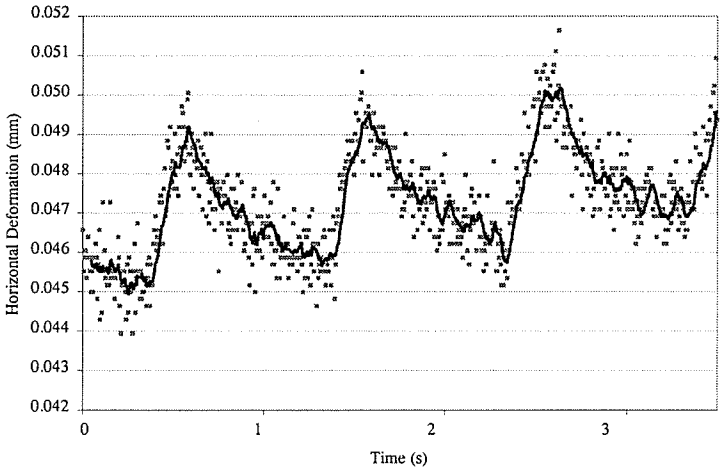

(b) Fitting a moving average to the raw data

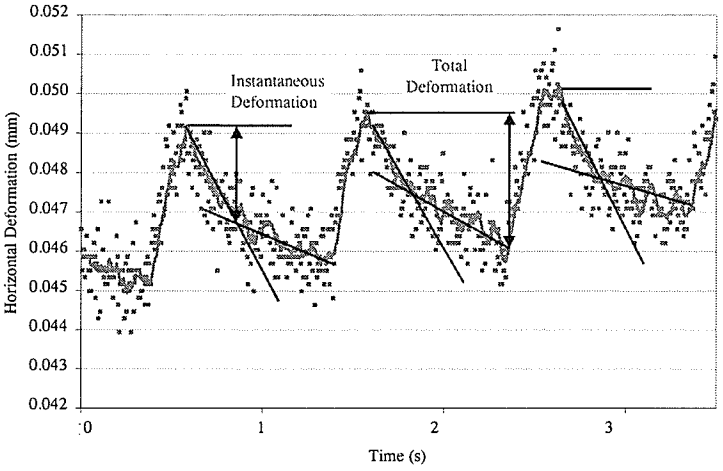

(c) Defining instantaneous and total deformations in three consecutive load cycles

Figure 5.9 Analysis of Deformation Data

The moving average was used to define two straight regression lines, in accordance to LTPP Protocol P07, as shown by Figure 5.9(c). The unloading portion of each cycle can be idealized into two, linear segments; the first shows a rapid rebound of deformation during the removal of the cyclic load while the second is the continued rebound of deformation after the removal of the cyclic load. The intersection of the two segments is used to identify the instantaneous portion of the deformation, while the total deformation is the difference between the peak deformation and the deformation at the end of the cycle, as shown in Figure 5.9(c).

The lines represent the unloading portion of the load cycle. The regression line was drawn on the instantaneous deformation portion of the unloading cycle while the second regression line was drawn from the start of the next load cycle along the moving average line of the current cycle. The intercept of the first straight regression line and the moving average line was used to illustrate the peak deformation experience by each cycle. The intercept of the two regression lines was used to calculate the instantaneous deformation while the intercept of the second regression line and the moving average line at the start of the next cycle was used to calculate the total deformation. The numerical values of the intercepts were found directly on the Excel plot.

The horizontal deformations from cycles 56, 57 and 58 were used to calculate the instantaneous and total resilient modulus values of each cycle. The average total resilient modulus value from the three cycles is reported. It has been found that the instantaneous recovered deformations are not well defined, whereas the total recovered displacements are easily defined (Von Quintus and Killingsworth, 1996).

5.1.2.1 Resilient Modulus

It should be noted that the initial stiffness calculated from static loading and the resilient modulus calculated from the dynamic loading will not be the same nor comparable. The differences between the stiffness values obtained from the two tests can be explained by the differences in the loading rates. Faster loading rates have higher computed stiffnesses because there is less time for the asphalt material to demonstrate a viscous response.

The resilient modulus of each asphalt core was calculated at each test temperature using raw deformation data, cyclic load, diameter and the thickness. As presented in Equation 5.3, the resilient modulus calculation used values obtained from the original deformation data.

$$Mr\{I,T\} = \frac{l \times Pcyclic_{avg}}{\Delta H_{avg}\{I,T\} \times d_{avg} \times t_{avg}} \qquad (5.3)$$

where

$M_r\{I,T\}$ = Instantaneous or Total resilient modulus (MPa)

l = Gauge length (mm)

$Pcyclic_{avg}$ = Average of 3 load cycles (N)

$H_{avg}\{I,T\}$ = Average instantaneous or total deformation of 3 cycles (mm)

d_{avg} = Average diameter of asphalt core (mm)

t_{avg} = Average thickness of asphalt core (mm)

The total resilient modulus takes into account the instantaneous recoverable deformation and the time dependent recoverable deformation during the rest period of one cycle of loading. The instantaneous resilient modulus is determined from the instantaneous deformation only. Only the total resilient modulus will be documented throughout this report.

Resilient Modulus at 10°C

Figure 5.10 compares the resilient modulus values for the Bit C mix to its corresponding Bit B mix that was calculated at 10°C using Equation 5.3. Project B had an extremely high Bit C resilient modulus value.

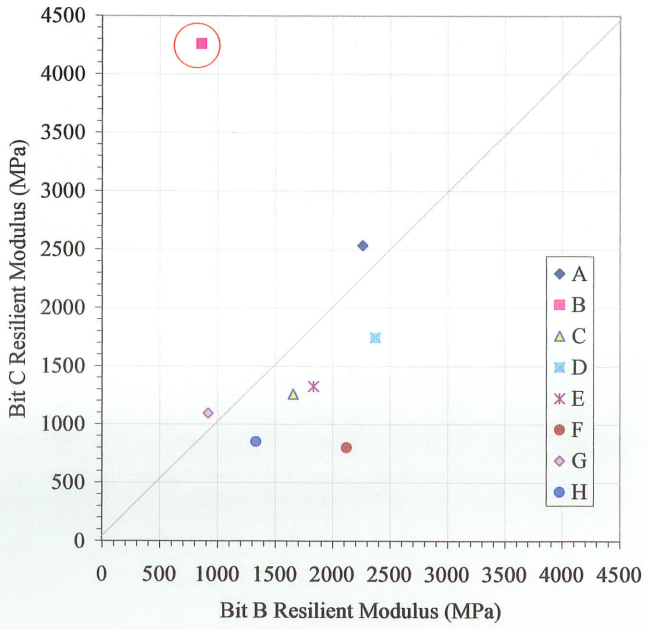

Figure 5.10 Resilient Modulus at 10°C

Table 5.3 Summary of Resilient Modulus at 10°C

Project ID	Resilient Modulus (MPa) 10°C		
	Bit B	Bit C	B:C ratio
A	2261	2535	0.89
B	858	4262	0.20
C	1656	1261	1.31
D	2370	1746	1.36
E	1833	1327	1.38
F	2120	803	2.64
G	917	1096	0.84
H	1333	853	1.56
Maximum	2370	4262	2.64
Minimum	858	803	0.20
Average	1669	1735	1.27

Table 5.3 is a summary of the resilient modulus values and the B:C ratio. The Bit B mix ranged from 858 MPa to 2370 MPa while the Bit C mix had a wider range due to the high Bit C modulus for Project B. The Bit B resilient modulus is, on average, 30% greater than its corresponding Bit C resilient modulus for the samples tested in this project. This sample size is too small to conclude that the Bit B mix has a greater resilient modulus than the Bit C mix at 10°C.

Resilient Modulus at 25°C

After the resilient modulus and creep tests were conducted at the 10°C temperature, they were conditioned in a temperature-controlled environment at 25°C for 24 hours. The resilient modulus test was then conducted. Figure 5.11 shows the resilient modulus comparison of all the projects that had cores for the Bit B and Bit C mix. Similar to the 10°C temperature, the Bit C mix from Project B has an extremely high resilient modulus value.

There were no test results for the Bit C sample from Project D because the sample failed during the temperature conditioning at the 25°C temperature. The Bit B sample from Project G was destroyed during testing at the 25°C temperature and therefore there is no test data. From the samples that were tested, the Bit B modulus values ranged from 250 MPa to 600 MPa, as reported in Table 5.4. With the exception of Project B, the Bit C mix ranged from 200 MPa to 350 MPa. The Bit C mixture has a narrower resilient modulus range than the Bit B mixture. No concise

conclusion can be made about the strength comparison of the two mixtures due to the small sample size.

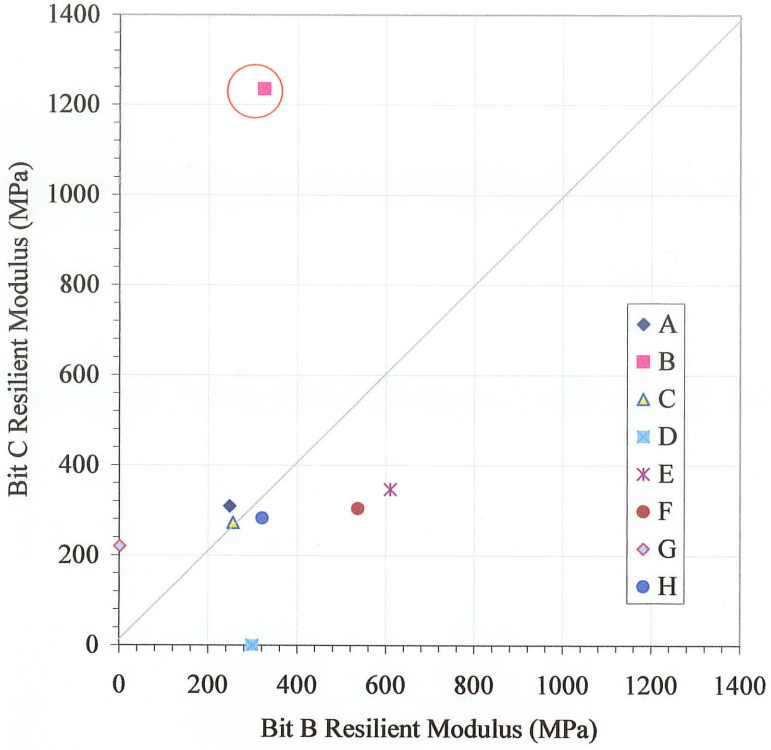

Figure 5.11 Resilient Modulus at 25°C

Table 5.4 Summary of Resilient Modulus at 25°C

Project ID	Resilient Modulus (MPa) 25°C		
	Bit B	Bit C	B:C ratio
A	248	309	0.80
B	324	1235	0.26
C	255	272	0.94
D	298	n/a	n/a
E	610	347	1.76
F	536	304	1.76
G	n/a	220	n/a
H	320	283	1.13
Maximum	610	1235	1.76
Minimum	248	220	0.26
Average	370	424	1.11

Resilient Modulus at 40 ℃

No dynamic testing was conducted at 40°C due to the limitations of the asphalt mixture. The asphalt samples that were prepared to be tested were too soft and too weak at 40°C. During the temperature conditioning process, the asphalt samples failed under self-weight. Tayebali et al. (1994) have also found that the resilient modulus could not be calculated at 40°C due to excessive vertical permanent deformations. They have reported that indirect tension testing to determine the resilient modulus should be limited to a maximum temperature of 20°C.

Temperature Ranges

Generally, the Bit B mix has higher resilient values at each temperature at which testing was conducted. The Bit B mix also exhibited a greater range of resilient modulus values than the Bit C mix, as shown in Figure 5.12. Because of the anomalous high resilient modulus values for the Bit C mix from Project B, Figure 5.12 does not include results from Project B.

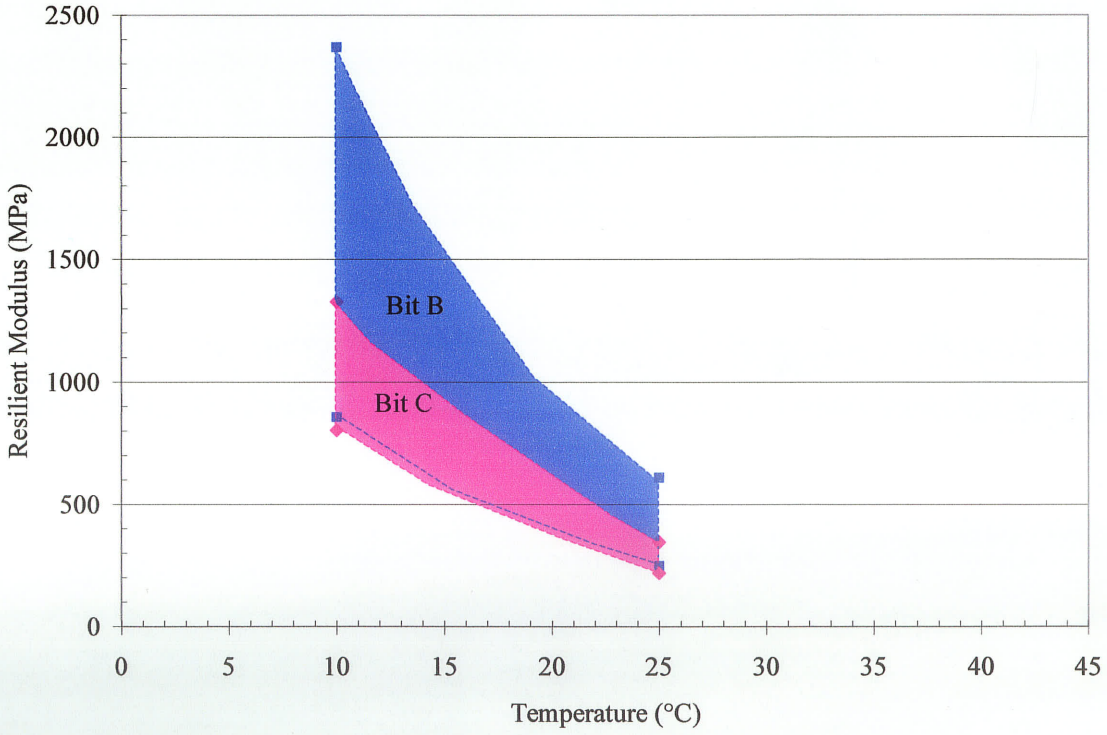

Figure 5.12 Ranges of Bit B and Bit C Mixes, Excluding Project B.

Table 5.5 summarizes the resilient modulus values determined from dynamic loading at the 10°C and 25°C temperatures. At 10°C, the B:C ratio ranges from 0.20 to 2.64. Project B had a B:C ratio of 0.20 with the lowest Bit B modulus but greatest Bit C modulus. At 25°C, the B:C ratio ranged from 0.26 to 1.76. Once again, Project B had the lowest ratio. For both the 10°C and 25°C temperatures, the Bit B mix generally had greater resilient modulus than the Bit C mix: at 10°C Bit B was 27% greater; and at 25°C Bit B was 11% greater than the Bit C.

Table 5.5 Summary of Resilient Modulus at Tested Temperatures

Project ID	Resilient Modulus (MPa)					
	10°C			25°C		
	Bit B	Bit C	B:C ratio	Bit B	Bit C	B:C ratio
A	2261	2535	0.89	248	309	0.80
B	858	4262	0.20	324	1235	0.26
C	1656	1261	1.31	255	272	0.94
D	2370	1746	1.36	298	n/a	n/a
E	1833	1327	1.38	610	347	1.76
F	2120	803	2.64	536	304	1.76
G	917	1096	0.84	n/a	220	n/a
H	1333	853	1.56	320	283	1.13
Maximum	2370	4262	2.64	610	1235	1.76
Minimum	858	803	0.20	248	220	0.26
Average	1669	1735	1.27	370	424	1.11

When analyzing the data without Project B, at 10°C the Bit B samples were 43% greater while the Bit B samples at 25°C were 28% greater than the corresponding Bit C samples.

The dynamic modulus values for the Bit B and Bit C samples tested at 25°C appear to be very low. It should be noted that the loading period for the dynamic testing was 0.3 seconds with a 0.7 second resting period, at a frequency of 1 Hz. The loading rate is greater than what was recommended in LTPP Protocol P07, which was 0.1 seconds. The loading duration and resting period implications are outlined in Section 2.4.1.4

Interpolated Resilient Modulus @ 20°C

The resilient modulus of the Bit B and Bit C asphalt samples tested was interpolated for a temperature of 20°C, as shown in Tables 5.6 and 5.7, respectively. This was done because the

effective modulus calculated from ELMOD, which is used to determine the modulus of each layer, is calculated for a temperature of 20°C. This will allow for a comparison of modulus values determined from laboratory testing and calculated from the FWD data.

There was no data for the resilient modulus from Bit C mix from Projects D nor the Bit B mix from Project G, therefore no data could be interpolated for these projects. Once again, the range of the Bit C mixture is a lot wider than the range for the Bit B mixture, due to Project B. Excluding Project B, the ranges are similar.

Table 5.6 Bit B Resilient Modulus Interpolated at 20°C

Project ID	Resilient Modulus (MPa)		
	10°C	Interpolated @ 20°C	25°C
A	2261	919	248
B	858	502	324
C	1656	722	255
D	2370	989	298
E	1833	1018	610
F	2120	1064	536
G	917	n/a	n/a
H	1333	658	320
Maximum	2370	1064	610
Minimum	858	502	248
Average	1669	839	370

Table 5.7 Bit C Resilient Modulus Interpolated at 20°C

Project ID	Resilient Modulus (MPa)		
	10°C	Interpolated @ 20°C	25°C
A	2535	1051	309
B	4262	2244	1235
C	1261	602	272
D	1746	n/a	n/a
E	1327	673	347
F	803	470	304
G	1096	512	220
H	853	473	283
Maximum	4262	2244	1235
Minimum	803	470	220
Average	1735	861	424

Figure 5.13 plots the comparison between the Bit B versus Bit C resilient modulus values interpolated at 20°C. Project B is highlighted, as the Bit C resilient modulus is extremely high. Similar to the 10°C and 25°C temperatures, the Bit B samples had greater resilient modulus values than the Bit C samples, with the exception of Project B and A. No concise conclusion can be made about the resilient modulus values due to the small sample size.

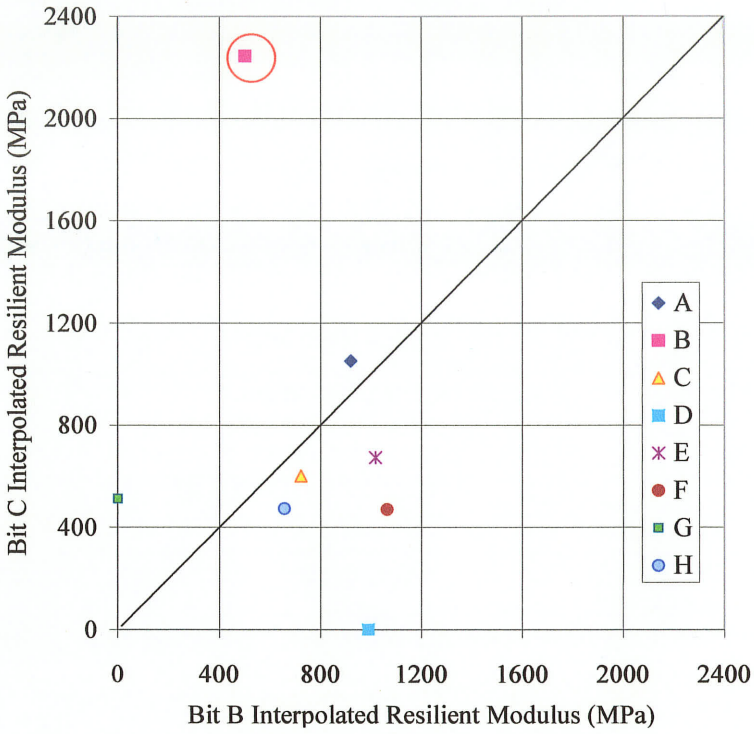

Figure 5.13 Resilient Modulus Interpolated at 20°C

5.2 Analysis of FWD Data

The FWD data that was obtained from MTGS was used to determine the resilient modulus of the entire pavement structure and the estimated resilient modulus of each pavement layer.

5.2.1 Backcalculation

An elastic layer analysis was completed using the ELMOD computer program, which uses backcalculation techniques in conjunction with surface deflections and pavement structure information to estimate the effective modulus for the entire pavement structure.

An assumption was made that the modulus of the subbase material was twice the modulus as the subgrade material. This value was used because when ELMOD was run without any assumption, ELMOD used a default ratio of 1.8-2.1. To maintain consistency, a ratio of 2.0 was used.

The total asphalt layer thickness and each individual layer thickness was measured in the laboratory from the cores that were extracted. The layer thickness measured at the University of Manitoba were compared with that reported by MTGS to ensure that the pavement structure was consistent. The measured pavement and granular base thicknesses reported by MTGS are found in Appendix F, Table F-1. These asphalt and aggregate base thicknesses were used by JEGEL. The thickness values used by the University of Manitoba can be found in Appendix F, Table F-2. The highlighted values are the values that were slightly different due to the information source, but will not significantly affect the results.

Figure 5.14 shows the effective modulus calculated by ELMOD at the University of Manitoba. The highlighted data point on Figure 5.14 is Project B. Project B showed high effective modulus values for the Bit B over Bit B and Bit B over Bit C section compared to the other seven projects tested.

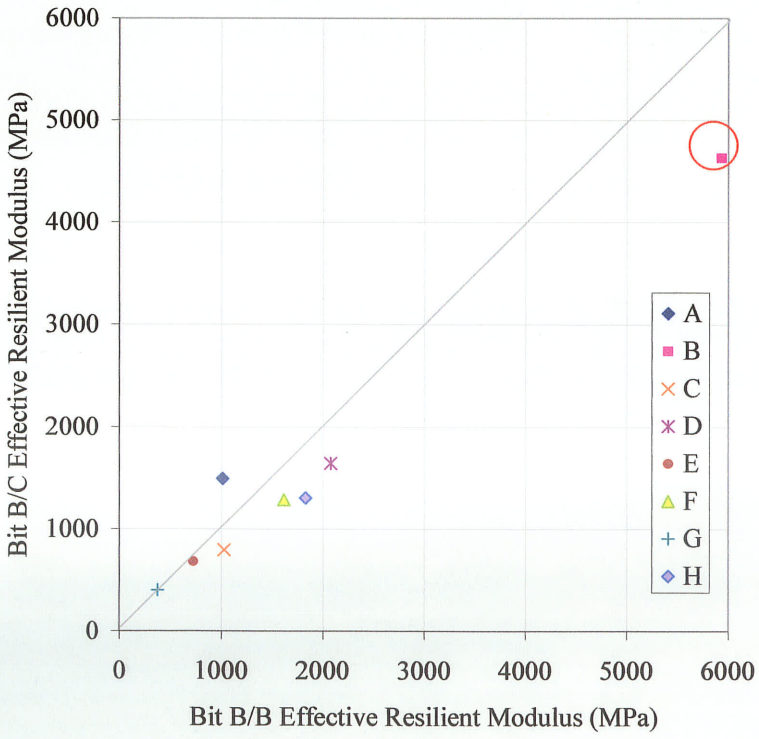

Figure 5.14 Backcalculated Effective Modulus

Project B, located on PTH 9 near Winnipeg Beach, is unique. The asphalt concrete mix from Project B contained 70% recycled asphalt pavement (RAP) and was constructed with 200-300 penetration grade asphalt. The other seven projects contained only 15 to 30% RAP and were constructed with 150-200 penetration grade asphalt. The high percent of RAP could explain the high modulus values obtained at this stage of analysis. Subsequent analysis showed that Project B always stood out from the other seven projects in this research.

Some of the projects showed similar effective modulus values for the two different pavement structures. As the effective modulus values increased, the Bit B over Bit B sections demonstrated a slightly higher effective modulus value than the Bit B over Bit C sections. The Bit B/B resilient modulus ranged from 375 to 6000 MPa while the Bit B/C resilient modulus ranged from 400 to 4600 MPa. These ranges include Project B, which shows much higher resilient modulus values.

Table 5.8 summarizes the effective modulus values for the Bit B over Bit B and the Bit B over Bit C pavement structures using ELMOD. For the modulus values obtained with ELMOD, the B:C ratio ranged from 0.68 to 1.40; with most ratios falling above 1.0. This indicates that the modulus values for the Bit B over Bit B sections generally have a greater stiffness than the Bit B over Bit C section.

Table 5.8 Effective Modulus Values

Project ID	ELMOD (MPa) Effective Modulus		
	Bit B/B	**Bit B/C**	**B:C ratio**
A	1012	1494	0.68
B	5935	4631	1.28
C	1026	796	1.29
D	2075	1645	1.26
E	725	680	1.07
F	1615	1288	1.25
G	375	400	0.94
H	1829	1305	1.40
Maximum	5935	4631	1.40
Minimum	375	400	0.68
Average	1824	1530	1.15

Although Project B had extremely high resilient modulus values, the B:C ratio falls within the minimum and maximum values. Project H has the greatest difference between the resilient modulus values, with the Bit B/B pavement having a 40% greater resilient modulus than the Bit

B/C section for that Project. Project G had the smallest variance between the two test sections; the Bit B/C section was 6% stiffer than the Bit B/B section.

A comparison was made between the effective modulus of the asphalt concrete layer that was calculated by JEGEL and the effective modulus was that calculated for this research (University of Manitoba). Figure 5.15 shows the comparison for all the eight projects. Once again, the highlighted data points indicate Project B. The backcalculated resilient modulus from the two sources, JEGEL and University of Manitoba, are very similar and confirm that the procedure is reliable.

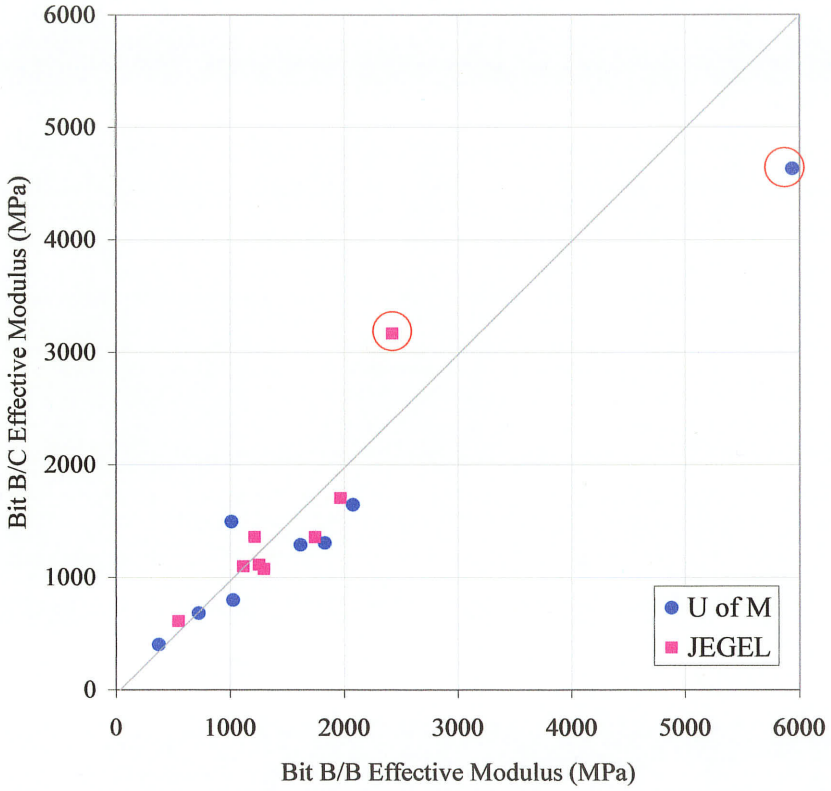

Figure 5.15 Effective Modulus calculated at U of M and the Consultant.

Both parties used the computer program ELMOD for the backcalculation process. The asphalt layer and aggregate thicknesses that were used for calculations varied slightly, as shown in Appendix F but will not significantly affect the results. This comparison was made to ensure that test results obtained by University of Manitoba using ELMOD were reasonable.

5.2.2 Temperature Sensitivity Analysis

In the laboratory, the asphalt specimens are tested at a constant, uniform temperature. The specimens are conditioned to the test temperature and therefore there is no temperature gradient throughout the test specimen. In the field, the asphalt concrete layer varies in temperature from the surface to the bottom of the layer. The temperature that was recorded during the FWD testing was the surface temperature of the asphalt concrete.

The backcalculated modulus values obtained from ELMOD are not corrected for temperature but can be corrected to a standard temperature by applying a temperature correction factor or equation to the data.

ELMOD has three different relationships to apply a temperature correction to the backcalculated modulus values:

1. E/E_{ref} ratio
2. exponential
3. semi-log

The correction factors and equations are approximate.

The ratio E/E_{ref} in Table 5.9 are provided to correct backcalculated modulus values, E, at any temperature ranging form -20 to 59°C to a standard temperature of 25°C. Note that these values are default values used by ELMOD and can be edited. For this study, the values in the table were not edited.

Equations 5.4 and 5.5 are two relationships that are used in the temperature sensitivity parameter in ELMOD. The regression constants in the exponential and semi-log equations, -0.06956 and -3.60 respectively, were altered until they resulted similar E/E_{ref} ratios.

$$\frac{E}{E_{ref}} = \exp\left(-0.06956\left(t - t_{ref}\right)\right) \qquad (5.4)$$

$$\frac{E}{E_{ref}} = 1 - 3.60 \log 10\left(\frac{t}{t_{ref}}\right) \qquad (5.5)$$

where

t = actual asphalt temperature at time of test (°C)

t_{ref} = reference temperature (°C)

E = backcalculated modulus (MPa)

E_{ref} = modulus at reference temperature (MPa)

Table 5.9 E/E_{ref} for Asphalt Concrete Temperatures

Temp.	E/E_{ref}	Temp.	E/E_{ref}	Temp.	E/E_{ref}	Temp.	E/E_{ref}
-20	5.988	0	2.022	20	1.150	40	0.632
-19	5.085	1	1.961	21	1.119	41	0.611
-18	4.557	2	1.903	22	1.088	42	0.590
-17	4.182	3	1.848	23	1.058	43	0.570
-16	3.891	4	1.794	24	1.029	44	0.550
-15	3.654	5	1.743	25	1.000	45	0.530
-14	3.453	6	1.694	26	0.972	46	0.510
-13	3.279	7	1.647	27	0.945	47	0.491
-12	3.126	8	1.601	28	0.918	48	0.472
-11	2.988	9	1.557	29	0.891	49	0.453
-10	2.864	10	1.514	30	0.866	50	0.434
-9	2.751	11	1.473	31	0.840	51	0.416
-8	2.646	12	1.433	32	0.815	52	0.398
-7	2.550	13	1.394	33	0.791	53	0.381
-6	2.460	14	1.356	34	0.767	54	0.363
-5	2.376	15	1.319	35	0.744	55	0.346
-4	2.297	16	1.284	36	0.721	56	0.329
-3	2.222	17	1.249	37	0.698	57	0.312
-2	2.152	18	1.215	38	0.676	58	0.295
-1	2.085	19	1.182	39	0.654	59	0.279

The equation and ratio methods are plotted at a reference temperature of 20°C and 25°C in Figures 5.16 and 5.17, respectively. These plots demonstrate the relationship between the three temperature correction methods for a temperature range of 2°C to 38°C. ELMOD stated that the exponential and semi-log equations were only valid for this temperature range and therefore the ratio method was only analyzed for this range.

At temperatures above the reference temperature, the ratio of E/E_{ref} is closer than at the lower temperatures (i.e. 0°C to 5°C). At both the 20°C and 25°C reference temperatures, the exponential and semi-log equations have similar E/E_{ref} ratios for the temperature range of 2°C to

38°C than compared to the ratio method. The exponential and semi-log methods suggest a greater variance in the resilient modulus obtained through backcalculation at lower temperatures than at higher temperatures.

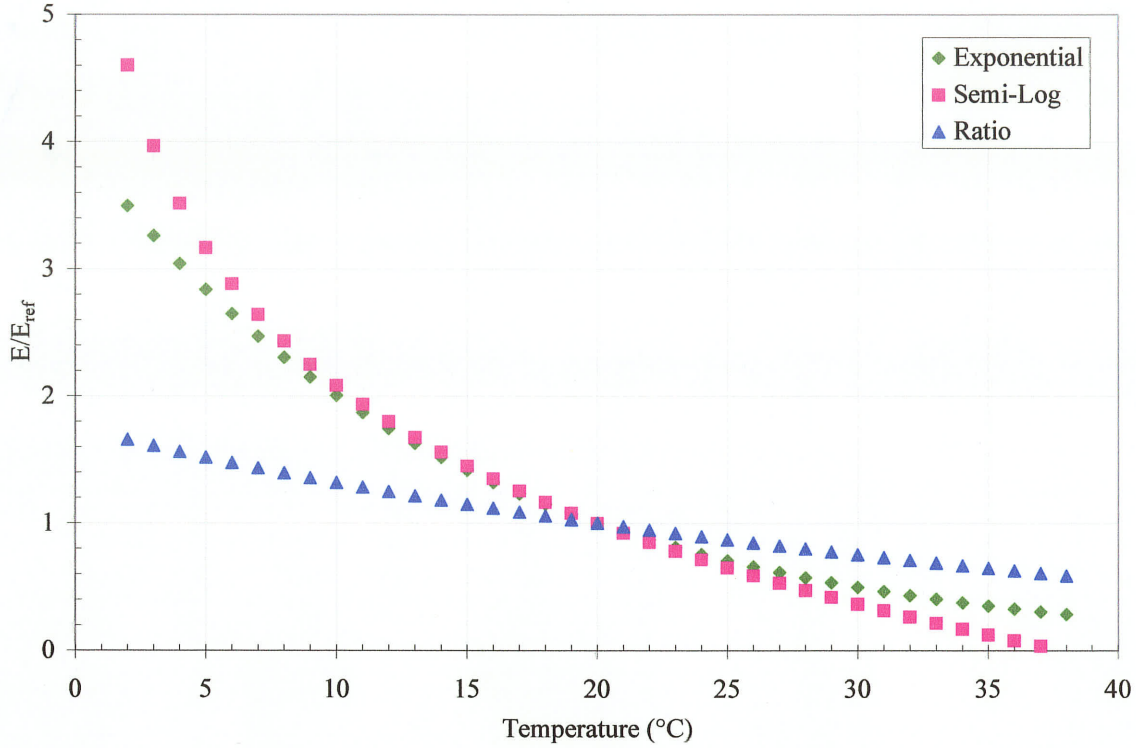

Figure 5.16 ELMOD Temperature Sensitivity Relations at 20°C Reference Temperature

From Figure 5.16, for a reference temperature of 20°C, Equations 5.6, 5.7 and 5.8 can be used for the three methods.

Semi-Log $$\frac{E}{E_{ref}} = -1.5635Ln(t) + 5.6837 \quad (5.6)$$

Exponential $$\frac{E}{E_{ref}} = 4.0197e^{-0.0696t} \quad (5.7)$$

Ratio $$\frac{E}{E_{ref}} = 0.0004t^2 - 0.0437t + 1.7273 \quad (5.8)$$

For a reference temperature of 25°C, Equations 5.9, 5.10, 5.11 can be used for the three methods.

Semi-Log $$\frac{E}{E_{ref}} = -1.5635Ln(t) + 6.0326 \quad (5.9)$$

Exponential $$\frac{E}{E_{ref}} = 5.6919e^{-0.0696t} \quad (5.10)$$

Ratio $$\frac{E}{E_{ref}} = 0.0004t^2 - 0.0502t + 1.9826 \quad (5.11)$$

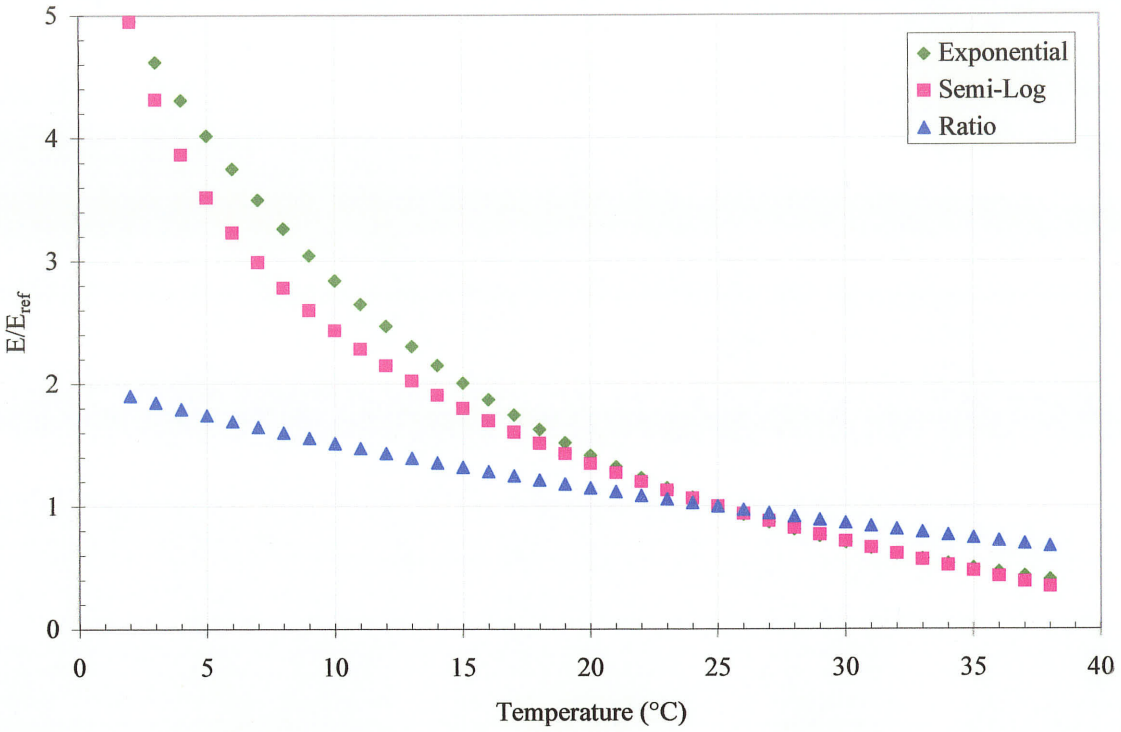

Figure 5.17 ELMOD Temperature Sensitivity Relations at 25°C Reference Temperature

Each of the three methods of temperature correction was applied to the backcalculated modulus values at the temperature the FWD testing was conducted. Tables 5.10 and 5.11 are a comparison of the Bit B/B modulus values at 25°C and 20°C, respectively. Tables 5.12 and 5.13 are a comparison of the Bit B/C modulus values at 25°C and 20°C, respectively.

Table 5.10 Bit B Modulus Comparison with Correction Factors at 25°C

Bit B

Project Identification	25°C			
	ELMOD	Exponential	Semi-Log	Ratio
A	1012	1647	1648	1242
B	5935	8404	8301	6853
C	1026	1557	1546	1221
D	2075	3621	3667	2624
E	725	2535	4765	1318
F	1615	2287	2259	1865
G	375	1064	1414	593
H	1829	2976	2979	2244

Table 5.11 Bit C Modulus Comparison with Correction Factors at 25°C

Bit C				
Project Identification	25°C			
	ELMOD	Exponential	Semi-Log	Ratio
A	1494	2431	2433	1833
B	4631	6557	6477	5347
C	796	1595	1679	1069
D	1645	2497	2478	1958
E	680	2218	3600	1152
F	1288	1955	1940	1533
G	400	1306	2119	678
H	1305	2617	2754	1754

Table 5.12 Bit B Modulus Comparison with Correction factors at 20°C

Bit B				
Project Identification	20°C			
	ELMOD	Exponential	Semi-Log	Ratio
A	1012	2332	2532	1428
B	5935	11899	12749	7881
C	1026	2205	2374	1405
D	2075	5126	5632	3017
E	725	3589	7318	1515
F	1615	3238	3469	2145
G	375	1507	2172	682
H	1829	4215	4575	2581

Table 5.13 Bit C Modulus Comparison with Correction Factors at 20°C

Bit C				
Project Identification	20°C			
	ELMOD	Exponential	Semi-Log	Ratio
A	1494	3442	3737	2108
B	4631	9284	9947	6149
C	796	2259	2578	1230
D	1645	3535	3806	2252
E	680	3141	5528	1325
F	1288	2768	2980	1763
G	400	1849	3254	780
H	1305	3705	4230	2018

A graphical comparison of Tables 5.10, 5.11, 5.12 and 5.13 is located in Appendix G.

5.2.3 Inertia Method

The Inertia Method was used to analyze the effective modulus results. This method was used in the Saskatchewan Surfacing Manual (1984) and the C-SHRP study on the Normalization of Asphalt Concrete Overlay Designs (EBA, 1996). The Inertia Method, Equation 5.12, uses the backcalculated effective modulus of the entire pavement structure and the equivalency of inertia (EI) to estimate the modulus of each asphalt layer. Note that the effective modulus values used for this analysis were not corrected for temperature and are the raw values obtained from ELMOD.

$$(d_1 + d_2)^3 E_{effective} = \left[(d_1 + d_2)\sqrt[3]{E_{eff}}\right]^3 = \left[d_1\sqrt[3]{E_1} + d_2\sqrt[3]{E_2}\right]^3 \qquad (5.12)$$

where

$E_{effective}$ = overall asphalt modulus back-calculated from ELMOD (MPa)

d_1 = thickness of Bit B layer (mm)

d_2 = thickness of Bit C layer (mm)

E_1 = modulus of Bit B layer (MPa)

E_2 = modulus of Bit C layer (MPa)

Figure 5.18 shows the comparison between the estimated Bit B modulus and the estimated Bit C modulus calculated from the Inertia Equation. This figure includes the results from all the projects, including Project B, which has been highlighted. As with the effective modulus value, Project B shows extremely high Bit B and Bit C values.

The modulus values for the each individual asphalt layer was then calculated using the Inertia Method and are also summarized in Table 5.14. The B:C ratio for the modulus values calculated using the Inertia Method range from 0.47 to 2.59. Except for two projects, Projects A and G, the Bit B modulus values are greater than the Bit C modulus values. Although Project B had very high modulus values for the Bit B and Bit C mixture, the B:C ratio was 1.46. For Project C and Project H, the Bit B modulus was over two times the value of the Bit C mixture.

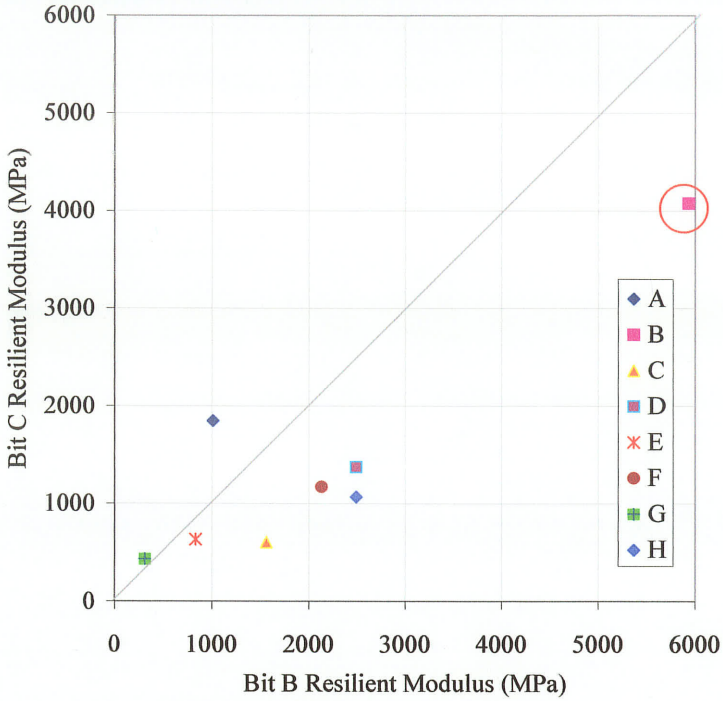

Figure 5.18 Estimated Modulus of the Bit B and Bit C layer Using the Inertia Equation

Table 5.14 Estimated Layer Modulus Calculated from the Inertia Method

Project ID	Inertia Method (MPa) Layer Modulus		
	Bit B	Bit C	B:C ratio
A	1012	1846	0.55
B	5935	4075	1.46
C	1564	604	2.59
D	2492	1374	1.81
E	833	633	1.32
F	2132	1170	1.82
G	310	432	0.72
H	2492	1067	2.34
Maximum	5935	4075	2.59
Minimum	310	432	0.55
Average	2096	1400	1.57

5.2.4 Subgrade Modulus

The resilient modulus of the subgrade material was estimated using the ELMOD computer program. Tables 5.15 and 5.16 list backcalculated subgrade resilient modulus values that were calculated at the University of Manitoba and by the Consultant, respectively.

The backcalculated values determined at the University of Manitoba were compared to the values obtained from the Consultant, as shown in Figure 5.19. This was done to confirm the values that were obtained at the University of Manitoba. Figure 5.19 indicates that the values calculated at the University of Manitoba are similar to the values calculated by the Consultant. Figure 5.20 is the same plot comparison but for the Bit B/C subgrade material. This figure indicates that the backcalculated subgrade resilient modulus values calculated at the University of Manitoba are very similar to the values obtained from the Consultant.

Table 5.15 Backcalculated Subgrade Resilient Modulus (U of M)

Project Identification	Back-calculated Subgrade Resilient Modulus (MPa)		
	Bit B/B	Bit B/C	Average
A	208	162	185
B	66	76	71
C	88	85	87
D	122	98	110
E	242	229	236
F	113	104	109
G	92	117	105
H	82	113	98
Maximum	242	229	236
Minimum	66	76	71
Average	127	123	125

Table 5.16 Backcalculated Subgrade Resilient Modulus (Consultant)

Project Identification	Back-calculated Subgrade Resilient Modulus (MPa)		
	Bit B/B	Bit B/C	Average
A	192	155	174
B	68	82	75
C	98	95	97
D	124	106	115
E	252	250	251
F	109	106	108
G	100	129	115
H	112	127	120
Maximum	252	250	251
Minimum	68	82	75
Average	132	131	132

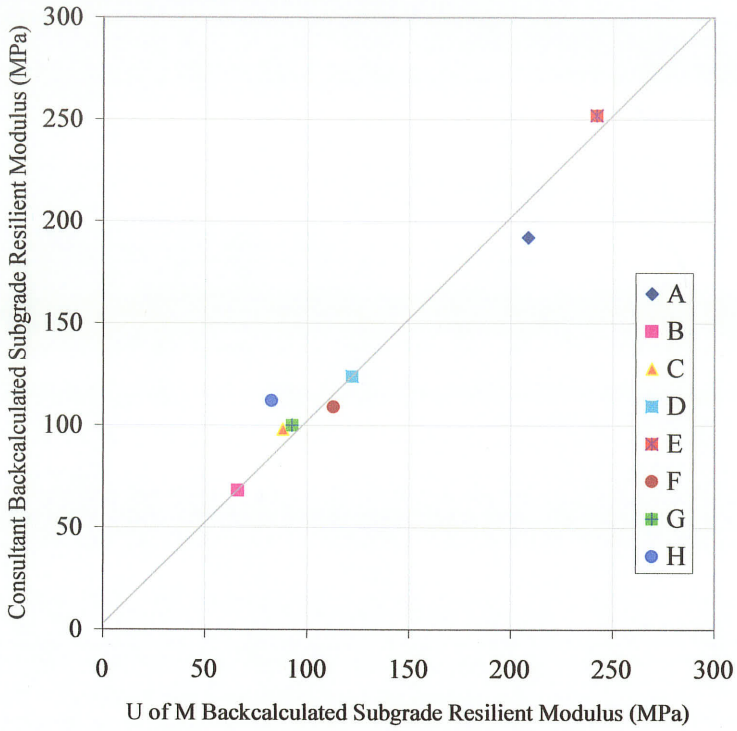

Figure 5.19 Subgrade Resilient Modulus Comparison for the Bit B/B sections

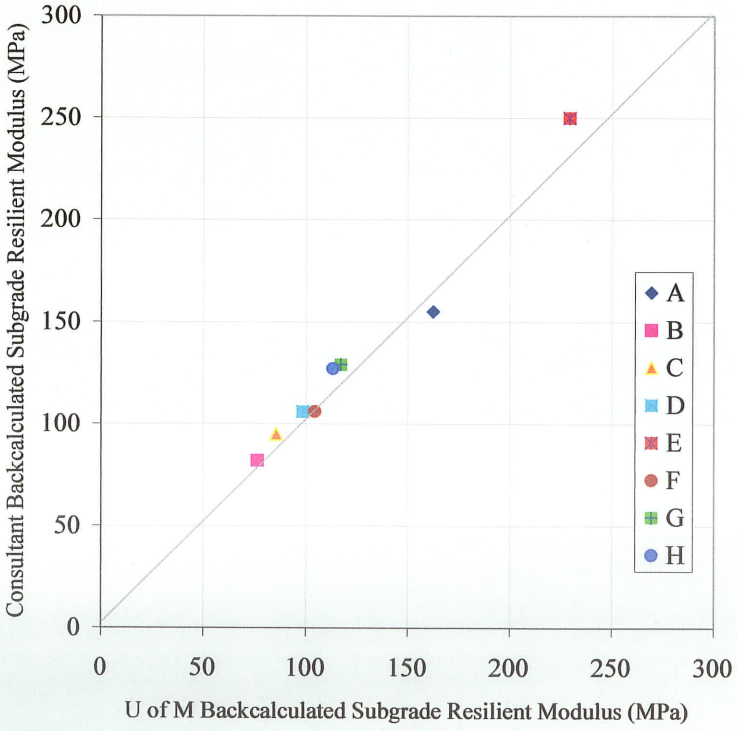

Figure 5.20 Subgrade Resilient Modulus Comparison for the Bit B/C sections

5.2.4.1 AASHTO Subgrade Resilient Modulus Equation

The subgrade modulus for each project site section was calculated using the AASHTO (1993) subgrade modulus Equation 5.13:

$$M_r = \frac{P\ (1-\mu^2)}{\pi\, D\, r} \qquad (5.13)$$

where

M_r = resilient modulus (MPa)

P = load (kN)

μ = Poisson's ratio (assumed = 0.35)

D = FWD deflection (mm)

r = sensor distance from centre of load plate (mm)

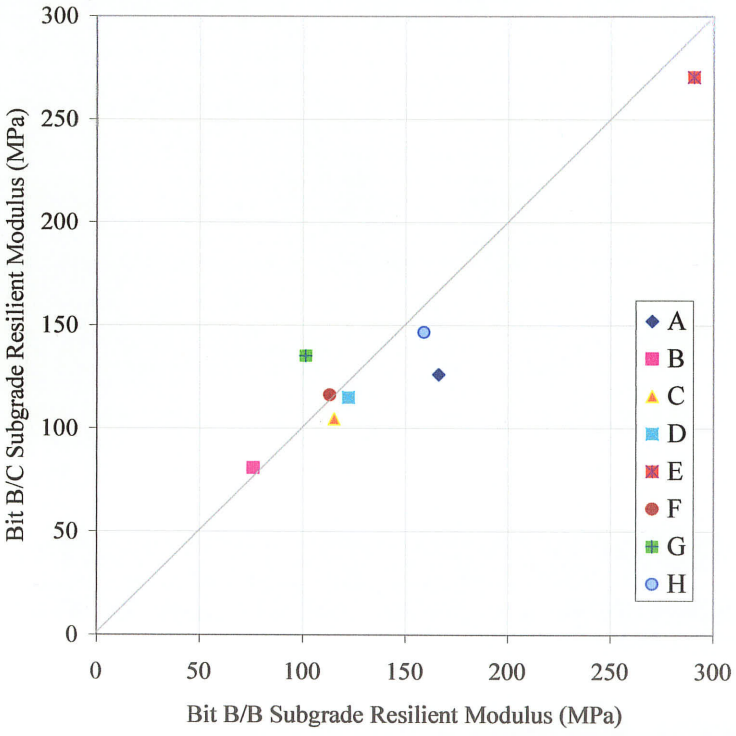

Figure 5.21 Subgrade Resilient Modulus of Bit B/B and Bit B/C Sections Using AASHTO Equation

The sensor distance from the centre of the load plate that was used in Equation 5.13, r, was 1200 mm. The average deflection and the average actual applied load at sensor 1200 for the load level

of 60 kN for each project was determined and used in the above equation. The subgrade modulus for each project site is plotted in Figure 5.21.

In general, the Bit B/B sections and Bit B/C sections had similar subgrade modulus values from each project site that ranged from 76 MPa at Project Site B to 290 MPa at Project Site E.

5.3 Comparison of Modulus Values

A brief comparison was made between the following:

- Interpolated laboratory resilient modulus at 20°C and the backcalculated effective resilient modulus.
- Interpolated laboratory resilient modulus at 20°C and the resilient modulus calculated using the Inertia Method.
- Laboratory resilient modulus at 10°C, 25°C, the backcalcuated effective modulus, resilient modulus calculated using the Inertial Method and the interpolated laboratory resilient modulus at 20°C.

Interpolated Modulus Versus Backcalculated Effective Modulus

Figure 5.22 compares the interpolated resilient modulus for the Bit B mixture at 20C to the backcalculated effective modulus of the Bit B/B section. The backcalucated effective modulus values used in this plot were not corrected for temperature. It can be seen that the backcalculated effective modulus values are generally greater than the interpolated resilient modulus. The interpolated values range from 502 MPa to 1064 MPa. The backcalculated effective modulus values have a wider range of 375 MPa to 5935 MPa. Project B has the greatest backcalculated effective modulus of 5935 MPa, which appears to be extremely high. The higher limit of the backcalculated effective modulus would be 2075 MPa if Project B were to be excluded from the analysis.

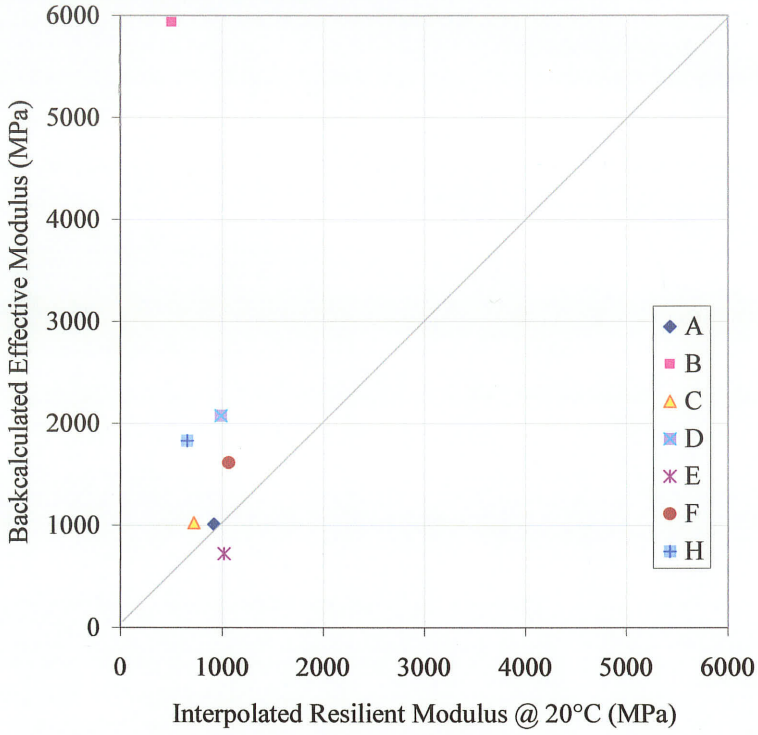

Figure 5.22 Interpolated Resilient Modulus of Bit B at 20°C Versus Backcalculated Effective Modulus of Bit B/B Section

Figure 5.23 shows a comparison of the resilient modulus values for the Bit C mixture interpolated at 20°C to the Bit B/C backcalculated effective modulus. Similar to the comparison made in Figure 5.22 with the Bit B versus Bit B/B modulus, the backcalculated effective modulus values typically were greater than the interpolated resilient modulus. The backcalculated effective modulus ranged from 400 MPa to 4631 MPa while the interpolated resilient modulus values ranged from 470 MPa to 2244 MPa. In both methods, the upper limit was from Project B. If Project B were excluded in the analysis, the upper range limits would be 1494 MPa and 1051 MPa, respectively.

Von Quintus and Killingsworth (1998) reported that backcalculated layer moduli are almost always greater than the laboratory measured values at comparable stress states and or temperatures. At 40°C, the backcalculated resilient modulus was found to be 4.0 times greater than the resilient modulus determined in the laboratory.

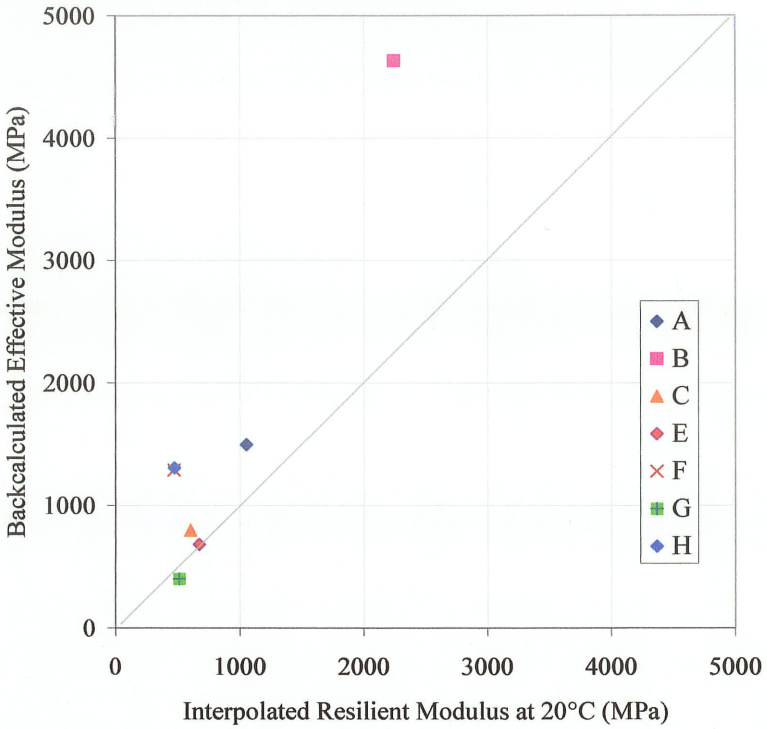

Figure 5.23 Interpolated Resilient Modulus of Bit C at 20°C Versus Backcalculated Effective Modulus of Bit B/C Section

Interpolated Modulus Versus Modulus Calculated from Inertia Equation

The modulus values calculated from the Inertia Equation are based on the effective modulus calculated from ELMOD. The effective modulus values are normalized to a temperature of 20°C. Therefore, comparison between the modulus obtained from the Inertia Equation and the dynamic laboratory testing must be made at a temperature of 20°C. In Section 5.1.2.1, the resilient modulus values obtained from dynamic laboratory testing were interpolated for the 20°C test temperature and will be used in this Section. Figure 5.24 is a plot of the Bit B samples that were dynamically tested versus the modulus calculated for the Bit B layer using the Inertia Equation.

The resilient modulus interpolated from laboratory data has a narrower range than the modulus calculated using the Inertia Equation. The laboratory resilient modulus interpolated at 20C ranged from 502 MPa to 1064 MPa while the modulus calculated from the Inertia Equation had a wider range of 310 MPa to 5935 MPa. Project B affected the range of the modulus values calculated by the Inertia Method. The range of modulus values calculated with the use of the Inertia Equation is 310 MPa to 2,492 MPa when Project B is excluded from the analysis. The

modulus calculated by both methods produces similar values until the modulus approaches 1,000 MPa. As the resilient modulus calculated from the Inertia Equation exceeds 1,000 MPa, the modulus of the interpolated laboratory data does not exceed 1,000 Mpa.

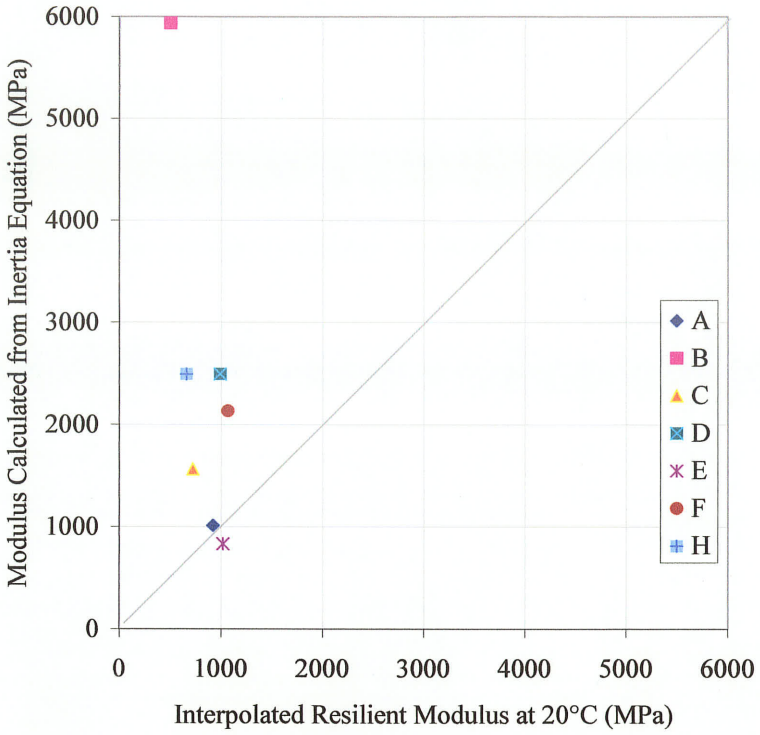

NOTE: The test data for the interpolated resilient modulus for Project G is not available

Figure 5.24 Resilient Modulus Interpolated at 20°C versus Modulus Calculated from Inertia Equation for Bit B

Table 5.17 is a summary of the modulus values from the two procedures including a ratio of the modulus calculated by the Inertia Method to the interpolated resilient modulus. This ratio ranged from 0.82 to 11.82, excluding Project B the ratio ranged from 0.82 to 3.79. The smallest difference in values was Project A, and the largest difference in methods was shown by Project B. The average Inertia modulus is approximately two times the interpolated modulus value, when Project B is excluded.

Figure 5.25 is a comparison of the Bit C interpolated and Inertia modulus values. The Inertia modulus and the laboratory modulus appear to have similar values until the modulus begins to exceed 1,000 MPa. At this limit, the Inertia modulus increases for some projects while the corresponding lab elastic modulus remained around 500 MPa. As the interpolated resilient modulus value increased the inertia resilient modulus almost doubles. It is apparent that the

Inertia modulus is generally greater than the lab modulus as the interpolated laboratory modulus approaches 750 MPa.

Table 5.17 Inertia and Interpolated Modulus for Bit B

Project ID	Resilient Modulus (MPa) Bit B		
	Interpolated	Inertia	Ratio
A	919	1012	1.10
B	502	5935	11.82
C	722	1564	2.16
D	989	2492	2.52
E	1018	833	0.82
F	1064	2132	2.00
G	n/a	310	n/a
H	658	2492	3.79
Maximum	1064	5935	11.82
Minimum	502	310	0.82
Average	839	2096	3.46

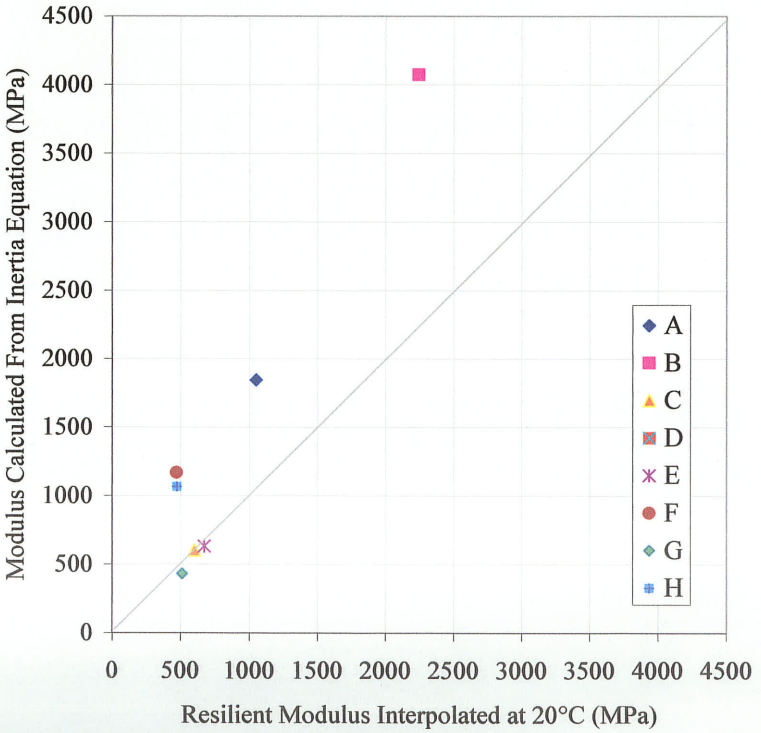

NOTE: The interpolated resilient modulus for Project D is not available.

Figure 5.25 Resilient Modulus Interpolated at 20°C versus Modulus Calculated from Inertia Equation for Bit C

Table 5.18 Inertia and Interpolated Modulus for Bit C

Project ID	Resilient Modulus (MPa) Bit C		
	Interpolated	Inertia	Ratio
A	1051	1846	1.76
B	2244	4075	1.82
C	602	604	1.00
D	n/a	1374	n/a
E	673	633	0.94
F	470	1170	2.49
G	512	432	0.84
H	473	1067	2.26
Maximum	2244	4075	2.49
Minimum	470	432	0.84
Average	861	1400	1.59

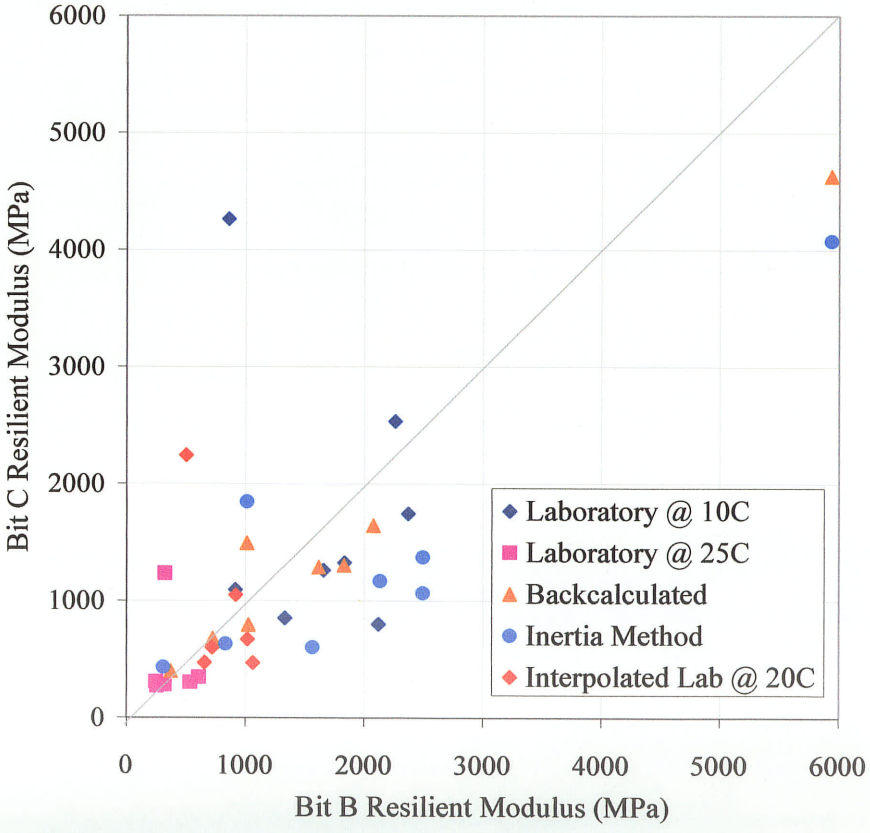

Figure 5.26 Overall Comparison of Resilient Modulus Values

Table 5.18 summarizes the modulus values and ratios for Bit C. For the Bit B mix, the Inertia modulus was as much as 3.8 times higher than the lab elastic modulus, while the Bit C Inertia

modulus increased to a factor of 2.5 greater than the lab elastic modulus. Crince and Baladi (2002) found that backcalculated modulus values were higher than the modulus of lab compacted samples but showed similar trends to the lab modulus values.

Overall Resilient Modulus Comparison

Figure 5.26 is a graphical comparison of all the resilient modulus values determined from laboratory testing at 10°C and 25°C, backcalculation, the Inertia Method and the resilient modulus interpolated at 20°C. From this plot, it is evident that in most cases the resilient modulus of the Bit B mixture is greater than the resilient modulus of the Bit C mixture.

5.4 Correlation Between Variables

In this chapter, various methods for determining the mix stiffness are determined. The stiffness of an asphalt paving mix is a primary indicator of the pavement response, and expected service life. In an effort to optimize pavement design in Manitoba, this research attempted to characterize the general mix categories defined as Bit B and Bit C.

The following strength parameters are discussed:

1. From static laboratory loading
   - Strength
   - Initial stiffness
2. From dynamic laboratory loading
   - Resilient modulus at 5, 25 and 40°C
   - Interpolated modulus at 20°C
3. From dynamic FWD tests
   - Surface modulus
   - Effective asphalt layer modulus
   - Individual layer modulus from Inertia Method
   - Temperature corrections using ratios, exponential and semi-log models

Tables 5.19 and 5.20 are a summary of the mixture properties and strength parameters for the Bit B and Bit C mix, respectively. A correlation matrix was constructed to examine the relationship between laboratory test results and mix parameters, as shown in Table 5.21. The correlation

matrix included all the values from the Bit B mixture and the Bit C mixture. Perfect correlation between the resilient modulus and mix parameters should not be expected. This research involved eight different projects with significant variability, such as location, aggregate source, contractor, environmental conditions, and traffic volumes. The bituminous mixtures were also tested under different conditions and procedures. Same numerical values should not be expected when using different test methods and loading modes.

Good correlation was found between some of the strength parameters found in the laboratory.

- Initial stiffness has good correlation with tensile strength and the resilient modulus at 25°C from dynamic loading.
- Resilient modulus at 10°C had good correlation with the resilient modulus at 25°C and interpolated resilient modulus at 20°C.
- Resilient modulus at 25°C correlated well with the resilient modulus at 20°C.

It should be noted that there was no correlation found between the resilient modulus determined in the laboratory using static or dynamic loading and the resilient modulus determined from FWD data.

As expected, there was a good correlation found between a few of the material properties.

- Bulk density has a good correlation with the air voids the percent voids filled with asphalt (%VFA)
- Percent air voids and percent voids filled with asphalt (%VFA)
- Recovered penetration has good correlation between the kinematic viscosity and absolute viscosity
- Kinematic viscosity and absolute viscosity

Good correlation was found between some of the strength parameters and material properties.

- Initial stiffness has good correlation with the recovered penetration, kinematic viscosity and the absolute viscosity
- Tensile strength has good correlation with the kinematic viscosity and the absolute viscosity
- Resilient modulus at 25°C using dynamic loading and the absolute viscosity
- Interpolated resilient modulus at 20°C and the absolute viscosity

It is interesting to note the strong correlation of viscosity to resilient modulus determined from laboratory testing. The correlation is a result of the viscoelastic behaviour of the asphalt concrete, which is dependant upon temperature. Traditional tests, such as the Marshall Stability and flow, generally show poor correlation to the material properties and the resilient modulus found in the laboratory and from FWD testing. The Marshall stability shows a 'good' correlation with the percent voids filled with asphalt (%VFA) and a 'fair' correlation to the Initial Stiffness, which is determined from static loading during the indirect tensile strength test. The flow shows no correlation with any of the material properties or the resilient modulus determined in the laboratory or through field testing.

The result from the correlation matrix justifies the need for more sophisticated tests to determine the strength properties of asphalt concrete mixtures.

Table 5.19 Bit B Parameters

Project Identification	Mix Parameters										Strength Parameters									
	Bulk Density (kg/m^3)	% Air Voids	Stability (kN)	Flow (0.25mm)	% VMA	% VFA	% Asphalt Content	Recovered Penetration	Kinematic Viscosity	Absolute Viscosity	Backcalculated Effective Modulus (MPa)	Backcalculated Temperature Corrected Effective Modulus (MPa)			Inertia Method Layer Modulus (MPa)	Initial Stiffness (kPa)	Tensile Strength (kPa)	Resilient Modulus at 10°C (MPa)	Resilient Modulus at 25°C (MPa)	Interpolated Resilient Modulus at 20°C (MPa)
												Exponential	Semi-Log	Ratio						
A	2417	2.8	8.764	10.4	15.7	81.9	6.1	108	342	1542	1012	2332	2532	1428	1012	3500	16.5	2261	248	919
B	2417	2.5	8.547	11	13.4	81.2	6.1	92	393	2036	5935	11899	12749	7881	5935	6300	30.8	858	324	502
C	2310	4.6	13.844	10.5	9.7	52.6	6.2	80	433	2215	1026	2205	2374	1405	1564	7100	22.6	1656	255	722
D	2353	4.2	11.334	10.1	14.5	71.4	5.7	85	367	1975	2075	5126	5632	3017	2492	2500	13.6	2370	298	989
E	2253	8.9	9.254	12.2	17.2	48.1	5.4	72	472	3004	725	3589	7318	1515	833	3900	24.3	1833	610	1018
F	2359	2.5	8.321	8.6	14.8	76.2	6.2	114	330	1417	1615	3238	3469	2145	2132	2000	13.2	2120	536	1064
G	2314	3.6	6.962	10.3	15.7	76.8	6.9	104	350	1626	375	1507	2172	682	310	700	4.3	917	n/a	n/a
H	2417	3.7	8.914	7.8	13.9	73.7	5.8	80	407	2371	1829	4215	4575	2581	2492	2200	7.4	1333	320	658

Table 5.20 Bit C Parameters

Project Identification	Mix Parameters										Strength Parameters									
	Bulk Density (kg/m^3)	% Air Voids	Stability (kN)	Flow (0.25mm)	% VMA	% VFA	% Asphalt Content	Recovered Penetration	Kinematic Viscosity	Absolute Viscosity	Backcalculated Effective Modulus (MPa)	Backcalculated Temperature Corrected Effective Modulus (MPa)			Inertia Method Layer Modulus (MPa)	Initial Stiffness (kPa)	Tensile Strength (kPa)	Resilient Modulus at 10°C (MPa)	Resilient Modulus at 25°C (MPa)	Interpolated Resilient Modulus at 20°C (MPa)
												Exponential	Semi-Log	Ratio						
A	2268	9.5	4.855	9.1	19.2	50.5	5.0	92	370	1843	1494	3442	3737	2108	1846	2800	9.2	2535	309	1051
B	2344	7.7	14.315	10.9	13.4	42.3	4.6	38	542	5873	4631	9284	9947	6149	4075	16300	45.8	4262	1235	2244
C	2164	11.2	11.14	13.3	12.9	13.5	4.9	83	466	2758	796	2259	2578	1230	604	6300	27.0	1261	272	602
D	2186	13.2	4.925	8.7	20.8	16.6	5.0	87	385	2100	1645	3535	3806	2252	1374	1800	13.6	1746	n/a	n/a
E	2333	5.5	11.999	11.3	13.2	58.2	4.7	80	453	2569	680	3141	5528	1325	633	8500	25.8	1327	347	673
F	2237	9.8	10.461	10.4	16.3	40.1	4.8	99	359	1656	1288	2768	2980	1763	1170	3100	17.6	803	304	470
G	2229	8.4	8.134	9.4	15.3	45.4	4.6	85	410	2121	400	1849	3254	780	432	1700	3.7	1096	220	512
H	2391	6.0	14.368	10.2	13.2	54.3	4.6	82	382	2048	1305	3705	4230	2018	1067	5700	18.9	853	283	473

Table 5.21 Correlation Matrix

Parameter	Bulk Density	Air Voids	Stability	Flow	VMA	VFA	Asphalt Content	Recovered Penetration	Kinematic Viscosity	Absolute Viscosity	Backcalculated Effective Modulus	Exponential	Semi-Log	Ratio	Inertia Method Layer Modulus	Initial Stiffness	Tensile Strength	Resilient Modulus at 10°C	Resilient Modulus at 25°C	Interpolated Resilient Modulus at 20°C
Bulk Density	1.00																			
Air Voids	-0.87	1.00																		
Stability	0.26	-0.05	1.00																	
Flow	-0.28	0.21	0.44	1.00																
VMA	-0.41	0.32	-0.80	-0.33	1.00															
VFA	0.86	-0.94	-0.05	-0.31	-0.24	1.00														
Asphalt Content	0.43	-0.58	-0.25	-0.17	-0.16	0.69	1.00													
Recovered Penetration	0.08	-0.34	-0.54	-0.29	0.25	0.40	0.52	1.00												
Kinematic Viscosity	-0.22	0.38	0.51	0.53	-0.33	-0.47	-0.47	-0.91	1.00											
Absolute Viscosity	-0.04	0.23	0.48	0.34	-0.22	-0.34	-0.42	-0.92	0.90	1.00										
Backcalculated Effective Modulus	0.42	-0.26	0.13	0.01	-0.16	0.20	0.04	-0.34	0.23	0.43	1.00									
Exponential Effective Modulus	0.43	-0.27	0.17	0.09	-0.16	0.21	-0.02	-0.42	0.31	0.47	0.98	1.00								
Semi-Log Effective Modulus	0.36	-0.24	0.17	0.22	-0.12	0.19	-0.08	-0.50	0.44	0.52	0.87	0.94	1.00							
Ratio Effective Modulus	0.43	-0.27	0.14	0.03	-0.16	0.21	0.02	-0.37	0.26	0.45	1.00	0.99	0.90	1.00						
Inertia Method Layer Modulus	0.50	-0.34	0.09	-0.10	-0.20	0.32	0.15	-0.27	0.15	0.33	0.97	0.95	0.83	0.97	1.00					
Initial Stiffness	0.15	0.10	0.69	0.46	-0.49	-0.20	-0.38	-0.78	0.79	0.86	0.51	0.54	0.54	0.52	0.41	1.00				
Tensile Strength	0.09	0.11	0.61	0.62	-0.40	-0.23	-0.29	-0.65	0.73	0.76	0.60	0.63	0.66	0.61	0.49	0.91	1.00			
Resilient Modulus at 10°C	0.11	0.05	0.14	-0.05	0.09	-0.05	-0.13	-0.51	0.40	0.66	0.33	0.31	0.27	0.33	0.32	0.54	0.44	1.00		
Resilient Modulus at 25°C	0.07	0.04	0.31	0.13	0.00	-0.14	-0.21	-0.69	0.63	0.87	0.47	0.49	0.53	0.48	0.39	0.73	0.68	0.77	1.00	
Interpolated Resilient Modulus at 20°C	0.11	0.00	0.18	0.01	0.10	-0.04	-0.08	-0.58	0.49	0.77	0.38	0.37	0.36	0.38	0.34	0.63	0.53	0.97	0.90	1.00

Note: Highlighted values identify material properties and strength parameters which have an absolute correlation coefficient higher than 0.70, ±1.00 representing perfect correlation

Chapter 6
CONCLUSIONS AND RECOMMENDATIONS

6.1 Summary and Conclusions

This research addresses the overall structural properties of the two commonly used mixes in Manitoba, Bituminous B and Bituminous C. While Bit B is a well graded mix with an optimum asphalt content, Bit C is only used as binder and leveling courses and has lower densities and higher air voids.

The research conducted at the University of Manitoba concluded that the sample size was too small to make any definitive statements about the numerical values of the tensile strength and resilient modulus. However, a comparison between the two mixes can be made.

6.1.1 Static Laboratory Testing

- Bit C mixes that are normally fine-graded, exhibited equal or even greater tensile strength values in several of the Projects than the corresponding Bit B mixes that are well-graded mixes, as tested in the indirect tensile test. This is not an unexpected result. Bit C mixes are made of sand asphalt mixtures, which have low asphalt contents and smaller aggregate size, contributing to the greater tensile strength.
- Initial stiffness, defined as the stiffness at 25% of the failure load during the indirect tensile strength test using a static load, was considered to be a suitable parameter for characterizing bituminous mixes. The initial stiffness calculated indicated that the Bit C mixture had greater initial stiffness values than the corresponding Bit B mixture for five of the projects.
- The moisture sensitivity test conducted on the Bit B mixture was inconclusive, as the results did not show any trend. Four of the projects were shown to be sensitive to moisture, with one project very sensitive to moisture by failing during the moisture conditioning process. The Bit C mixture did not withstand the moisture conditioning process and therefore further testing must be conducted to determine the cause of the low durability. The limited number of tests indicates that Bit B is more durable than Bit C. It would be desirable to test a larger number of samples. It can be concluded that the Bit B mixture is more durable than the Bit C mixture.

6.1.2 Dynamic Laboratory Loading

- Dynamic loading was used with the indirect tensile strength test to determine the material properties of the asphalt concrete when a moving load is applied. The indirect tensile strength test was conducted at 10°C, 25°C and 40°C. It was not possible to complete the tests at 40°C and therefore only the results at 10°C and 25°C were presented. The resilient modulus values that were found at 10°C and 25°C were lower than expected when compared with other resilient modulus values that have been published because it appears the asphalt pavements used in Manitoba are much softer.
- At the 10°C test temperature, the Bit B mix had greater resilient modulus values than the corresponding Bit C mixtures, with the exception of Project B and Project G. The resilient modulus values for the Bit B samples generally were 30% higher than the Bit C values. The Bit B values were 55% greater than the Bit C values if Project B is excluded.
- Considering all the test results, the Bit B resilient modulus was found 17% greater than the Bit C resilient modulus at the 25°C test temperature. Excluding Project B, the Bit B values are generally 40% greater than the Bit C values. It can be stated that the resilient moduli of the Bit B mixtures were greater than the Bit C mixtures.
- At each testing temperature, the variations of resilient modulus values of samples cored from different projects were quite high. In this regard, Bit B mixes showed greater variations both at 10°C and 25°C compared with Bit C mixes. The main reason for the variability is that there are no mechanistic tests performed at the mix design stage. Employing such tests will improve the design reliability and prediction of performance.
- One project was found to have significantly high resilient modulus values for the Bit C, being well beyond the expected range in the other projects. Upon further investigation, up to 70% reclaimed asphalt pavement (RAP) had been used in the mix, while the other projects contained a maximum of 30% RAP. This high percent of RAP could be the cause of the anomalous modulus values for this Project.

It is imperative that several parallel designs be completed using the laboratory resilient modulus values presented in this report and compared to existing designs so that a correlation be established and the impact of the resilient modulus values on the overall design be determined.

6.1.3 FWD Analysis

- The Bit B over Bit B pavement structure generally had greater effective modulus values than the corresponding Bit B over Bit C pavement, except for Projects A and G. Project B had extremely high resilient modulus values, but the difference in resilient modulus between the two sections was not 'out of the ordinary'.
- The asphalt layer modulus values obtained from the Inertia Equation had similar trends to the performance of the asphalt mixture in the laboratory. Project B had the greatest modulus values, while Project G had the lowest modulus values.
- The subgrade resilient modulus values obtained from the Consultant were similar to the values calculated for this research with the use of ELMOD, giving credit to the values found in this research.

6.1.4 Testing Procedures

- The laboratory resilient modulus values were slightly lower than the resilient modulus values obtained from backcalculation, although the same trends exist. The strong pavements displayed high values in the laboratory and for backcalculation, while the weaker pavements demonstrated to be weaker in the laboratory, during conditioning and in the data from FWD analysis.
- Dynamic testing using the indirect tensile strength test to determine the resilient modulus of asphalt is a procedure that is new to the laboratories at the University of Manitoba. Some work is needed to improve the testing procedure and equipment. Some improvements include; utilizing a 0.1 second load period; using an environmental chamber to achieve test temperatures.

6.2 Recommendations and Future Work

The research performed in this thesis has presented the initial development of laboratory testing to determine the resilient modulus of asphalt mixtures. Much work still remains to improve the laboratory testing procedures to expand on this research.

- The static indirect tensile strength test is not known to be a repeatable test. Only one Bit B and one Bit C asphalt sample were tested in the static mode. More tests are recommended to be undertaken to reduce the uncertainty of the single test results. The test results are representative of the particular project in which the samples were taken from. There is variability in the asphalt mixtures themselves.

- The asphalt samples were taken from eight randomly selected construction projects throughout the Province of Manitoba. The binder, aggregates, fines and construction crew varied from project to project. It is recommended that mixture samples are prepared in the laboratory to reduce variability of the materials used, such as the binder, aggregates, and fines. The material properties of the laboratory prepared samples can then be controlled. This will ensure that there are comparable Bit B and Bit C samples and that the same materials have been used.
- The design of a computer program to precisely calculate the instantaneous and total deformations to use in the resilient modulus calculation would reduce human error. The computer program would determine the two regression lines in the unloading portion of the loading-unloading cycle, determine the intercepts of the two lines and calculate the deformations.
- Determine a better way to estimate the load applied to the specimens by reviewing the correlations that were made. Loads were arbitrarily selected based on previously tested samples in the laboratory, sometimes too high and sometimes too low. Determining the load that should be applied beforehand, would eliminate this problem.
- The high resilient modulus values obtained in Project B should be further investigated. Manitoba Department of Transportation and Government Services indicated that 70% RAP was used in the mixture design for this Project while the remaining Projects only had approximately 15-30% of RAP. The use of RAP and its affects on pavement performance should be further investigated.

Section 2.4.1.4 outlined the factors that influence the resilient modulus values obtained from dynamic loading. The following are brief comments of some recommendations with regards to the influencing factors.

- *Temperature control.* A better attempt should be made to use an environmental chamber to control the temperature of the cores during temperature conditioning and during testing. A cold room has proven to not be sufficient enough.
- *Material Properties.* The affect of each material property, such as air voids, density, asphalt content, etc., should be studied.
- *Diameter of core.* The testing procedure and resilient modulus calculations outlined LTPP Protocol P07 was followed for this research. There were no direct strain limits outlined for 6 inch diameter cores so therefore the limits that were stated for the 4 inch

diameter cores was used. A testing protocol should be developed for 6 inch cores or 4 inch cores should be used in future laboratory testing.

- *Load or cycle frequency.* The effect of load frequency should be examined for asphalt mixtures in Manitoba. Other studies have shown the cycle frequency to sway the resilient modulus values due to the shorter or longer recovery time.
- *Loading period/duration.* For dynamic testing to determine the resilient modulus of the asphalt samples, the loading period must be further evaluated. In the literature review, it was found in some research projects that the load duration did not affect the resilient modulus calculations at the 5°C testing temperature (Barksdale et al., 1997). This was explained by the asphalt specimen acting like an elastic material at this temperature. However, at 25°C and 40°C an increase in load duration will decrease the resilient modulus and produce more damage than a shorter loading period. The longer loading period results in a shorter resting period that reduces the time the asphalt core has to recover from the deformation experience.
- *Loading rate.* For the static testing conducted for this research, the loading rate was much slower than the rate outlined in LTPP Protocol P07.
- *40°C test temperature.* It has been concluded that the asphalt binder used in Manitoba appears to be very soft compared to asphalt used by other States and Agencies. The test temperatures should be chosen to better suit the materials used in Manitoba.

REFERENCES

AASHTO, American Association of State Highway and Transportation Officials, *AASHTO Guide for Design of Pavement Structures*, Washington, D. C., 1993.

AASHTO T283-89 Standard Method of Test for *Resistance of Compacted Bituminous Mixture to Moisture Induced Damage*

Almudaiheem, Jamal A., Al-Sugair, Faisal H., *Effect of Loading Magnitude on Measured Resilient Modulus of Asphaltic Concrete Mixes*, Transportation Research Record 1317, 1991.

Appea, Alexander K., Al-Qadi, Imad L., *Assessment of FWD Deflection Data in Stabilized Flexible Pavements,* Prepared for Annual Meeting of the Transportation Research Board, Washington, D.C., January 9-13, 2000.

ASTM D113-99, *Standard Test Method for Ductility of Bituminous Materials*

ASTM D2041-00, *Standard Test Method for Theoretical Maximum Specific Gravity and Density of Bituminous Paving Mixtures*

ASTM D2170-01a *Standard Test Method for Kinematic Viscosity of Asphalts (Bitumens)*

ASTM D2171-01 *Standard Test Method for Viscosity of Asphalts by Vacuum Capillary Viscometer*

ASTM D3381-92 (1999) is the *Standard Specification for Viscosity-Graded Asphalt Cement for Use in Pavement Construction.*

ASTM D3497-79 (1995), *Standard Test Method for Dynamic Modulus of Asphalt Mixtures*

ASTM D4123-82 (1995), *Standard Test Method for Indirect Tensile Test for Resilient Modulus of Bituminous Mixtures*

ASTM D4867/D4867M-96, *Standard Test Method for Effect of Moisture on Asphalt Concrete Paving Mixtures*

ASTM D5-97, *Standard Test Method for Penetration of Bituminous Materials*

ASTM D8-02, *Standard Terminology Relating to Materials for Roads and Pavements.*

Atkins, Harold N., *Highway Materials, Soils and Concretes*, Prentice-Hall Inc., Third Edition, 1997.

Baladi, Gilbert Y., *Resilient Modulus*, Proceedings of the Workshop on Resilient Modulus Testing, Oregon State University, Corvallis, OR, pp. III-68 – III-91, March 1990.

Barksdale, Richard D., Alba, Jorge, Khosla, N. Paul, Kim, Richard, Lambe, Phil C., Rahman, M. S., *Laboratory Determination of Resilient Modulus for Flexible Pavement Design*, NCHRP Web Document 14, Project 1-28, Contractor's Final Report, June, 1997.

Boudreau, Richard L., Hicks, R. Gary, Furber, Arthur M., *Effects of Test Parameters on Resilient Modulus of Laboratory-Compacted Asphalt Concrete Specimens*, Transportation Research Record 1353, 1992.

Brown E. R., and Foo, Kee Y., *Evaluation of Variability in Resilient Modulus Test Results (ASTM D 4123)*, National Center for Asphalt Technology, NCAT Report No. 91-6, October 1989.

Chen, Dar-Hao, Lin, Huang-Hsiung, Bilyeu, John, Murphy, Mike, *Temperature Correction on FWD Meausurements*, 2000.

Cochran, George R., *Minnesota Department of Transportation Experience with Laboratory MR Testing*, Proceedings of the Workshop on Resilient Modulus Testing, Oregon State University, Corvallis, OR, pp II-69 – I-94, March 1990.

Collop, A. C., Cebon, D., and Hardy, M. S. A., *Viscoelastic Approach to Rutting in Flexible Pavements*, Journal of Transportation Engineering, Vol. 121, No 1, pp. 82-93, January/February 1995.

Davis, Harmer E., Troxell, Greorge Earl, Hauck, George F. W., *The Testing of Engineering Materials*, McGraw-Hill Inc., Fourth Edition, 1982.

Drescher, Kenneth N., Korfaitis, George P., Ezeldin, A. Samer, *Materials for Civil and Highways Engineers*, Prentice-Hall Inc., Fourth Edition, 1998.

EBA, *Normalization of Asphalt Concrete Overlay Designs for the C-LTPP Test Sections*, TAC, December 1996.

Emery, John, and Seddik, Hoda, *Moisture Damage of Asphalt Pavements and Antistripping Additives: Causes, Identification, Testing and Mitigation*, Prepared for Transportation Research Board, Ottawa, Canada, 1997.

Epps, Amy, Harvey, John T., Kim, Y. Richard, Roque, Reynaldo, *Structural Requirements of Bituminous Paving Mixtures,* A2D04: Committee on Characteristics of Bituminous Paving Mixtures to Meet Structural Requirements, Transportation Research Board, 2000.

ERES Consultants, Participant's Manual, *Mechanistic-Empirical Pavement Analysis and Design Workshop*, April 4-5, 2001.

Drescher, A., Newcomb, D. E., Zhang W., *Interpretation of Indirect Tension Test Based on Viscoelasticity*, Transportation Research Record 1590, pp. 45-51, 1997.

Fairhurst, C.E. Kosla, N.P., Kim Y.R., *Resilient Modulus Testing of Asphalt Specimens in Accordance with ASTM 4123,* Proceedings of the Fourth International Symposium held by RILEM, 1990.

FHWA, *LTPP Protocol: P07, Test Method for Determining the Creep Compliance, Resilient Modulus and Strength of Asphalt Materials Using the Indirect Tensile Test Device*, , FHWA-LTPP Technical Support Services Contractor, Version 1.1, August 2001.

FHWA, *Proceedings of the Workshop on Resilient Modulus Testing*, Federal Highway Administration, Research Development and Technology, Turner-Fairbank Highway Research Center, Publication No. FHWA-TS-90-031, March 1990.

Finn, F. N., and Epps, J. A., *Compaction of Hot Mix Asphalt Concrete, Research Report 214-21*, Texas Transportation Institute, Texas A&M University, College Station, Texas, August 1980.
Hass, Ralph, *Pavement Design and Management Guide*, Transportation Association of Canada, Ottawa, Canada, 1997.

Hanna, Amir N., *Determination of Insitu Material Properties of Asphalt Concrete Pavement Layers from Nondestructive Tests*, National Cooperative Highway Research Program, Research Results Digest, December, Number 271, 2002.

Huang, Yang H., *Pavement Analysis and Design*, Prentice Hall, Englewood Cliffs, New Jersey 07632, 1993.

Kandhal, Prithvi S., and Chakraborty, Sanjoy, *Effect of Asphalt Film Thickness on Short and Long Term Aging of Asphalt Paving Mixutres*, NCAT Report No. 96-1, January 1996.

Kandhal, Prithvi S., Foo, Kee Y., Mallick, Rajib B., *A Critical Review of VMA Requirements in Superpave*, NCAT Report No. 98-1, January 1998.

Kennedy, T. W., and Hudson W. R., *Application of the Indirect Tensile Test to Stabilized Materials*, Highway Research Record No. 235, Highway Research Board, Washington, D.C., pp. 36-48, 1968.

Khanal, Punya P., and Mamlouk, Michael S., *Tensile Versus Compressive Moduli of Asphalt Concrete*, Transportation Research Record 1492, pp.144-150, 1995.

Khosla, N. Paul, Birdsall, Brian G., and Kawaguchi, Sachiyo, *Evaluation of Moisture Susceptibility of Asphalt Mixtures Using Conventional and New Methods*, Submitted for presentation at Transportation Research Board Annual Meeting, Washington, D.C., 2000.

Kim, Y.R., Shah, K.A., Khosla, N.P., *Influence of Test Parameters in SHRP P07 Procedure on Resilient Moduli of Asphalt Concrete Field Cores*, Transportation Research Record 1353, pp 82-89, 1992.

Lukanen, Erland O., Stubstad, Richard, Briggs, Robert, *Temperature Predictions and Adjustment Factors For Asphalt Pavement,* Federal Highway Administration, Publication No. FHWA-RD-98-085, June 2000.

Mahoney Joe P., Newcomb, David E., *Elastic Pavement Analysis*, Prepared for Workshop on Resilient Modulus Testing, Oregon State University, Corvallis, OR, March 28-30, 1989, Federal Highways Administration, Publication Number FHWA-TS-90-031, March 1990.

Mamlouk, Michael S., and Sarofim, Ramsis T., *Modulus of Asphalt Mixtures – An Unresolved Dilemma*, Transportation Research Record 1171, pp 193-198, 1988.

Manitoba Department of Transportation and Government Services, *Standard Construction Specifications*, March 2003.

Manitoba Department of Transportation and Government Services, *Standard Test Method for: Dynatest Falling Weight Deflectometer*, Standard No. MRB7-08, 1998.

Mohammad, Louay N., Paul, Harold R., *Evaluation of Indirect Tensile Test for Determining Structural Properties of Asphalt Mix*, Transportation Research Record 1417, pp 58-63, 1993.

Monismith, C. L., *Resilient Modulus Testing: Interpretation of Laboratory Results for Design Purposes*, Proceedings of the Workshop on Resilient Modulus Testing, Oregon State University, Corvallis, OR, pp. IV-3 – IV-39, March 1990.

Nukunya, Bensa, Roque, Reynaldo, Tia, Mang, and Mehta, Yusuf A., *Effect of Aggregate Structure on Rutting Potential of Dense-Graded Asphalt Mixtures*, Transportation Research Board, 81st Annual Meeting, Washington, D.C., January 2002.

Pologruto, Michael, *A Procedure for Using an FWD to Determine the Structural Layer Coefficients for Flexible Pavement Materials*, Prepared for Annual Meeting of the Transportation Research Board, Washington, D.C., January 9-13, 2000.

Qi, Xicheng and Witczak, M. W., *Time-Dependent Permanent Deformation Models for Asphaltic Mixtures*, Transportation Research Board, 1998.

Radovskiy, Boris, *Analytical Formulas for Film Thickness in Compacted Asphalt Mixture*, Transportation Research Board, 82nd Annual Meeting, Washington, D.C., January 2003.

Roberts, Freddy L., Kandhal, Prithvi S., Brown, E. Ray, Lee, Dah-Yinn, Kennedy, Thomas W., *Hot Mix Asphalt Materials, Mixture Design and Construction*, Second Edition, Lanham, Maryland, 1996.

Roque, Reynaldo, Buttlar, William G., Ruth, Byron E., Dickison, Stephen W., *Short-Loading-Time Stiffness from Creep, Rsilient Modulus, and Strength Tests Using the Superpave Indirect Tension Test*, Transportation Research Board, 77th Annual Meeting, Washington D.C., January 1998.

Saskatchewan Department of Transportation, *Surfacing Manual*, 2000.

Shatanwi, Shakir R., and Van Kirk, Jack, *Premature Asphalt Concrete Pavement Distress Caused by Moisture-Induced Damage*, Transportation Research Record 1417, 1993.

Stroup-Gardiner, Mary, Newcomb, David E., Crow, Benita, Kussman, William and Wegman, Dan, *Moisture Sensitivity in Asphalt Concrete Mixtures*, Final Report 1994-1995, November 1995.

Stubstad, Richard N., *LTPP Data Analysis: Feasibiltiy of Using FWD Deflection Data to Characterize Pavement Construction Quality*, National Cooperative Highway Research Program (NCHRP), NCHRP Web Document 52 (Project 20-50[9]), 2002.

Tayebali, Akhtarhusein A., Tsai, Bor-Wen, and Monismith, Carl L., Stiffness of Asphalt-Aggregate Mixes, SHRP-A-388, Strategic highway Research Program, National Research Council, Washington, D.C., 1994.

Thiessen, Myron, *Strength and Rutting Characteristics of Asphalt Pavements in Manitoba*, Thesis for Partial Completion of Master of Science, University of Manitoba, 2001.

Ullidtz, Per and Coetzee, N. F., Analytical Procedures in Nondestructive Testing Pavement Evaluation, Transportation Research Board, Research Record 1482, pp 61-66, 1995.

Ullidtz, Dr. Per, *Analytical Tools for Design of Flexible Pavements*, Keynote Address, International Society for Asphalt Pavements, 2002.

Vinson, Ted S., *Fundamentals of Resilient Modulus Testing*, Prepared for Workshop on Resilient Modulus Testing, Oregon State University, Corvallis, OR, March 28-30, 1989, Federal Highways Administration, Publication Number FHWA-TS-90-031, March 1990.

Von Quintus, Harold, and Killingsworth, Brian, *Analyses Relating to Pavement Material Characterizations and Their Effects on Pavement Performance*, Federal Highway Administration, LTPP, Publication Number FHWA-RD-97-085, January 1998.

Von Quintus, Harold, and Killingsworth, Brian, *Design Pamphlet for the Determination of Design Subgrade Moduli in Support of the 1993 AASHTO Guide for Design of Pavement Structures*, Federal Highway Administration, Publication Number: FHWA-RD-97-083, September 1997.

Wallace, Keith, and Monismith, C. L., *Diametral Modulus Testing on Nonlinear Pavement Materials*, AAPT Volume 49, pp 633-649, 1980.

Wimsatt, Andrew J., *Direct Analysis Methods for Falling Weight Deflectometer Deflection Data*, Prepared for Annual Meeting of the Transportation Research Board, Washington, D.C., January 1999.

Appendix A
Test Section Locations

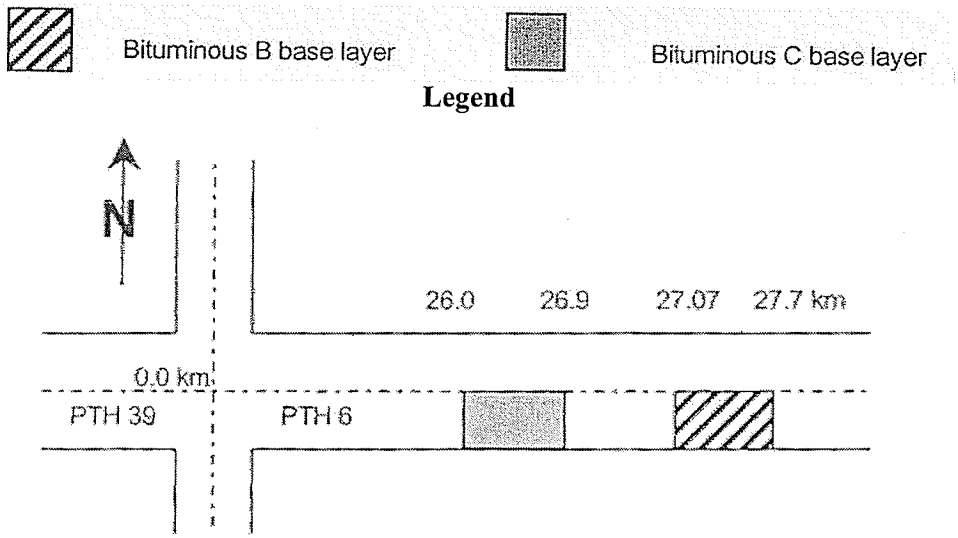

Figure A-1 Project A (PTH 6, North of PTH 39 to PR 373, Ponton)

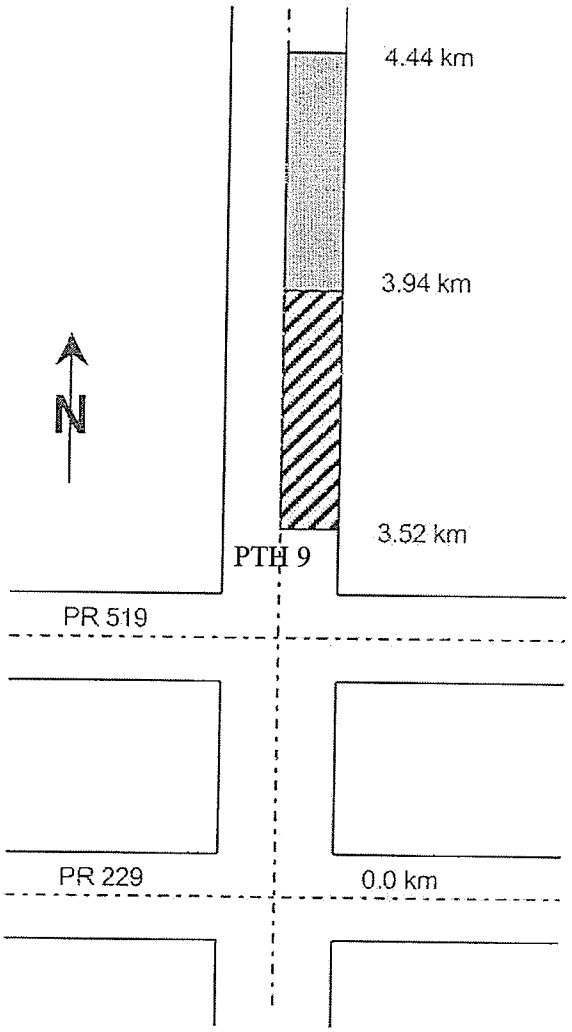

Figure A-2 Project B (PTH 9, PR 519 to Willow Creek, Winnipeg Beach)

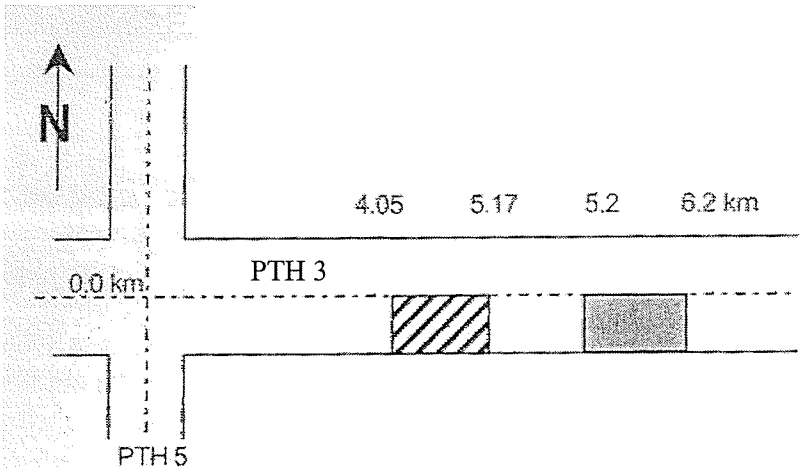

Figure A-3 Project C (PTH 3, PTH 5 to PR 442, Cartwright)

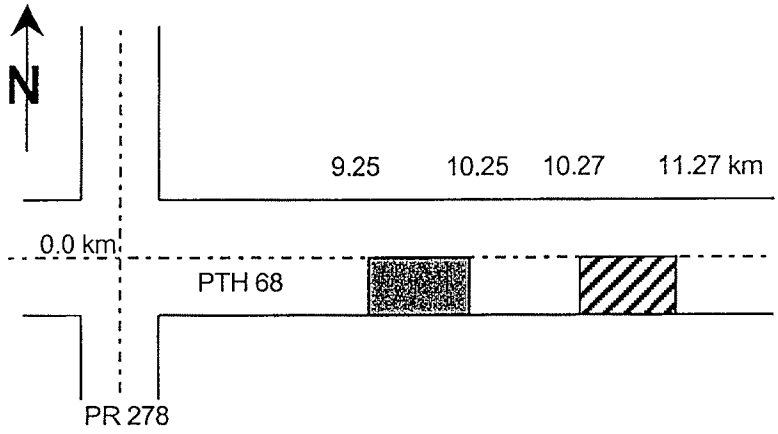

Figure A-4 Project D (PTH 68, Eddystone)

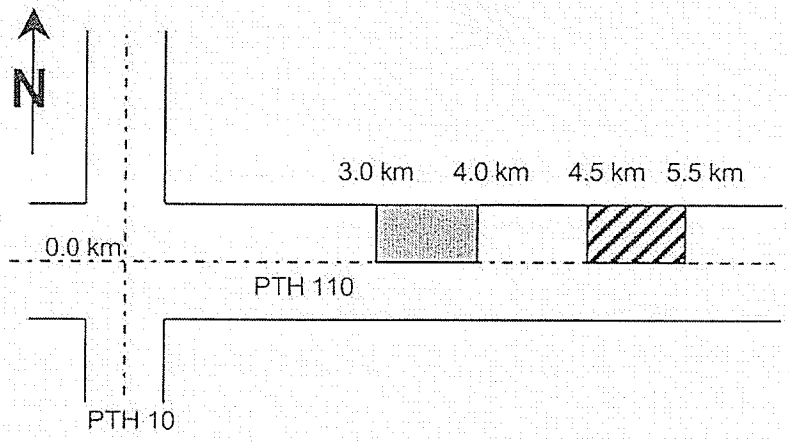

Figure A-5 Project E (PR 110, PTH 10 to Richmond Avenue, Brandon)

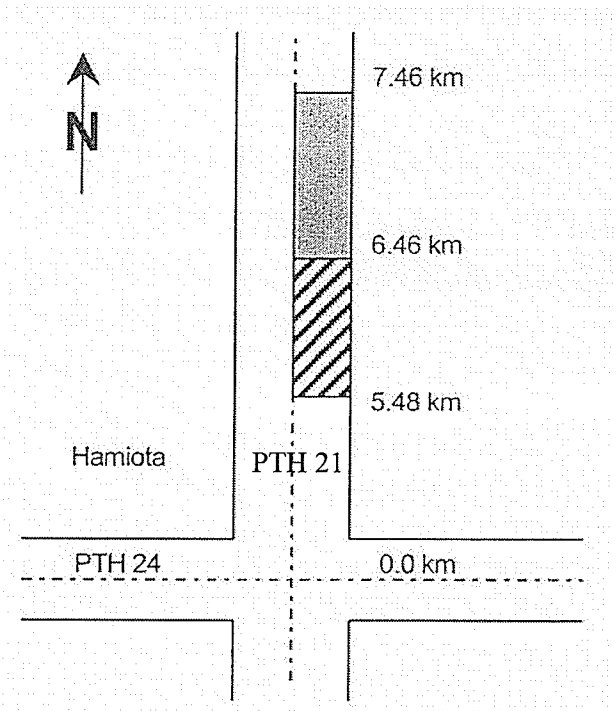

Figure A-6 Project F (PTH 21, Hamiota)

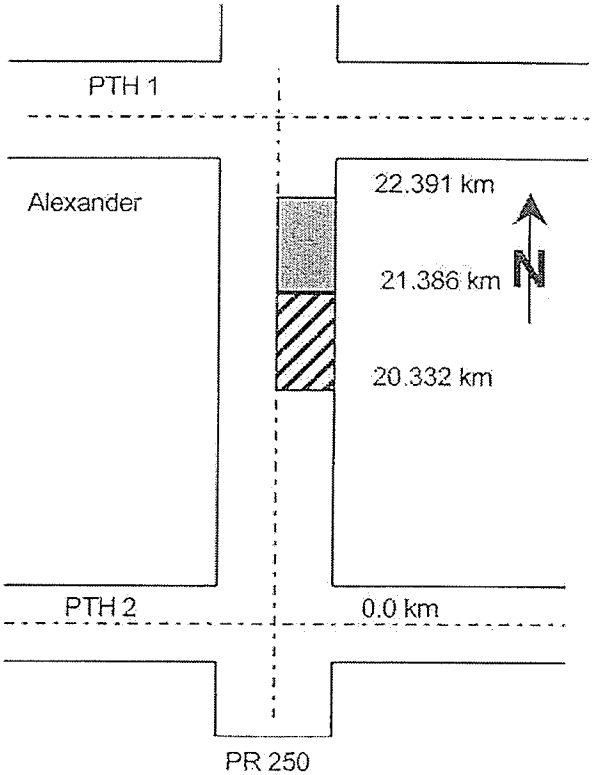

Figure A-7 Project G (PR 250, PTH 2 to Trans Canada Highway, Alexander)

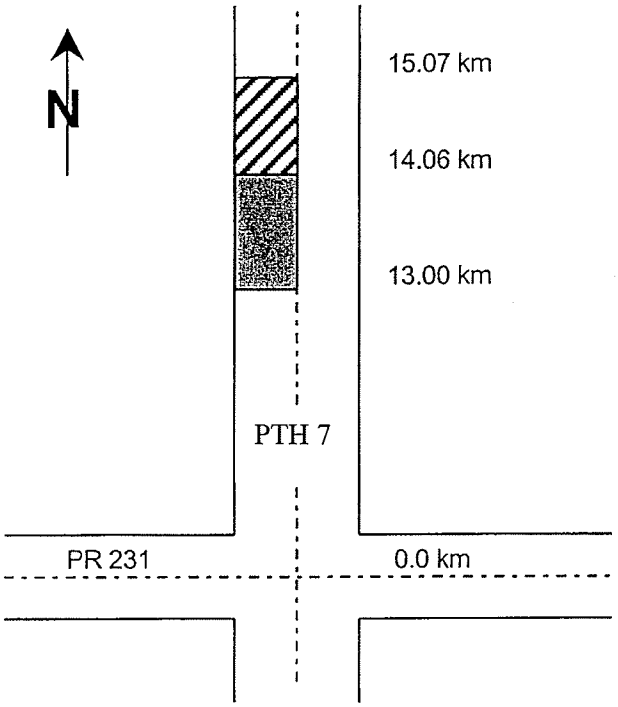

Figure A-8 Project H (PTH 7, PR 231 North, Arborg)

Appendix B

Measured Layer Thicknesses

Table B-1 Specimen Thicknesses

Measured Core Thickness After Cutting (mm)

Project Identification	Core and Layer		Measurement (mm)				
			1	2	3	4	Average
A	Bit B/B	Bit B (top)	45	44	40	42	**43**
		Bit B	40	40	39	39	**40**
	Bit B/C	Bit B (top)	37	42	43	40	**41**
		Bit C	35	38	45	40	**40**
B	Bit B/B	Bit B (top)	27	28	30	27	**28**
		Bit B	38	38	39	34	**37**
	Bit B/C	Bit B (top)	27	28	32	30	**29**
		Bit C	29	29	30	32	**30**
C	Bit B/B	Bit B (top)	50	49	51	51	**50**
		Bit B	45	45	46	45	**45**
	Bit B/C	Bit B (top)	34	33	34	36	**34**
		Bit C	42	43	41	41	**42**
D	Bit B/B	Bit B (top)	37	38	37	38	**38**
		Bit B	44	44	45	44	**44**
	Bit B/C	Bit B (top)	**SAMPLE BROKE**				
		Bit C	49	50	52	50	**50**
E	Bit B/B	Bit B (top)	43	42	44	42	**43**
		Bit B	49	49	48	49	**49**
	Bit B/C	Bit B (top)	40	41	41	40	**41**
		Bit C	44	46	46	47	**46**
F	Bit B/B	Bit B (top)	41	42	45	42	**43**
		Bit B	48	51	48	48	**49**
	Bit B/C	Bit B (top)	48	47	48	48	**48**
		Bit C	39	40	42	40	**40**
G	Bit B/B	Bit B (top)	39	34	35	36	**36**
		Bit B	32	32	35	34	**33**
	Bit B/C	Bit B (top)	28	30	33	32	**31**
		Bit C	28	28	29	30	**29**
H	Bit B/B	Bit B (top)	40	40	40	40	**40**
		Bit B	40	39	40	40	**40**
	Bit B/C	Bit B (top)	38	37	42	39	**39**
		Bit C	41	43	45	43	**43**

Appendix C
Material Properties

Table C-1 Bit B Material Properties

Project Identification	Bulk Density (kg/m^3)	% Air Voids	Stability (kN)	Flow (0.25 mm)	% VMA	% VFA	% Asphalt Content	Recovered Penetration	Kinematic Viscosity	Absolute Viscosity
A	2417	2.8	8.764	10.4	15.7	81.9	6.1	108	342	1542
B	2417	2.5	8.547	11	13.4	81.2	6.1	92	393	2036
C	2310	n/a	13.844	10.5	9.7	52.6	6.2	80	433	2215
D	2353	4.2	11.334	10.1	14.5	71.4	5.7	85	367	1975
E	2253	8.9	9.254	12.2	17.2	48.1	5.4	72	472	3004
F	2359	n/a	8.321	8.6	14.8	76.2	6.2	114	330	1417
G	2314	3.6	6.962	10.3	15.7	76.8	6.9	104	350	1626
H	2417	3.7	8.914	7.8	13.9	73.7	5.8	80	407	2371

Table C-2 Bit C Material Properties

Project Identification	Bulk Density (kg/m^3)	% Air Voids	Stability (kN)	Flow (0.25 mm)	% VMA	% VFA	% Asphalt Content	Recovered Penetration	Kinematic Viscosity	Absolute Viscosity
A	2268	9.5	4.855	9.1	19.2	50.5	5.0	92	370	1843
B	2344	7.7	14.315	10.9	13.4	42.3	4.6	38	542	5873
C	2164	n/a	11.14	13.3	12.9	13.5	4.9	83	466	2758
D	2186	13.2	4.925	8.7	20.8	16.6	5.0	87	385	2100
E	2333	5.5	11.999	11.3	13.2	58.2	4.7	80	453	2569
F	2237	n/a	10.461	10.4	16.3	40.1	4.8	99	359	1656
G	2229	8.4	8.134	9.4	15.3	45.4	4.6	85	410	2121
H	2391	6.0	14.368	10.2	13.2	54.3	4.6	82	382	2048

Appendix D
Deflection Basins

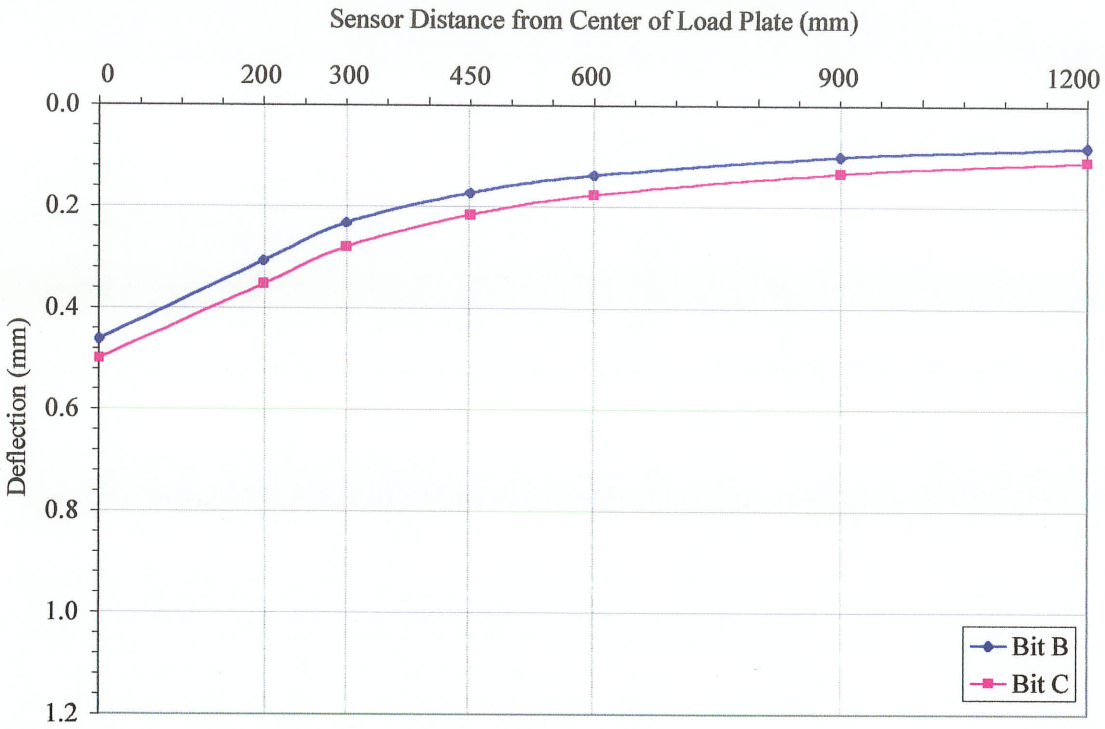

Figure D-1 Project A

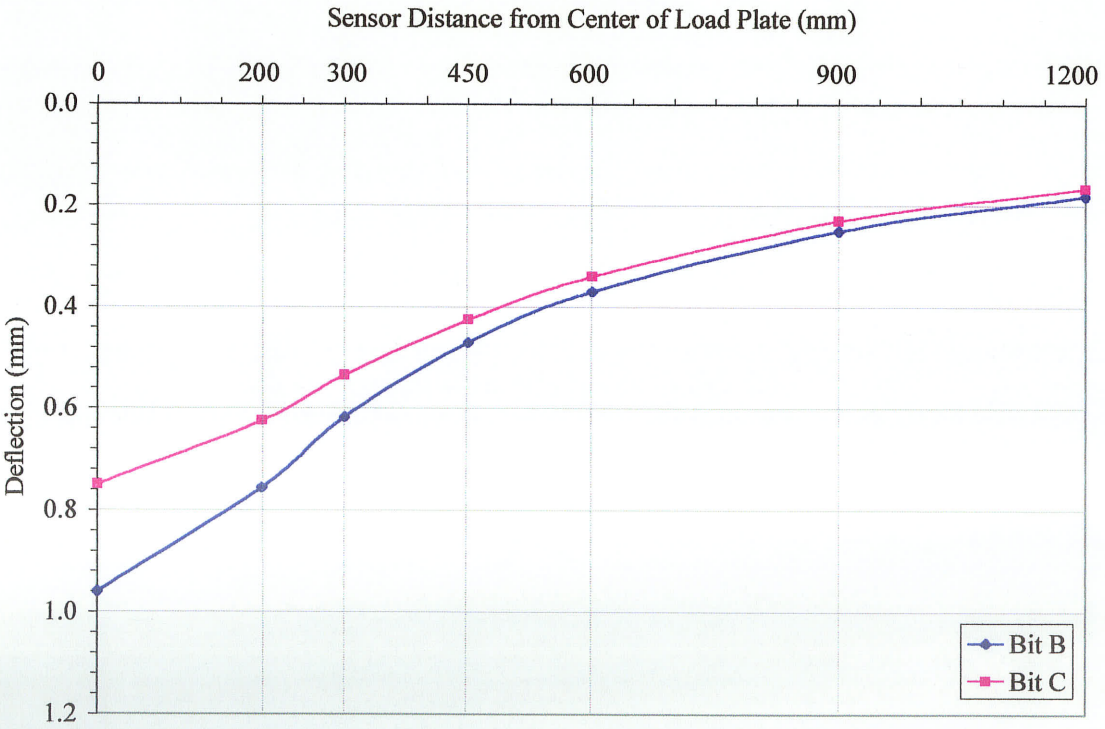

Figure D-2 Project B

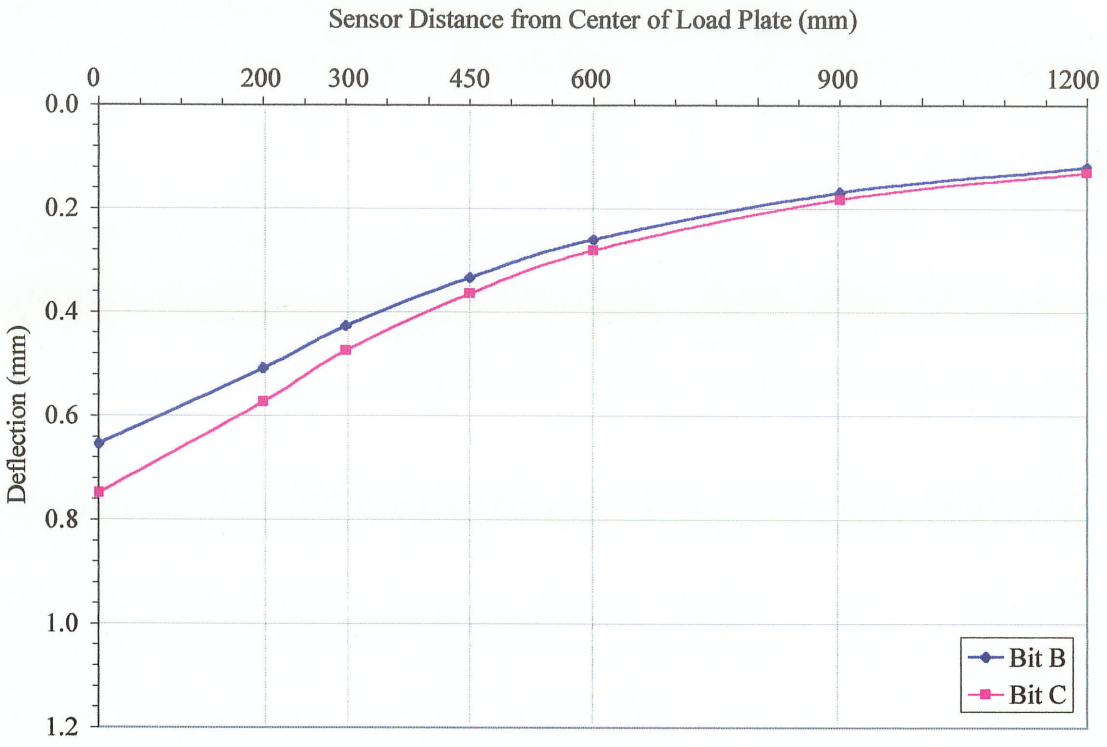

Figure D-3 Project C

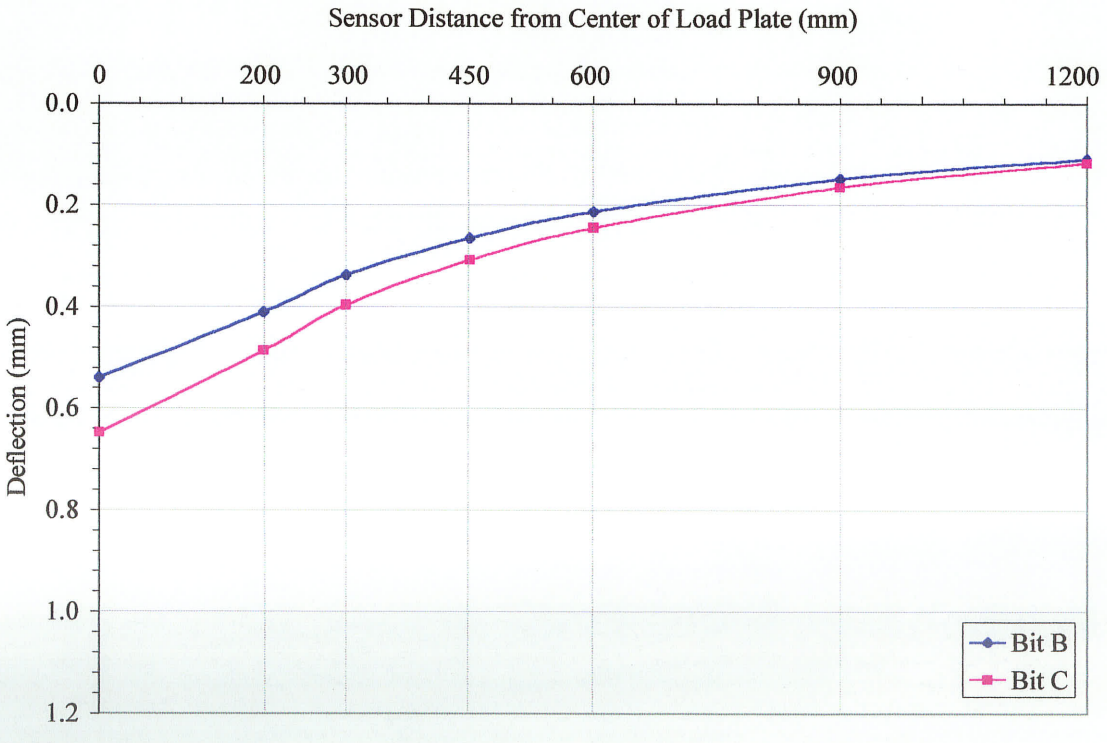

Figure D-4 Project D

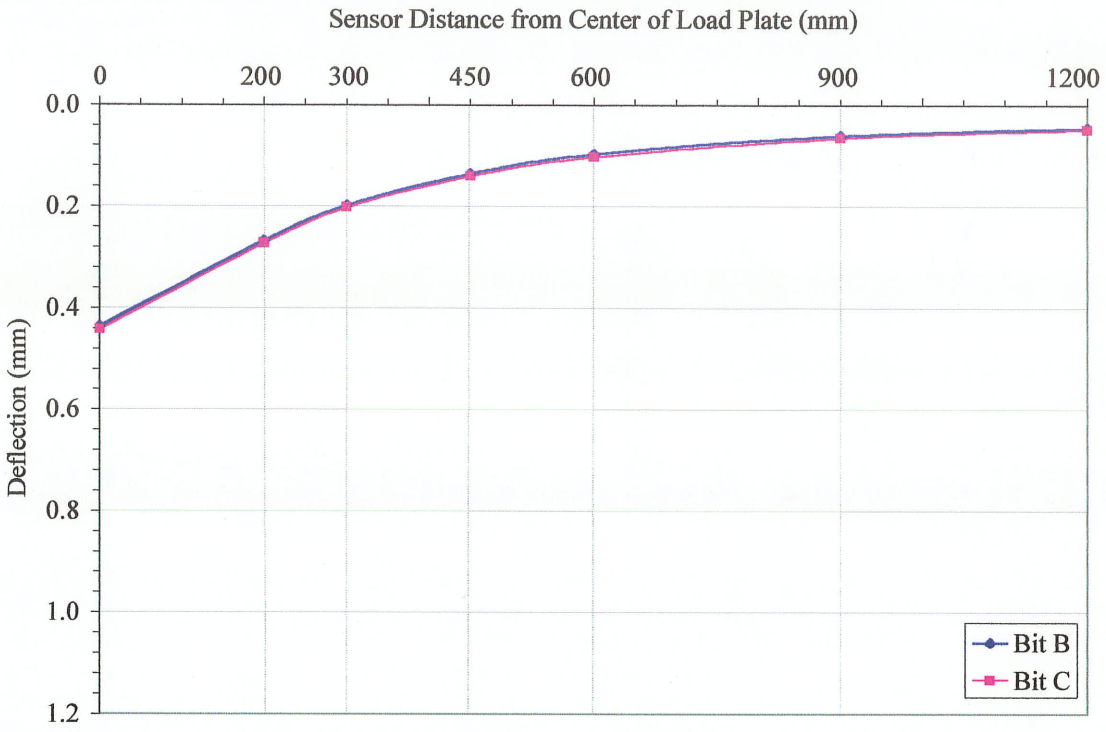

Figure D-5 Project E

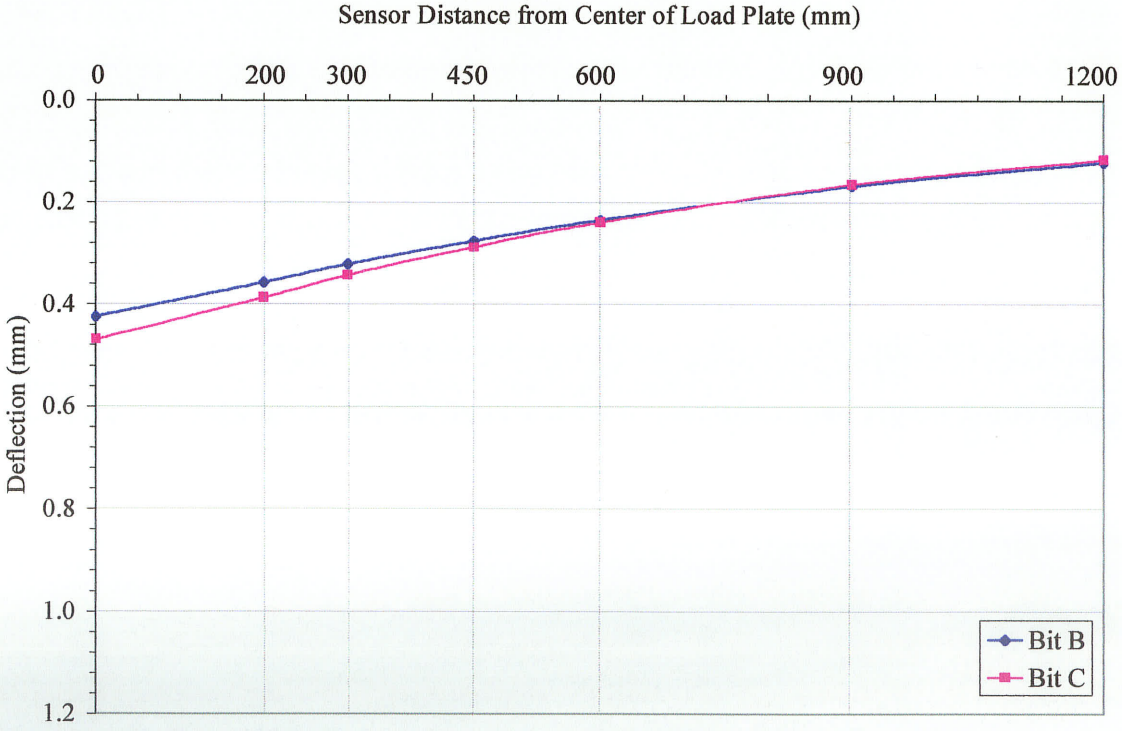

Figure D-6 Project F

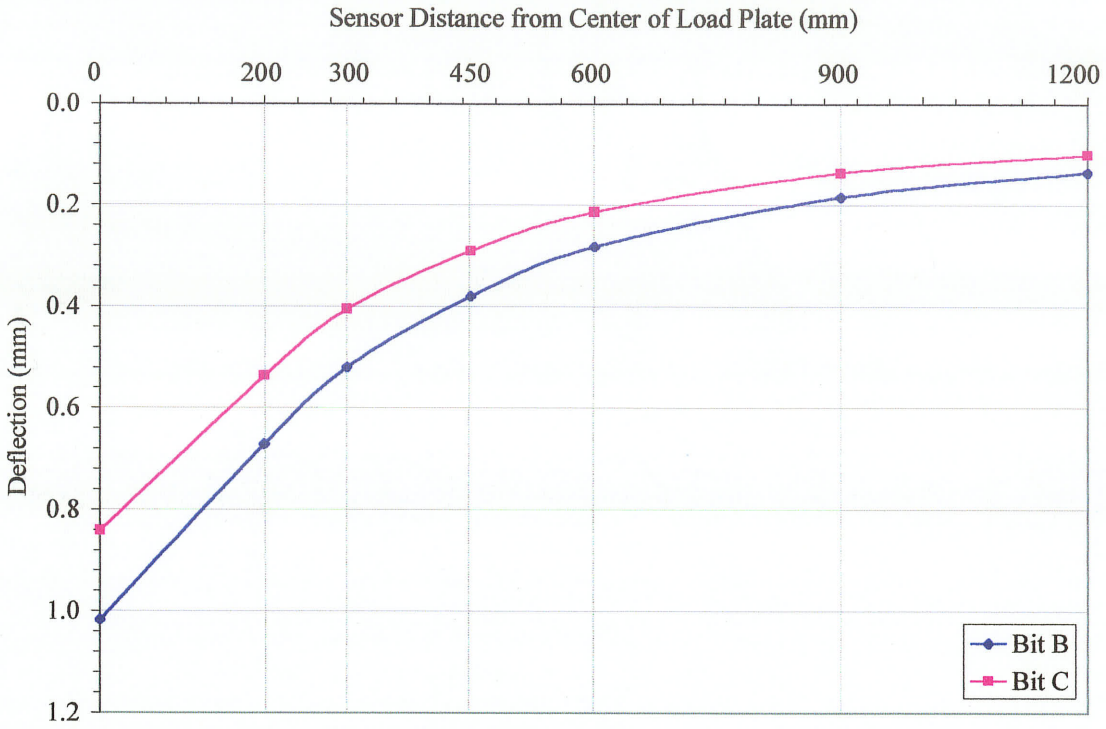

Figure D-7 Project G

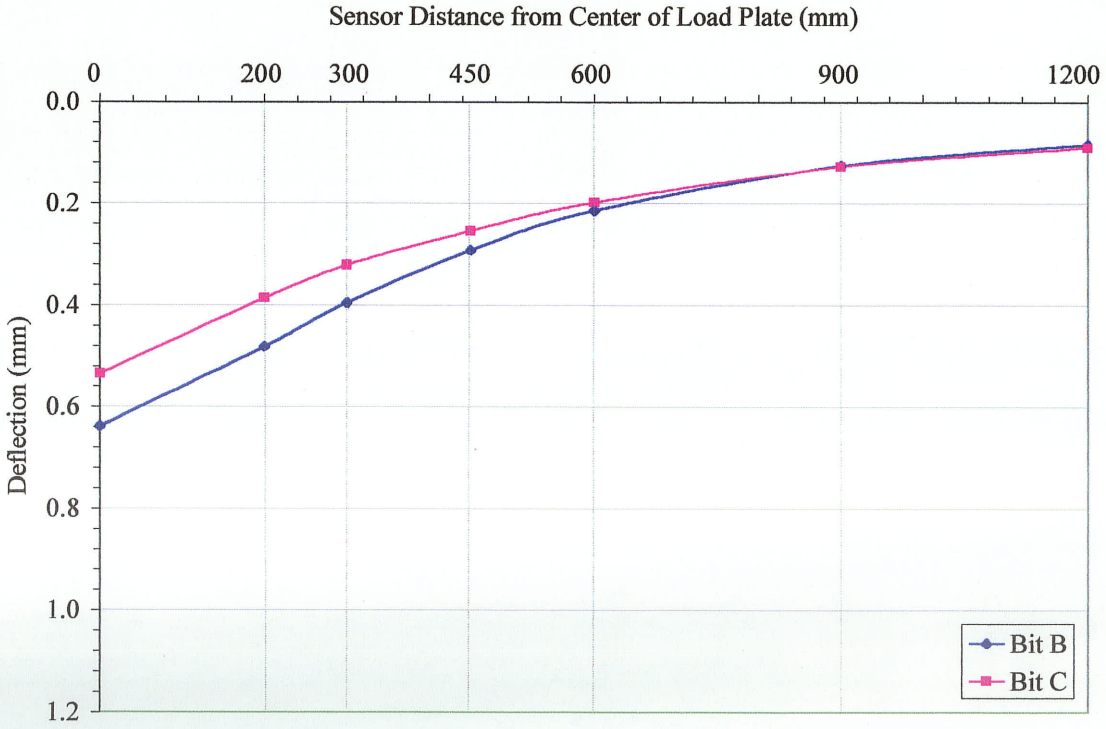

figure D-8 Project H

Appendix E

Peak Load and Tensile Strength

Table E-1 From Static Loading

Project Identification	Layer	Peak Load (N)	Tensile Strength (kPa)
A	Bit B	158	16.5
	Bit C	88	9.2
B	Bit B	273	30.8
	Bit C	329	45.8
C	Bit B	244	22.6
	Bit C	271	27.0
D	Bit B	143	13.6
	Bit C	166	13.6
E	Bit B	286	24.3
	Bit C	284	25.8
F	Bit B	154	13.2
	Bit C	169	17.6
G	Bit B	34	4.3
	Bit C	26	3.7
H	Bit B	71	7.4
	Bit C	195	18.9

Appendix F
FWD Information

Table F-1 Thicknesses Used by JEGEL

Project Identification	Bit B over Bit B		Bit B over Bit C	
	Asphalt	Granular	Asphalt	Granular
A	131	187	136	227
B	99	188	135	193
C	226	160	201	175
D	143	164	148	162
E	214	172	207	204
F	317	154	303	139
G	192	194	190	210
H	181	197	240	180

Table F-2 Thicknesses Used by University of Manitoba

Project Identification	Bit B over Bit B		Bit B over Bit C	
	Asphalt	Granular	Asphalt	Granular
A	131	187	136	227
B	99	188	136	193
C	226	164	225	175
D	143	164	149	162
E	214	172	207	204
F	332	154	348	139
G	192	194	190	210
H	181	197	240	180

Appendix G

Temperature Sensitivity Analysis

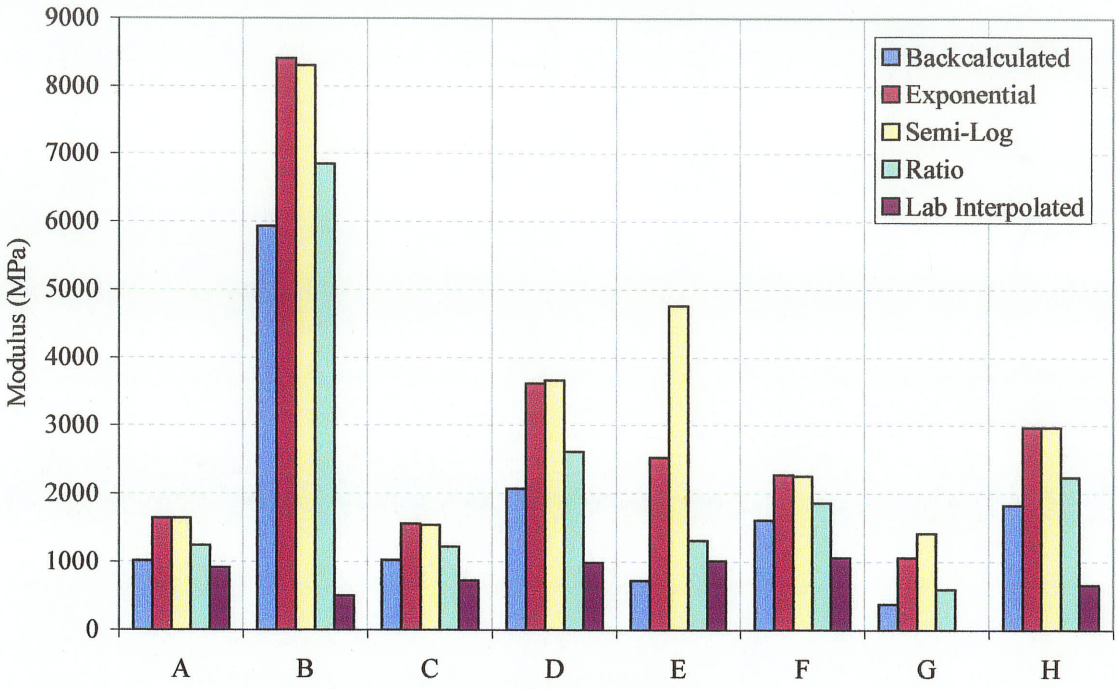

Note: There is no lab interpolated data for Project G.

Figure G-1 Temperature Corrected Modulus Comparison at 25°C for Bit B Mixture

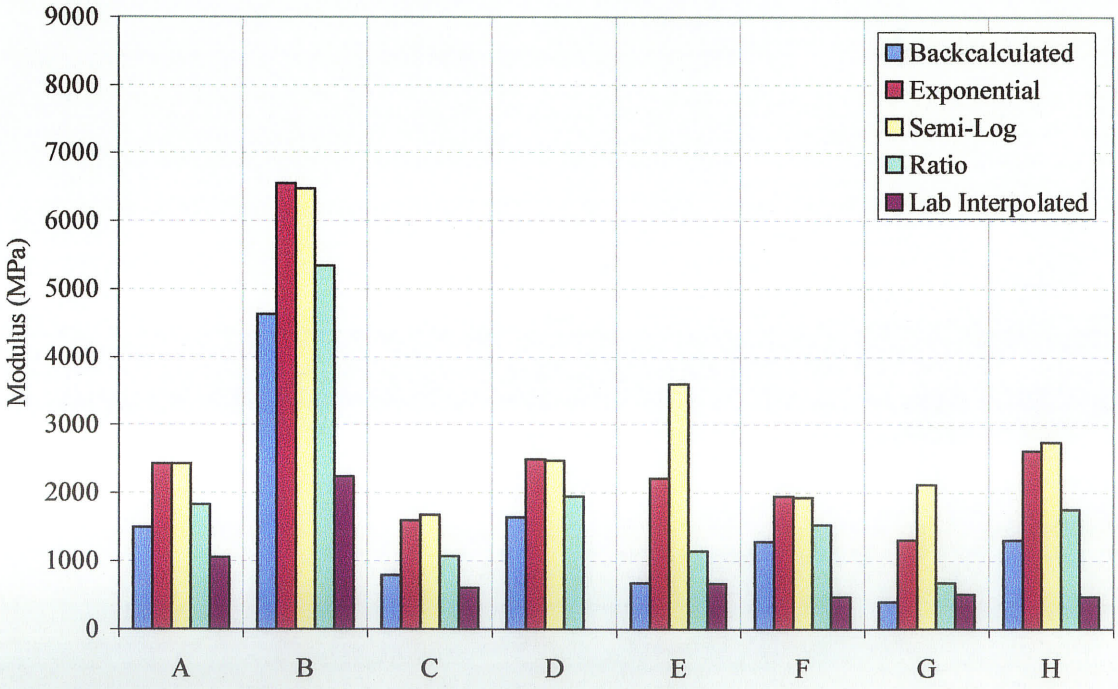

Note: There is no lab interpolated data for Project D.

Figure G-2 Temperature Corrected Modulus Comparison at 25°C for Bit C.